Overview of The 2016 Kumamoto Earthquake

*Noriko Kamaya[1], Naoyuki Yamada[1], Yuzo Ishigaki[1], Kiyoshi Takeda[1], Hidekuni Kuroki[1], Satoshi Takahama[1], Ken Moriwaki[1], Mugi Yamamoto[1], Mitsuharu Ueda[1], Takahiko Yamauchi[1], Miho Tanaka[1], Youko Komatsu[1], Kouji Sakoda[1], Nobuyuki Hirota[1], Jun-ichi Suganomata[1], Akio Kawai[1], Yuki Morita[1], Satoshi Annoura[1], Yuji Nishimae[1], Shigeki Aoki[1], Naoto Koja[1], Koji Nakamura[1], Gen Aoki[1], Tetsuo Hashimoto[1]

1.Japan Meteorological Agency

1. Introduction

A big earthquake of M6.5 occurred at 21:26 on 14 April, 2016 in Kumamoto region of Kumamoto Prefecture. Its focal depth was estimated at 11km, and the maximum JMA seismic intensity scale was 7, which is the strongest of the scale. After 28 hours of the earthquake, a rather bigger earthquake of M7.3 occurred in the same region, and the seismically active area was spread up to about 150km long, from Kumamoto Prefecture to Oita Prefecture. Just after the latter biggest earthquake (M7.3), another earthquake of M5.7 occurred in the central region of Oita Prefecture (The M5.7 is a reference value. JMA Seismic intensity of this earthquake is unknown because of overlapping seismic waves from M7.3 event.), and one and a half hour after the biggest earthquake (M7.3), another earthquake of M5.9 occurred in Aso region of Kumamoto Prefecture (maximum JMA seismic intensity is 6+). Seismic intensities were over 5- for 18 big earthquakes (as of 11 May). JMA named the sequence of this seismic activity “The 2016 Kumamoto Earthquake”. This seismic activity occurred in crust, and Earthquake Research Committee of Headquarters of Earthquake Research Promotion evaluated that this seismic activity is caused by parts of Futagawa Fault and Hinagu Fault.

2. Distribution of hypocenters and Mechanisms of the earthquakes

Hypocenters are distributed along a belt area from Northeast to Southwest direction within Beppu-Shimabara Graben in central Kyushu. Detailed analysis of the distribution of hypocenters by using Double-Difference method suggests vertical or steeply dipping fault planes inclining toward Northwest. In addition, it shows that there are complex planes around the junction of the Futakaga Fault and the Hinagu Fault. In the central Oita Prefecture, the hypocenters of the new seismic activity are distributed in the areas where seismicity had been inactive.
The mechanisms of the earthquakes are mainly strike slip type with North-South Tension axis. Some Normal fault type earthquakes occur around Futagawa Fault.

3. Analysis of Source Process and Source Scanning Algorithm

Source process analysis on the biggest earthquake (M7.3) in Kumamoto region of Kumamoto Prefecture by using strong-motion seismic records of near seismometers shows that the fault slip propagated from the hypocenter toward Northeast and finally reached around Mt. Aso.
Source Scanning Algorithm on the same earthquake (M7.3) shows that emission of energy started around the Futagawa Fault, and spread to the Hinagu Fault.

4. Earthquake information issued by JMA

After the first big earthquake (M6.5) in Kumamoto Prefecture on 14 April, Japan Meteorological Agency (JMA) issued Early Earthquake Warning (EEW) for 19 earthquakes of this seismic activity. Regarding to Intensity Scale for Long-period Ground Motion, the maximum intensities of 3 and 4 were observed at following earthquakes.
M6.5 on 14 April: Intensity 3 in Kumamoto region of Kumamoto Prefecture.

M6.4 on 15 April: Intensity 4 in Kumamoto region of Kumamoto Prefecture.
M7.3 on 16 April: Intensity 4 in Kumamoto region and Aso region of Kumamoto Prefecture.
It was the first time to observe the intensity 4 which is the strongest intensity in the Intensity Scale for Long-period Ground Motion since the start of issuance of this information by JMA in March 2013.
JMA issued information about aftershock probability after the first big earthquake of M6.5, however, JMA stopped issuance of following information because this seismic activity is not considered to be a simple mainshock -aftershock series after the occurrence of the bigger earthquake (M7.3) on 16 April. Instead of issuance of information about aftershock probability, JMA called attention to people to prepare high seismicity in this region from a point of view of disaster prevention.

Keywords: Kumamoto Earthquake, Double-Difference Method, Seismic Source Process Analysis, Source Scanning Algorithm, Long-period Earthquake Ground Motion, Earthquake Information

The 2016 Kumamoto Earthquake -Seismic Activity and Earthquake Information issued by JMA-

*Noriko Kamaya[1], Naoyuki Yamada[1], Yuzo Ishigaki[1], Kiyoshi Takeda[1], Hidekuni Kuroki[1], Satoshi Takahama[1], Ken Moriwaki[1], Mugi Yamamoto[1], Mitsuharu Ueda[1], Takahiko Yamauchi[1], Miho Tanaka[1], Youko Komatsu[1], Kouji Sakoda[1], Nobuyuki Hirota[1], Jun-ichi Suganomata[1], Akio Kawai[1], Yuki Morita[1], Satoshi Annoura[1], Yuji Nishimae[1], Shigeki Aoki[1], Naoto Koja[1], Koji Nakamura[1], Gen Aoki[1], Tetsuo Hashimoto[1]

1.Japan Meteorological Agency

A big earthquake of M6.5 occurred at 21:26 on 14 April, 2016 in Kumamoto region of Kumamoto Prefecture. Its focal depth was estimated at 11km, and the maximum JMA seismic intensity scale was 7, which is the strongest of the scale. After 28 hours of the earthquake, a rather bigger earthquake of M7.3 occurred in the same region, and the seismically active area was spread up to about 150km long, from Kumamoto Prefecture to Oita Prefecture. Just after the latter biggest earthquake (M7.3), another earthquake of M5.7 occurred in central region of Oita Prefecture (The M5.7 is a reference value. JMA Seismic intensity of this earthquake is unknown because of overlapping seismic waves fromM7.3 event.), and one and a half hour after the biggest earthquake (M7.3), another earthquake of M5.9 occurred in Aso region of Kumamoto Prefecture (maximum JMA seismic intensity is 6+). Seismic intensities were over 5- for 18 big earthquakes (as of 11 May). JMA named the sequence of this seismic activity “The 2016 Kumamoto Earthquake”. In this poster, JMA will report analysis of this seismic activity and earthquake information issued by JMA. Please see relevant abstract “Overview of The 2016 Kumamoto Earthquake” by JMA.

Keywords: Kumamoto Earthquake, Double-Difference Method, Seismic Source Process Analysis, Source Scanning Algorithm, Long-period Earthquake Ground Motion, Earthquake Information

The 2016 Kumamoto earthquake M7.3

*Yuzo Ishikawa[1]

1.The National Institute of Advanced Industrial Science and Technology

1. Introduction
01:25 on April 16 M7.3 earthquake occurred in Kumamoto prefecture and JMA Intensity 7 was observed. There were M6.5 and M6.4 two big foreshocks. M6 foreshock is rare case in Japan. Only one event was known such case. It was that off Boso M7.5 1909 earthquake had M6.7 foreshock.
M7.3 mainshock induced new seismic activity in Aso region and the central Ooita prefecture. These earthquakes were also researched.

2. The characteristics of each earthquake group
The Kumamoto M7.3 earthquake had so many aftershocks. It was the most number of aftershocks of inland event in Japan from 1997. The induced earthquakes by the Mainshock were occurred in Aso region and the central Ooita prefecture. The hypocenters of these earthquakes avoided the past source areas of 1975 M6.1 Aso earthquake and 1975 M6.4 west of Ooita earthquake and Mt. Kujyu volcano.
The fault plane solutions of large events are all strike slip (E-W compression and N-S tension)by Global CMT group.
The b-value of M6.4 on 2016/04/14 is 0.74 and some smaller than the b-value of the mainshock 0.85. But M5.0 earthquake occurred along the Hinagu fault on 2000 June 8 nad its b value is 0.61. So, it is very hard to suppose that M6.5 was the foreshock by b-value. The b-values in west Aso followed M5.9 on April 16, in east Aso followed M5.8 and in the central Ooita were 0.9-1.0, 0.8, and 1.0.

3. Other problems
Intensity distribution of the mainshock showed that stations in east from the hypocenter were shaken hardly compared to other direction.
Past large earthquake inland Kyushu had never directly induced volcanic eruptions. Only the 1922 M6.9 earthquake in the Tachibana bay followed Aso eruption about one month later. But the source fault of the Kumamoto earthquake arrived at the end of Mt. Aso and it is the first case that the source of M7 event arrived at the volcanic area. So, we must observe volcanoes more carefully.
The hypocenter data of Hi-net automatically determined were very useful to check the seismicity. So, the hypocenter data is needed to keep them in homepage in long time.

Keywords: Kumamoto earthquake, b value, volcanic eruption

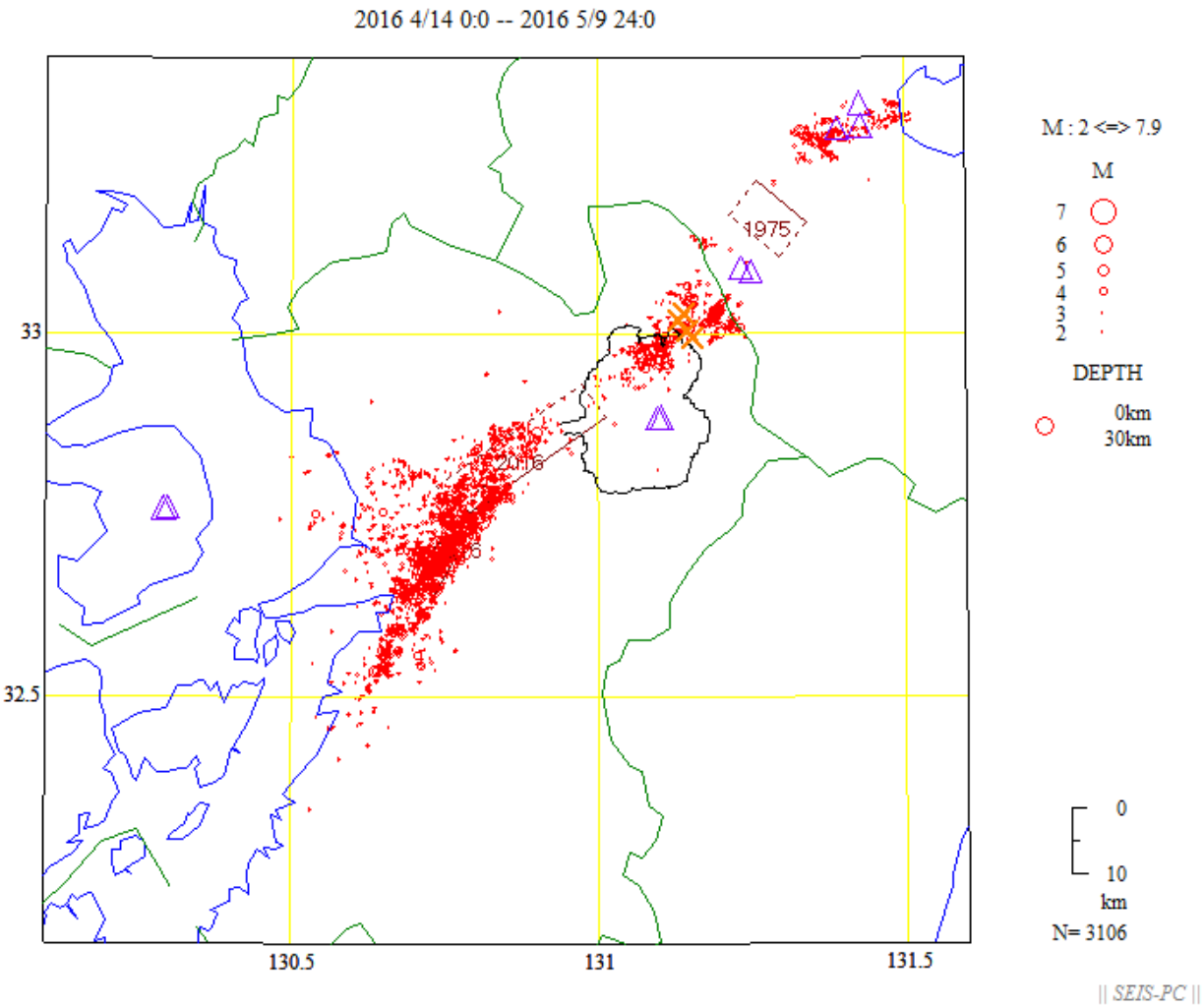

Focal mechanisms of 2016 Kumamoto earthquake activity and its relation to the stress field (preliminary report)

*Satoshi Matsumoto[1], Yusuke Yamashita[2], Manami Nakamoto[1], Masahiro Miyazaki[2], Shin'ichi Sakai[3], Yoshihisa Iio[2], Group for urgent joint seismic observation of the 2016 Kumamoto earthquake

1.Institute of Seismology and Volcanology, Faculty of Sciences, Kyushu University, 2.Disaster Prevention Research Institute, Kyoto University, 3.Earthuake Research Institute, University of Tokyo

The 2016 Kumamoto earthquake occurred in middle Kyushu Island, Japan where stress field is in strike-slip or normal fault regime. The minimum principal compression stress (s3), with its near north-south trend, is dominant throughout the entire region. In this study, we determined focal mechanisms related to the seismic activity from first P wave polarity data by urgent seismic observation deployed in the hypocentral area.
Generally, the earthquakes in strike-slip and normal fault types occurred around focal area, indicating maximum principal stress is similar magnitude to moderate one as suggested by the result of stress tensor inversion by Matsumoto et al. (2015). The focal mechanisms show spatial and temporal variation during the activity. The solution for main shock (M7.3) reveals different strike angle from centroid moment tensor solution by F-net (NIED). This suggests the mainshock rupture change its direction to the Futagawa fault.
In addition, the result is indicative of change in stress condition associated with the occurrence of the main shock (M7.3) around Futagawa and Hinagu faults.
Acknowledgement
We also used seismic waveform data at stations operated by Kyushu, Kyoto, Kagoshima Universities, JMA, and NIED. This study was supported by the Ministry of Education, Culture, Sports, Science and Technology (MEXT) of Japan, under its Earthquake and Volcano Hazards Observation and Research Program.This work is partly supported by MEXT KAKENHI Grant Number16H06298.

Keywords: 2016Kumamoto earthquake, focal mechanisms, stress field

The significance of seismicity after The 2016 Kumamoto Earthquake sequence

*Tomoko Elizabeth Yano[1], Makoto MATSUBARA[1]

1.National Research Institute of Earth Science and Disaster Resilience

We applied the double-difference method (hypoDD; Waldhauser and Ellsworth, 2000) using cross-correlation of waveform data as well as the ordinal differential picking time data for the 2016 Kumamoto Earthquake sequence including the largest earthquake with magnitude (M) of 7.3 occurred on April 16, 2016 following the second largest earthquake with M6.5 on April 14, 2016. A total 5,272 events are consisted of three different subgroups; 1) events (M > 0) between the M6.5 event and the M7.3 event, 2) events (M > 0) after the M7.3 event to April 19, 3) otherwise event (M > 3) from April 19 to April 27, 2016. Waveforms obtained by the multi-institute networks such as NIED Hi-net, JMA, Kyushu university, and Kagoshima university are adopted for preparing both cross-correlation of their waveform data and ordinal differential picking time data for differential travel times used by hypoDD. Therefore, the final relocated earthquake distribution made sharper lines and confined clusters. Particularly for this study area, the final hypocenter distributions are easily traceable following the known active fault traces such as the Hinagu fault range and its surroundings while the Futagawa fault range shows more complicated shapes than the Hinagu fault. Particularly, along the vertical planes or planes with high angle dips become apparent shape of seismicity during this earthquake sequence. Orientations of these planes agree the strike direction of the focal mechanisms estimated by the first motion phase arrivals, which routinely or manually determined by the NIED Hi-net.

Immediately after the first M6.5 event, the seismicity extremely increases along the Hinagu fault range. After the largest M7.3 event, the seismicity increases along the Futagawa fault as well as the Hinagu fault and spread to the northeastern of the Futagawa fault such as the Mt. Aso area, and Ohita region. These two main events are occurred at the complicated region where the Hinagu and the Futagawa faults marge each other. Although the nucleation of these two main events are not clear whether on the Futagawa or Hinagu fault, our relocation results show that the clear location of very high seismicity on the Hinagu fault range immediately after the M6.5 event but not on the Futagawa fault range at this moment. The active seismicity on the Futagawa fault range started after the M7.3 event.

The seismicity between the northeastern tip of Futagawa fault and southwest of the caldera of the Mt. Aso has isolated by extremely fewer than its surroundings whereas seismicity dramatically increases after the M7.3 event. In this region and surroundings had been a moderate seismicity area and not been observed any significant difference from surroundings in terms of seismicity according to the background seismicity over 10 years due to JUICE catalog (Yano et al., 2015) in which all inland shallow hypocenters were determined by NIED Hi-net are re-determined by hypoDD. This region coincides with the area where coseismic slip amplitude during the M7.3 event becomes the maximum about 5 m in the depth down to 10 km, according to source inversion result by Kubo et al. (2016). This zone also coincides with thick low P-wave velocity zone (Matsubara and Obara, 2011) underneath.
The area around the Mt. Aso and Ohita prefecture have been seismic region from the past, according the JUICE catalog. The seismicity in this area has been observed along the lines, which run in both vertical and north dipping direction. After the M7.3 event, the seismicity in this area increased significantly. Majorities of the events can be traced where background seismicity had occurred

particularly in vertical direction. However, there are some aftershocks occurred where seismicity is not apparent from JUICE catalog. Their new activity has shaped a linear pattern running from northwest to southeast.

Keywords: Kumamoto earthquake, Seismicity, Earthquake relocation

Normal-fault components in the focal mechanisms of earthquakes in April 2016, Kyusyu region, Japan

*Akiko Takeo[1]

1.Earthquake Research Institutute, the University of Tokyo

A swarm of earthquakes occurred in Kyushu region, Japan in April 2016. The activity includes two major earthquakes in Kumamoto prefecture with moment magnitudes of Mw6.1 on April 14th and Mw7.1 on April 16th. Many large aftershocks (Mw > 4) have been excited at least one month since the first Mw6.1 earthquake. The overall activity might be defined by a foreshocks-mainshock-aftershocks sequence. According to moment tensor catalog by F-net and Hi-net systems operated by National Research Institute for Earth Science and Disaster Prevention (NIED), the three major earthquakes seem to have occurred near the intersection point between the known Hinagu and Futagawa faults with mostly strike-slip focal mechanisms, whereas some potion of aftershocks seem to have occurred at the western extension of the Futagawa fault and northern/southwestern areas out of the Futagawa fault with focal mechanisms including normal-fault components. For revealing the contribution of normal-fault system during this swarm activity, I estimated the centroid moment tensor solutions of the major three earthquakes and large aftershocks (Mw > 4) by a grid-search algorithm (Takeo et al. 2010) and their uncertainties by the bootstrap method. The datasets are the records of F-net strong motion velocitymeters for two major earthquakes, and records of F-net broadband seismometers and three broadband seismometers in the southwestern Shikoku island installed by Earthquake Research Institute, the University of Tokyo in 2015. As a result, I obtained both strike-slip and normal-fault reliable solutions for aftershock sequence (4 < Mw < 6). The normal-fault solutions often appeared at off fault area of the Futagawa fault. The two major earthquakes had significant non-double couple components, which can be explained by the linear combination of the strike-slip double-couple solutions along the known fault systems and the normal-fault double-couple solutions along the fault systems. The contribution of Hinagu and Futagawa faults is hard to distinguish by the centroid moment tensor analysis because the difference in the strike angles of these fault system is not large enough. On the other hand, the total contribution of normal-fault solutions could be estimated to be about 15% for the Mw6.1 first earthquake and about 30% for the largest Mw7.1 earthquake. These values may be useful for the slip inversion of these earthquakes and for interpreting surface faulting. The total contribution of normal-fault solution will be estimated, which might have contribution for discussing the tectonics of the Beppu-Shimabara graben widely located off north of the Futagawa fault.

Keywords: Kumamoto earthquake, Centroid moment tensor analysis

Time evolution of the 2016 Kumamoto Earthquake I

*Masahiro Miyazaki[1], Satoshi Matsumoto[2], Yoshihisa Iio[1], Yusuke Yamashita[1], Hiroshi Shimizu[2], Takeshi Matsushima[2], Manami Nakamoto[2], Kazunari Uchida[2], Megumi Kamizono[3], Group for urgent joint seismic observation of the 2016 Kumamoto earthquake Group for urgent joint seismic observation of the 2016 Kumamoto earthquake

1.Disaster Prevention Research Institute, Kyoto University, 2.Institute of Seismology and Volcanology, Faculty of Sciences, Kyushu University, 3.Department of Earth and Planetary Sciences, Graduate School of Sciences, Kyushu University

Mjma6.5 event was occurred on the Northeast part of the Hinagu fault zone on 14 April 2016. Aftter about 28 hours, Mjma 7.3 event occurred on the Futagawa fault zone and triggered seismic activities happened at the Northeast part of the Mt. Aso and near Beppu city. From the spreading source region and its magnitudes, it seemed that the first Mjma6.5 event was foreshock and the Mjma 7.3 event was main shock. However, time evolution of the sequence must be discussed to reveal the relation of the two events.

In this study, we detected after shocks events using the Matched-filter technique (Gibbons and Ringdal, 2006; Shelly et al., 2007) in the continuous records. We mainly selected the events that occurred deeper part of the fault zones as templates and use the temporal observation data including the network just above the aftershock region. Using that datasets, we could distinguish among the events that were close to each other in time and space.

We obtained the results as follows. First, the number of the detected events was higher than the regions surrounded by the foreshock and the aftershock rather than other region. In addition, activity rates of the detected events in the inner region were higher than that of outer region. These suggested that foreshock activities at the deeper part of the fault zones was affected to the occurrence of the main shock. Second, numbers of detected events that using the templates between the foreshock and the main shock was decrease after the main shock. We considered two reasons as follows. One is the effect of the migration of active area. The other is that the stress field and/or structures surrounding fault zones were disturbed by the main shock.

In addition, we investigated the influence to the non-volcanic tremor occurred at the southwestern part of the Hinagu fault zone (Miyazaki et al., 2015; Chao and Obara, 2016). We found that tremors were activated after the large events. Long term activity rates were seems to be unchanged before the 2016 Kumamoto earthquake. Activities at the seismogenic zone above the tremor sources were relatively lower than that of other regions. These suggested that magnitude of the direct influences from the 2016 Kumamoto earthquakes was small. However, we need careful observation to reveal the effect to the whole Hinagu fault zone.

Acknowledgements
We use the dataset recorded at Kyushu University, Japan Meteorological Agency (JMA), National Research Institute for Earth Science and Disaster Prevention (NIED) and Group for urgent joint seismic observation of the 2016 Kumamoto earthquake. This study was supported by the Ministry of Education, Culture, Sports, Science and Technology (MEXT) of Japan, under its Earthquake and Volcano Hazards Observation and Research Program.This work is partly supported by MEXT KAKENHI

Grant Number16H06298. and Earthquake Research Institute, University of Tokyo under Joint Usage Program.

Reference

Chao, K., and K. Obara (2016), Triggered tectonic tremor in various types of fault systems of Japan following the 2012 Mw8.6 Sumatra earthquake, J. Geophys. Res. Solid Earth, 121, 170–187, doi:10.1002/2015JB012566.

Gibbons, S. J., and F. Ringdal (2006), The detection of low magnitude seismic events using array-based waveform correlation, Geophysical Journal International, 165(1), 149-166, doi: 10.1111/j.1365-246X.2006.02865.x.

Miyazaki, M., S. Matsumoto, and H. Shimizu (2015), Triggered tremors beneath the seismogenic zone of an active fault zone, Kyushu, Japan,
Earth Planets Space, 67, 179, doi:10.1186/s40623-015-0346-4.

Shelly, D. R., S. Ide, and G. C. Beroza (2007), Non-volcanic tremor and low-frequency earthquake swarms, Nature, 446(7133), 305-307, doi: 10.1038/nature05666.

Keywords: the 2016 Kumamoto Earthquake, seismic activty, non-volcanic tremor, Futagawa-Hinagu fault zone , hypocenter distribution, urgent joint seismic observation

Spatio-temporal evolution of seismicity following the 2016 Kumamoto earthquake: Migrations of early aftershocks following M6.5 earthquake

*Aitaro Kato[1], Jun'ichi Fukuda[1], Shigeki Nakagawa[1]

1.Earthquake Research Institute, the University of Tokyo

A series of powerful earthquakes and the following aftershocks has struck the Kumamoto area in Kyusyu, Japan, from 14th April, 2016. These powerful earthquakes have caused destructive damages in the central part of Kyusyu. We relocated a bunch of earthquakes associated with the 2016 Kumamoto earthquake (~2700 events), applying a double-differential code to arrival time data set constructed by JMA, and waveform cross-correlation technique. Then, we newly detected numerous earthquakes using these relocated earthquakes as template events, applying a matched filter technique to continuous waveform data recorded at 35 seismic stations in the central Kyusyu area. Most of relocated hypocenters are aligned along nearly vertical planes or north-westward dipping plane. Hypocenters before M7.3 earthquakes were concentrated near surface traces of active faults in northernmost segment of “Hinagu” and a part of “Futagawa”. After M7.3 earthquake, they shifted toward northwest ward and aligned gently northwest ward dipping plane. Early aftershocks following M6.5 earthquake clearly expanded along fault strikes during a half day. But, aftershock zone slightly continued to expand perpendicular to fault strikes until the generation of M7.3 earthquake. The M7.3 earthquake has immediately boosted a widespread seismicity along the northeastern extension of the Futagawa fault, as well as the northwestern section of the Hinagu fault.

Keywords: Kumamoto earthquake, Seismicity, Migrations of aftershocks

Effect of complex fault systems and volcanic areas on the 2016 Kumamoto-Oita earthquake sequence

*Takahiko Uchide[1], Haruo Horikawa[1], Misato Nakai[1], Reiken Matsushita[1], Norio Shigematsu[1], Ryosuke Ando[2,1], Kazutoshi Imanishi[1]

1.Research Institute of Earthquake and Volcano Geology, Geological Survey of Japan, National Institute of Advanced Industrial Science and Technology (AIST), 2.Demartment of Earth and Planetary Science, Graduate School of Science, the University of Tokyo

The 2016 Kumamoto-Oita earthquake sequence breaking out on the night of April 14, 2016 (all time and date in this abstract are written using local time (UTC+9)) ruptured a pair of fault systems and volcanic areas. The first large event (referred to as "event #1") was Mw 6.2 at 21:26 on April 14, followed by an Mw 6.0 event ("event #2") at 0:03 on the 15th. The largest event (Mw 7.0; "event #3") took place at 1:25 on the 16th. Not only the strong ground motion from individual events, but also the series of large and medium earthquakes for a long time brought painful experiences to residents. The seismicity became active in three separated areas: the Futagawa and Hinagu fault systems where the abovementioned three large events occurred; the northern Aso area; and the Beppu-Yufuin area. We address the following questions: (1) Why were the faults ruptured by three different large earthquakes, not by a single large earthquake at once? (2) Why did the spatial gaps of seismicity appear?

We performed a relocation of hypocenters in this seismicity using hypoDD (Waldhauser and Ellsworth, 2000). The result suggests underground complex fault geometries corresponding to the Futagawa and Hinagu fault systems, composed of the NW-dipping faults and nearly vertical faults. The hypocenter of the event #1 was on a vertical fault, while that of the event #2 was on a dipping fault. The event #3 started on another vertical fault, as indicated by the first-motion polarity mechanism, close to the intersection with the dipping fault. The irregularity of the fault geometry probably prevented the further rupture propagation and, at the same time, helped the nucleation for the next large earthquake. This resulted in the rupture by the series of three large earthquakes.

The seismicity gap (referred to as "Aso gap") between the Futagawa fault system and the northern Aso was ruptured by the event #3, as revealed by the slip inversion analysis using strong-motion data from KiK-net of NIED. It is probable that the event #3 completely ruptured the Aso gap and remained little stress to produce its aftershocks. This condition should be somehow related to the volcanic structure of Mt. Aso, although rigorous discussions require a detailed structure model and resultant fault behaviors.

At Yufuin, we found a dynamic triggering event by visual inspection of highpass-filtered seismograms from K-NET and KiK-net of NIED. The dynamic triggering events have often been found in volcanic areas (e.g., Hill et al., 1993). A simple comparison of the amplitudes of seismograms highpass-filtered at 16 Hz with those of the nearby Mw 5.1 event that occurred at 7:11 on April 16, 2016 implies that the triggered event is mid-M6. The estimated magnitude is consistent with the rupture length inferred from the InSAR image by GSI from ALOS-2 and the extent of the area where the seismicity became active after the event #3. This dynamic triggering mechanism produced the apparent gap in seismicity between Yufuin and northern Aso area.

Our careful data analyses revealed the mechanism of the curious seismic activity in the 2016

Kumamoto-Oita earthquake sequence, although a number of questions are still remained, such as the mechanism of the formation of the complex fault system, and the relationship between the Aso gap and Mt. Aso. The influence of this earthquake sequence on the volcanic activities is also of interest. These studies will help us to make better assessment of seismic and volcanic hazards.

Acknowledgement
We used the phase data from the JMA Unified Earthquake Catalog based on data from seismic stations maintained by JMA, NIED, and Kyushu University; material from NIED: seismograms from Hi-net, KiK-net, and K-NET, and the F-net Moment Tensor Catalog; and the moment tensor catalog from the Global CMT Project.

Keywords: Seismology, The 2016 Kumamoto earthquake, Dynamic triggering of earthquakes, Slip inversion analysis of earthquake, Hypocenter relocation, Mt. Aso

Triggered significant seismicity in Oita following the M7.3 Kumamoto earthquake in 2016

*Masatoshi Miyazawa[1]

1.Disaster Prevention Research Institute, Kyoto University

On 16 April 2016, the M7.3 Kumamoto earthquake occurred in Kyushu. At a seismic station in Oita located about 80 km north-eastwards from the hypocenter, large seismic signals from another large earthquake were observed during the passage of seismic waves from the M7.3 event. The event identified in Oita was located by picking P and S wave arrivals using seismograms at K-NET and KiK-net stations. The Oita earthquake occurred about 33 sec after the M7.3 event, the hypocenter located at a depth of about 7 km beneath Yuhuin geothermal region, and its local magnitude was estimated about 6.0. The static and dynamic stress changes at this region from the M7.3 event were on the order of about 1 kPa and 1 MPa, respectively.

Keywords: 2016 Kumamoto earthquake, Triggered seismicity in Oita

Matched Filter Method implemented as a semi-automatic hypocenter location system - Application to the 2016 Kumamoto Earthquake -

*Shiro Ohmi[1]

1.Earthquake Hazards Division, Disaster Prevention Research Institute, Kyoto University

Seismic activity of the 2016 Kumamaoto Earthquake was analyzed by using the Matched Filter Method (MFM). In this analysis, MFM was implemented as a semi-automatic hypocenter relocation system. Since the hypocenters are scattered in wide area, we have to select template earthquake to match each earthquake cluster. For this purpose, we selected template earthquakes using the conventional automatic hypocenter location system using STA/LTA ratio. During one week since the start of the activity, we automatically selected about 300 templates. We inspected these templates one by one manually and scanned the continuous data. We could detect more than 6,400 events in this time range. One problem raised is that the performance of this 'modified MFM method' depends on the performance of the conventional automatic relocation system to select templates. Seismicity pattern obtained by this method is similar to that from manually inspected catalogue by JMA. We suppose MFM is one of the powerful tools to semi-automatically obtain preliminary results for the seismic activity

Keywords: 2016 Kumamoto Earthquake, automatic hypocenter relocation system, Matched Filter method

Seismic quiescence prior to the 2016 Kumamoto Earthquakes

*Toshiyasu Nagao[1], Nobuhiro Furuse[1], Jun Izutsu[2]

1.Institute of Oceanic Research and development, Tokai University, 2.International Digital Earth Applied Science research center, Chubu University

We developed new algorithm named RTM detecting seismic quiescence before large earthquakes. The RTM algorithm is a kind weighted parameter survey method, which taking into account region (R), time (T) and size of earthquakes (M) (Nagao et al., EPS, 2011). The most notable feature of the RTM algorithm is very sensitive to detect small change of seismicity.
We applied the above RTM algorithm to 2016 Kumamoto Earthquake swarm and detected clear seismic quiescence in the western Kyushu Island. The seismic quiescence started at around beginning of 2015 and ended March 2016. The main shock of M7.3 occurred just the edge of seismic quiescence region. It is well consistent with the past examples (e.g. 1995 Kobe EQ). In the presentation, we would like to present the results of parameter search and robustness of the obtained quiescence.
The figure shows the maximum of the seismic quiescence prior to the 2016 Kumamoto Earthquakes.
This study was partly supported by the Ministry of Education, Culture, Sports, Science and Technology (MEXT) of Japan, under its Earthquake and Volcano Hazards Observation and Research Program, and Resarch projects of Institue of Oceanic Research and Development, Tokai university.

Keywords: seismic quiescence, Kumamoto

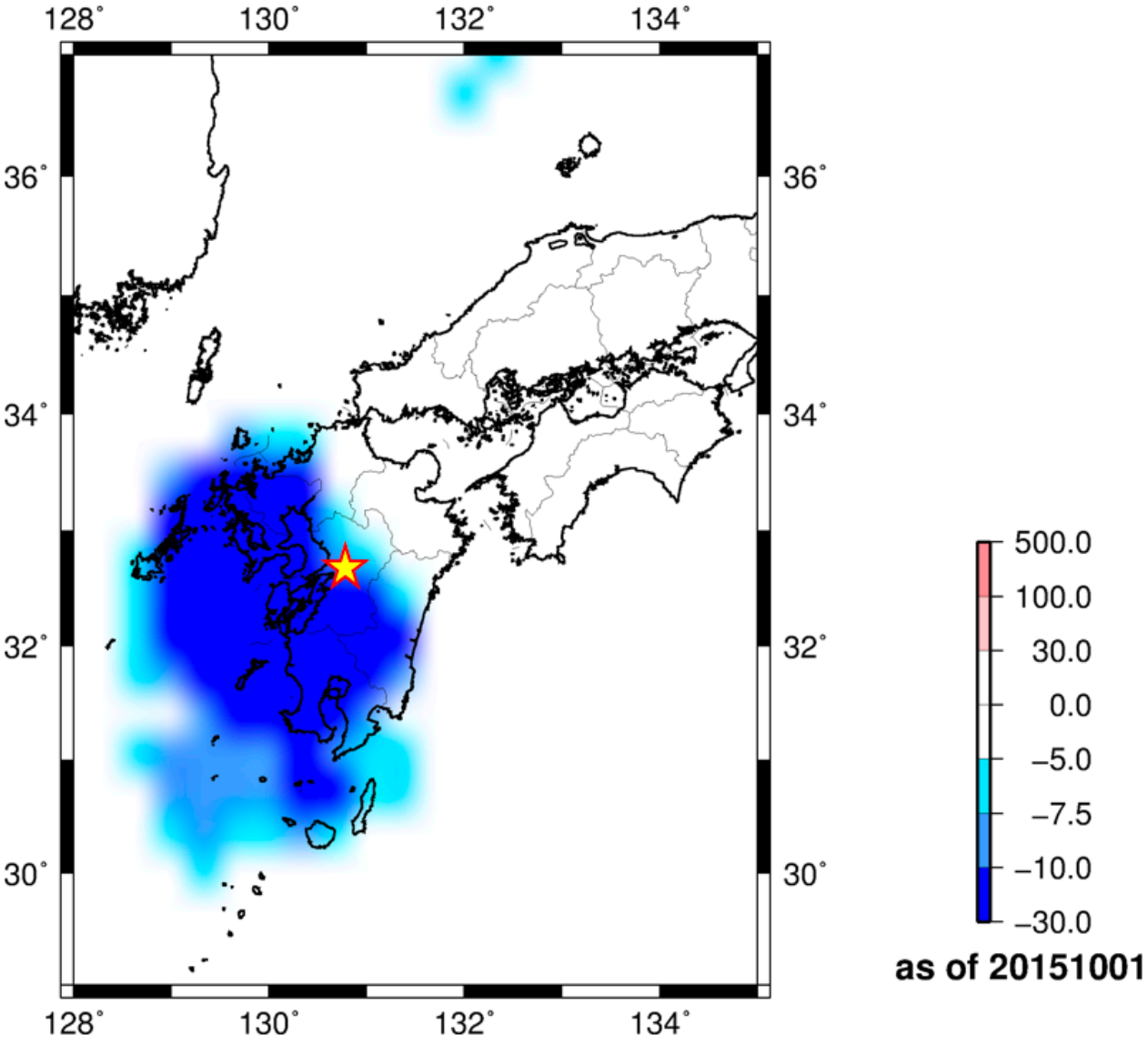

Temporal and spatial changes in b-value for the 2016 Kumamoto Earthquakes

*Takaaki Kobari[1], Pen Han[1], Kastumi Hattori[1]

1.Department of Earth Sciences, Graduate School of Science, Chiba University

At 09:26, on April 14, 2016(LT), the first Kumamoto EQ (Mj6.5) occurred at depth of 11 km in Kumamoto Prefecture. This EQ is thought the foreshock of the main shock (Mj7.3) at 01:25 on April 16 (LT). In this paper, we will show the results of b-value changes in time and space for the 2016/04/16 Kumamoto Earthquakes base on Gutenberg-Richter law. We used the JMA earthquake catalog (2010/01/01-2016/04/16) and earthquakes shallower than 20 km depth. For the investigation of spatial changes, we analyzed the region of E129-133 (deg.) and N31.0-34.5 (deg) with interval of G=0.05 (deg). We take the circle with radius R = 60 (km) and the number of earthquake N in the circle for computation. We set N=80,100 as a threshold and if N<80 or 100, we do not compute b-values. For the investigation on temporal changes, we used the moving window method of a certain number of earthquakes. We take the number of earthquake of the windows 200 and 100 with shift of 100 and 50, respectively. The details will be shown in the presentation.

Keywords: Earthquake, b-value

Change in *b*-values following the three *M*6 or 7-class earthquakes in the 2016 Kumamoto earthquake sequence

*Takaki Iwata[1]

1.Tokiwa University

This study investigates whether or not *b*-values of the Gutenberg-Richter law change following the three events (*M*6.5 on 14 April, *M*6.4 on 15 April, and *M7*.3 on 16 April) in the 2016 Kumamoto earthquake sequence. To examine the statistical significance of the change, a Bayesian approach developed and used in Iwata [2008, 2013, GJI; 2016, Pageoph] was applied to the sequence. This approach introduces a statistical model of a magnitude-frequency distribution covering the entire magnitude range proposed by Ogata & Katsura [1993, GJI]. The proposed distribution contains a parameter representing the quality of detection capability of earthquakes. With the aforementioned Bayesian approach, we can estimate a *b*-value with the consideration of the temporal change in the quality of detectability; all observed events are used in the estimation while we discard events of which magnitude is less than a cut-off magnitude in an conventional method to find a *b*-value. This is the advantage of the Bayesian approach to examine the significance of the change in *b*-values.

Data analyzed in this study was taken from the JMA catalog (last accessed on 11 May 2016). A study area was chosen to cover the aftershock area just before the *M7*.3 event and the epicenter of the *M* 7.3 event, and four periods were considered: from 1 August 2015 to the occurrence of the *M*6.5 event (Period 0), between the occurrences of the *M*6.5 and *M*6.4 events (Period 1), between the occurrences of the *M*6.4 and *M7*.3 events (Period 2), and after the M7.3 event (Period 3). For each of the four periods, the *b*-value and temporal change in detection capability (i.e, the parameter of the magnitude-frequency distribution proposed by Ogata & Katsura [1993]) were estimated simultaneously. Cases with the constraint of a common *b*-value over successive periods (e.g., *b* -values of Periods 1, 2, and 3 are the same while the one in Period 0 is different.) were also considered. In total, there were eight cases (models), depending on which periods have a common *b* -value, and the best model was selected from the eight with Akaike's Bayesian Information Criterion (ABIC).

The best model is the case where Periods 0, 1, and 2 have a common *b*-value of 0.736 and only Period 3 has a different value of 0.941; the *b*-value varies at the timing of the *M7*.3 event whereas it does not change with the *M*6.5 and *M*6.4 events. The difference of ABIC values between this model and the one where the *b*-values over the four periods are the same is 7.9, which suggests the statistical significance of the best model. Remarkable increase in the *b*-value following a major/megathrust earthquake has been found [e.g., Tormann et al., 2015, Nature Geoscience]. This increase will correspond to decrease of stress due to a large slip, because it has been suggested that the *b*-value is correlated inversely with stress [e.g., Scholz, 2015, GRL]. From this viewpoint, the result of this study suggests that the high stress in the focal area of the Kumamoto sequence was not decreased by the *M*6.5 and *M*6.4 events but the *M7*.3 event has released it.

Keywords: b-value, stress, detectability of earthquake, Bayesian estimation, aftershock sequence, Gutenberg-Richter law

Observation of transient signatures in atmosphere and ionosphere prior to the 2016 Kumamoto earthquake in Japan. Preliminary results.

*Dimitar Ouzounov[1,5], Katsumi Hattori[2,5], Sergey Pulinets[3,5], Leonid Petrov[4]

1.Center of Excellence in Earth Systems Modeling & Observations (CEESMO) , Schmid College of Science & Technology Chapman University, Orange, California, USA, 2.Chiba University, Yayoi 1-33, Inage, Chiba, 263-8522, Japan, 3.Space Research Institute, Russian Academy of Sciences, Moscow, Russian Federation, 4.Astrogeo Center, Falls Church VA, USA, 5.International Space Science Institute, Beijing, China

The 2016 Kumamoto series of earthquakes started with M6.2 foreshock (12:26 UTC) on April 14, 2016 and continued with M7.0 series of 16:25 UTC on April 15) beneath Kumamoto City on Kyushu Region, Japan. The two earthquakes killed at least 48 people and injured about 3,000 others in total. We prospectively and retrospectively analyzed transient variation of specific physical parameters characterizing the state of the atmosphere and ionosphere several days before the onset of this earthquake, namely: outgoing earth radiation (OLR) on the top the atmosphere), atmospheric chemical potential (ACP) related to the thermodynamic proprieties in the lower atmosphere and for ionosphere the *F2*-layer critical frequency (*foF2)*. On April 1st , 2106 the satellite monitoring over Japan has shown a rapid increase of OLR near Kumamoto epicentral area. The ongoing analysis of satellite radiation revealed another transient anomaly over the epicentral area on April 12 (-3 days before the M7). The retrospective analysis of ACP from satellite assimilation data shows similar patterns of rapid increases on April 11-12 several hours earlier to the satellite transient anomalies. *F2* -layer critical frequency data from Okinawa/Ogimi Ionosond (26.68°N, 128.15°E) show repeatable pattern of *foF2 i*ncrease in the nighttime of April 13 (36 hours before the foreshock of M6.2 on April 14) and in the early morning hours of April 15 (20 hours before eth M7.0 0f April 15th). Our preliminary results show correlation between the appearance of pre-earthquake transients anomalies in atmosphere and ionosphere (with a short time-lag, from hours up to few days) and the occurrence of 2016 Kumamoto, Japan earthquake series.

Keywords: pre-eartqhauke signals, Satelitte thermal anomaly, Ionosond foF2

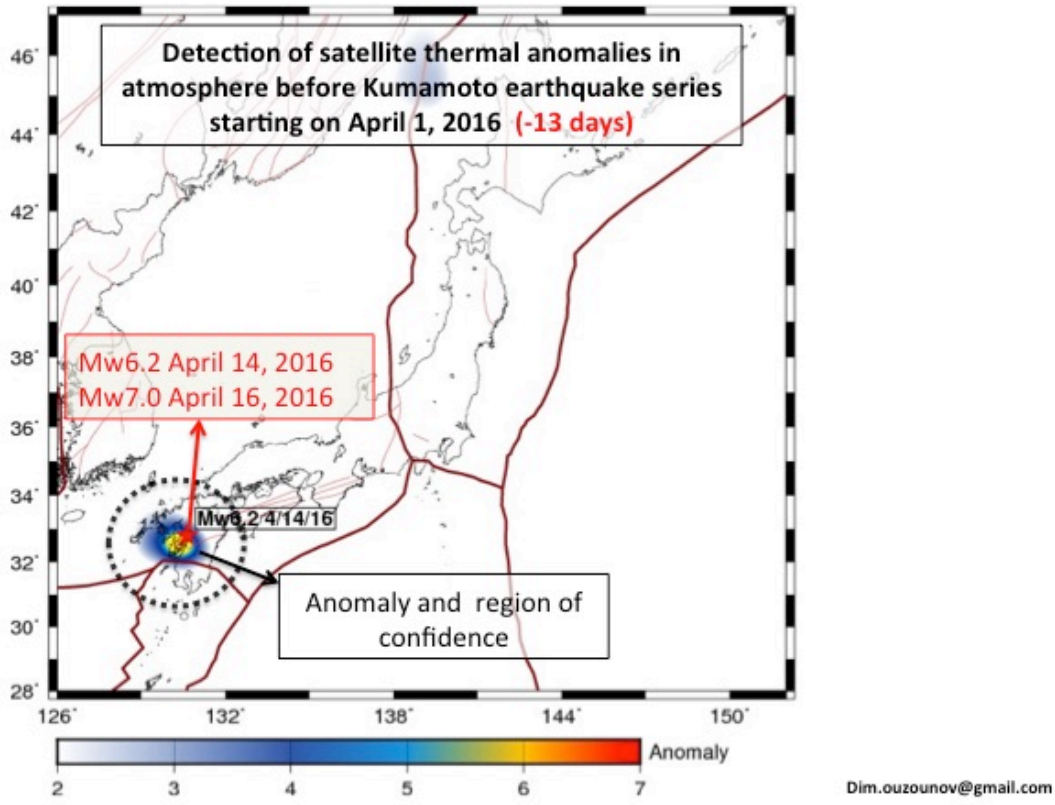

Probability of successive occurrences of large earthquakes and triggering of volcanic eruptions: in response to 2016 Kumamoto earthquake activity

*Takeshi Nishimura[1]

1.Department of Geophysics, Graduate School of Science, Tohoku University

The 2016 Kumamoto earthquake activity consists of a main shock of M7.5 earthquake on April 16 that followed a large foreshock of M6.5 on April 14. Such successive occurrences of large earthquakes have not often occurred. Since the Kumamoto earthquakes with high aftershock activity are occurring in the Beppu-Shimabara graben, activations of the earthquakes in the central fault lines of Japan and nearby volcanoes such as Aso are worried about. To understand the possibility of these activities, I examine worldwide database of earthquakes and volcanic eruptions.
We analyze the CMT solutions provided by Columbia university, and search successive occurrences of large earthquakes with magnitudes of > 7. The results show that after an occurrence of large earthquake, occurrence rate of large earthquakes increases in the region within about 1000 km distance from the first eq. The seismic activity approaches to the common level for more than 2 years. We also find that the number of volcanic eruptions increase after the occurrence of large earthquakes within a distance of about 200 km.

Keywords: large earthquake, volcanic eruptions, successive occurrence

Prediction of the 2016 Kumamoto Earthquake

*Takao Saruwatari[1]

1.none

1.Predictive method

When as a result of having analyzed many earthquakes, time and the low pressure that a typhoon became the extratropical cyclone developed, an intense downward air current occurred and knew that an earthquake occurred at the point that hit the ground, the surface of the water several months later. At the point where a downward air current was, increase of the maximum instantaneous wind speed was recognized. In addition, it was revealed that it came out as a domain without the cloud by the satellite image.

1) It is very likely to be the earthquake occurrence at the point where the maximum instantaneous wind speed for the first time in several years was recorded from several months.

2) Because width of the strong wind area or the width of the domain without the cloud accords with the width of the focal region as for the volume of earthquake, I can suppose it.

3) An earthquake is generated in a rear-entry position for seven months from one week from a strong wind day.

4) The direction of the wind near the epicenter accords with the axis of the mechanism solution.

2. Proof of the predictive method

After prediction method is announced by Seismological Society of Japan in 2010, there are many prediction examples and analysis samples 2011 northeastern offing earthquake, and I'm thinking this prediction method was proved.

3.Earthquake prediction from the low pressure which developed of April 7, 2016

The low pressure with the front goes ahead through the Sea of Japan; passing through the neighborhood of Tohoku at night to the Sanriku offing. It rained, and wind of the southerliness strongly blew nationwide in West Japan and East Japan.

Maximum instantaneous wind speed 43.9 meters (wind of the south-southwest) (it is nine years since then since 2007) was observed in Kumamoto Mount Aso at 09:53 a.m. In addition, in Nagasaki, 35.2m/s (southwestern wind) was observed in Nagasaki in 29.3 meters of maximum instantaneous wind speed (south wind), Unzendake. A record of around April 1 was updated. Based on a predictive method, it was predicted that I ran near Mount Aso from Unzendake, and the earthquake was possible. It was predicted with seven months later after one week at the outbreak time and occurred seven days later.

4.The 2016 Kumamoto earthquake

April 14 21:26 Kumamoto, Kumamoto district M6.5

April 16 01:25 Kumamoto, Kumamoto district M7.3

5.Detailed analysis and conclusion

I showed the maximum instantaneous wind speed of April 7 of all observation points of Kumamoto, Oita of the Meteorological Agency in a separate table, the other figure. The deficit is the point that the maximum instantaneous wind speed is high in. A red frame of the other figure is a frame of the epicenter distribution map of the Meteorological Agency making. From the southwest of Mount Aso to the northeast, there is the domain that the maximum instantaneous wind speed is higher in than the outskirts. This domain almost fits an epicenter distribution map (red frame) of the distinction illustrated Meteorological Agency making. In other words, as well as many other earthquakes, I can predict the scene of earthquake and the volume of earthquake from the maximum instantaneous wind speed before the earthquake occurrence.

Mantle convection and an active fault are not the causes of the earthquake, and the strong wind of the downward air current should think with the cause of the earthquake.

References
1. http://www2.jpgu.org/meeting/2011/yokou/MIS036-P85.pdf
2. http://www2.jpgu.org/meeting/2015/PDF2015/S-CG56_P.pdf

Keywords: earthquake prediction, maximum instantaneous wind speed , nuclear power plant

地点	熊本県 最大瞬間			地点	大分県 最大瞬間		
	風速	風向	起時		風速	風向	起時
鹿北	18.1	南南東	7:41	国見	9.2	南東	5:19
伎明	16.1	南南西	9:21	中津	14.1	南西	12:16
菊池	17.7	南	7:58	豊後高田	19.1	南東	0:48
南小國	18	南南東	10:16	院内	12.5	西南西	8:09
阿蘇乙姫	29.4	南西	10:21	杵築	12.5	西北西	16:07
阿蘇山	43.9	南西	9:53	日田	18.5	西南西	12:00
熊本	19.5	西	13:35	玖珠	19.7	南南西	7:00
益城	19.5	南西	10:16	湯布院	26.2	南西	9:11
南阿蘇	21.4	西南西	7:50	大分	19.6	南南西	9:54
高森	24.6	西南西	9:37	犬飼	16	南南西	11:21
三角	18.9	南西	9:55	竹田	14.8	西	8:55
甲佐	17.9	南	10:26	佐伯	11.6	南南西	9:13
本渡	26.7	南南西	9:58	宇目	9	南東	7:12
松島	19	南	8:54	浦江	15.1	南	5:19
八代	20.9	南南西	8:35				
牛深	20.1	南西	8:14				
水俣	13.2	東南東	1:00				
人吉	12.7	西南西	13:23				
上	12.8	西南西	8:54				

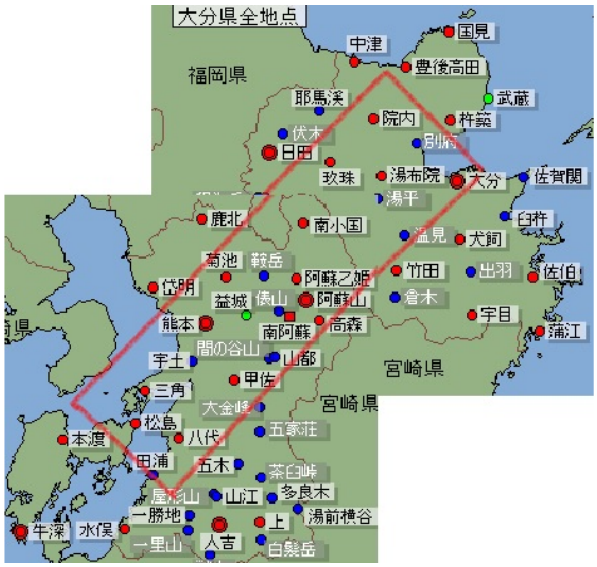

Urgent joint seismic observation of the 2016 Kumamoto earthquake - Dense seismic observation -

*Manami Nakamoto[1], Satoshi Matsumoto[1], Takeshi Matsushima[1], Shin'ichi Sakai[2], Yusuke Yamashita[3], Masahiro Miyazaki[3], Yoshihisa Iio[3], Tomomi Okada[4], Hiroaki Takahashi[5], Toshiki Watanabe[6], Kazuhiko Goto[7], Youichi Asano[8], Hiroshi Shimizu[1], Group for urgent joint seismic observation of the 2016 Kumamoto earthquake

1.Institute of Seismology and Volcanology, Kyushu University, 2.Earthquake Research Institute, The University of Tokyo, 3.Disaster Prevention Research Institute, Kyoto University, 4.Research Center for Prediction of Earthquakes and Volcanic Eruptions, Tohoku University, 5.Institute of Seismology and Volcanology, Hokkaido University, 6.Earthquake and Volcano Research Center, Nagoya University, 7.Nansei-Toko Observatory for Earthquakes and Volcanoes, Kagoshima University, 8.National Research Institute for Earth Science and Disaster Resilience

On April 16, 2016, a large earthquake of M 7.3 occurred in Kumamoto prefecture, Kyushu island, southwestern Japan, accompanied by an earthquake of M 6.5 on April 14. Many aftershocks occur and spread across a wide area from Kumamoto to Oita prefecture. After the first large earthquake, temporal seismic stations were immediately installed around the focal area by the group for urgent joint seismic observation of the 2016 Kumamoto earthquake. Until May 1, we installed 37 seismic stations consist of short period seismometers and in 10 stations of them waveform data were telemetered. Moreover, we installed 10 seismometers each area, Yatsushiro city and northeast area of Aso caldera and west of Kumamoto city, corresponding to central part of the Hinagu fault zone, NE-extension of the Fukagawa fault zone and west of the joint area of the two faults, respectively. Continuous wave data will be totally recorded in 67 stations. Kyushu University has also deployed temporal seismic stations in and around Beppu-Shimabara graben before the event on April 14. These data sets help us to determine the hypocenters and analyze focal mechanisms of aftershocks accuracy, and it is expected to reveal characteristics of the 2016 Kumamoto earthquake.
Acknowledgements:
This work is partly supported by MEXT KAKENHI Grant Number 16H06298, the Ministry of Education, Culture, Sports, Science and Technology of Japan under its Earthquake Research Institute, The University of Tokyo under Joint Usage Program.

Keywords: the 2016 Kumamoto earthquake, seismic observation

Fault Structure of the 2016 Kumamoto earthquake using relocated aftershocks

*Yusuke Yamashita[1], Satoshi Matsumoto[2], Manami Nakamoto[2], Takeshi Matsushima[2], Masahiro Miyazaki[1], Hiroshi Shimizu[2], Yoshihisa Iio[1], Group for urgent joint seismic observation of the 2016 Kumamoto earthquake

1.Disaster Prevention Research Institute, Kyoto University, 2.Institute of Seismology and Volcanology, Kyushu University

We estimated the fault structure of the 2016 Kumamoto earthquake using relocated aftershocks for 1 week after the Mj 6.5 foreshock (21:26 14 April 2016). Aftershocks relocation was performed using double-difference method [Waldhauser and Ellsworth, 2000]. For analyzing many events, we picked first arrival times of P and S-waves using automatic picking system (Home Seismometer Corporation) applying to the data of temporal seismic observation around the Futagawa-Hinagu Faults by group for urgent joint seismic observation of the 2016 Kumamoto earthquake. The station using relocation were selected within 50 km distance from epicenter. We firstly calculated initial location using HYPOMH [Hirata and Matsu'ura, 1987] with 1-D velocity model (routine analysis in Kyushu University). Then, we applied tomoDD code [Zhang and Thurber, 2003] with 3-D velocity model [Saiga et al, 2011]. Total number of relocated event is approximately 10,000, which is approximately 5 times compared with JMA catalog. Preliminary result shows some complex alignment of aftershocks associated with foreshock, mainshock, and induced earthquakes.

Acknowledgements: This work is partly supported by MEXT KAKENHI Grant Number 16H06298, the Ministry of Education, Culture, Sports, Science and Technology of Japan under its Earthquake and Volcano Hazards Observation and Research Program, and Earthquake Research Institute, The University of Tokyo under Joint Usage Program.

Keywords: 2016 Kumamoto earthquake

Three-dimensional seismic velocity structure in Kyushu including the source region of the 2016 Kumamoto earthquake

*Azusa Shito[1], Satoshi Matsumoto[1], Hiroshi Shimizu[1], Group for urgent joint seismic observation of the 2016 Kumamoto earthquake

1.Institute of Seismology and Volcanology, Kyushu University

The 2016 Kumamoto earthquake is a series of earthquakes, including an earthquake with magnitude of Mj=7.3 which occurred on April 16, 2016 beneath Kumamoto City, the preceding earthquake with magnitude of Mj=6.5 which occurred on April 14, 2016, and many triggered aftershocks. The two main earthquakes were located along the Futagawa and Hinagu fault zones in the west area of Beppu-Shimabara graben.

The purpose of the study is to reveal detailed crustal structures and its tectonic process of the successive large earthquakes generation. We estimated three-dimensional seismic wave velocities in the crust beneath Kyushu including the source region of the Kumamoto earthquakes by applying double-difference tomography method [Zhang and Thurber, 2003]. The local earthquake data (from January 2000 to July 2013, m > 2, depth < 30 km) were collected by the Institute of Seismology and Volcanology (SEVO), Kyushu University. For the tomographic inversion, we used 159,103 P-wave and 115,265 S-wave arrival times from 4,126 local earthquakes. The initial velocity model is the same as the one used for routine earthquake location processing in SEVO, Kyushu University.

We will discuss the relation between the 2016 Kumamoto earthquakes and the tectonic background inferred from the seismic wave velocity structure.

Acknowledgements
This work is partly supported by JSPS KAKENHI Grant Number JP15J40067, MEXT KAKENHI Grant Number 16H06298, MEXT under its Earthquake and Volcano Hazards Observation and Research Program, and Earthquake Research Institute, The University of Tokyo under Joint Usage Program. We thank Dr. Okada and Dr. Nakajima for their constructive comments.

Keywords: The 2016 Kumamoto earthquake

Temporal changes of seismic velocity structure after the 2016 Kumamoto earthquake

*Tomotake Ueno[1], Tatsuhiko Saito[1], Kaoru Sawazaki[1], Katsuhiko Shiomi[1]

1.National Research Institute for Earth Science and Disaster Resilience

Seismic velocity structure often changes after large earthquakes or during seismic swarms. On April 2016, a large earthquake (Mjma7.3) occurred at Kumamoto Prefecture in the Kyushu district. Aftershocks have been occurred around the Futagawa fault and the Hinagu fault, which are located at southwest part in the source area. For northeast part of the source area, aftershock activity seems to reach to near Mt. Aso. Induced earthquakes have also been activated in the northern Oita prefecture, which is located northeastward from the aftershock area. Using the seismic interferometry method, we detected co-seismic velocity changes after the 2016 Kumamoto earthquake in the Kyusyu district.

We use seismic records of Hi-net, which were provided by National research Institute for Earth science and Disaster resilience (NIED). We use Auto-Correlation-Functions (ACFs) of the ambient seismic noise record to calculate velocity fluctuation of the subsurface structure. To obtain an ACF, we applied a 1 - 3 Hz bandpass filter to 1 hour waveform data, and applied one-bit amplitude normalization to the filtered data to reduce effects of large seismic signals. To avoid daily pattern of ambient seismic noise, we calculate one-week average of the ACFs. These stacked ACFs were calculated every day, and they were compared to the referenced ACF through the stretching method. The referenced ACF was reproduced from average of the ACFs obtained in 2013. Temporal velocity change was calculated if the velocity change was larger than twice the standard deviation of the velocity fluctuation obtained one month before the 2016 Kumamoto earthquake.

Our preliminary result demonstrated the co-seismic velocity changes at the source region of the Kumamoto earthquake, Mt. Aso, and a part of the northern Oita prefecture. For the southwest part of the source area, we obtained 0.5 -3.0 % velocity decreases at three stations: N.MSIH, N.MSMH, and N.TYNH. For the northeast part of the source area near Mt. Aso, significant velocity decreases of 1.5 -6.0 % were obtained at stations N.ASVH, N.HKSH, and N.NMNH. In a part of the northern Oita prefecture, velocity decreases of 0.5 -1.0 % were obtained at stations N.KKEH and N.SNIH, which are located at a seismic gap between the swarms of Mt. Aso and northern Oita prefecture.

Keywords: The 2016 Kumamoto earthquake, temporal changes of seismic velocity structure, Auto Correlation function, Hi-net

Change in stress and seismicity after the 2016 Kumamoto, Japan, earthquake sequence and implication on regional seismic hazard

*Chung-Han Chan[1], Yu-Chih Huang[2]

1.Earth Observatory of Singapore, Nanyang Technological University, 2.Aso Volcanological Laboratory, Institute of Geothermal Sciences, Kyoto University

We evaluate evolution of stress and seismicity after the 2016 Kumamoto earthquake sequence and assess rupture probability for the neighbouring active faults. Following the Kumamoto earthquakes, including the April 14th M_W 6.1 and the April 16th M_W 7.0 events, consequent aftershocks took place both north-eastward and south-westward along the Futagawa-Hinagu fault system. In addition to the strike-slip mechanism, which is consistent with the behaviour of the Futagawa-Hinagu fault system, some aftershocks with normal mechanisms were observed. Such aftershock patterns in space and mechanism could be associated with coseismic Coulomb stress change on optimally oriented planes (OOPs), determined based on the stress perturbation of an earthquake and prior regional stress. The model shows significant stress increase along the Futagawa-Hinagu fault system and the OOP were favorable to either strike-slip or normal faulting, consistent with observations. In addition to spatial distribution of consequent events, we forecasted their temporal distribution through the modified Omori Law. In comparing with background seismicity rate, this sequence could last for ca. 1 year, similar as the duration of the sequence that follows the 2000 M5.0 earthquake took place in this region. To assess regional seismic hazard after the mainshock, we evalauted short-term rate change on neighboring active faults through the rate-and-state friction model. Due to stress enhanced, seismicity rate elevation for more than 4 times is expected on the Takano-Shirahata and Hinagu segments of the Hinagu fault zone. Considering their long-term rupture probability of 6 % in the coming 30 years, the hazard near these segments are further elevated after the Kumamoto earthquakes. Our results provide the basis to rapidly re-assess seismic hazard, which would be beneficial for emergency response regarding victim relocation and building reinforcement.

Keywords: Kumamoto sequence, Coulomb stress change, modified Omori Law, rate-and-state friction model, seismic hazard assessment

Stress fields in and around the focal area of the 2016 Kumamoto earthquake

*Keisuke Yoshida[1], Akira Hasegawa[2], Tatsuhiko Saito[1], Youichi Asano[1], Sachiko Tanaka[1], Kaoru Sawazaki[1], Yumi Urata[1], Eiichi Fukuyama[1]

1.National research institute for earth science and disaster prevention, 2.Tohoku University

An M6.5 earthquake occurred in the Futagawa-Hinagu fault zone in Kumamoto Prefecture at 21:26 (JST) on 14 April, 2016. Two days after, the M 7.3 Kumamoto earthquake occurred at 1:25 on 16 April. GPS and strong motion waveform analyses revealed that the significant slip of M6.5 and M7.3 earthquake occurred on the Hinagu and Futagawa fault, respectively. Many earthquakes were induced along the fault zone even in the Oita prefecture, 100 km away the mainshock fault.
To understand the generation mechanism of the series of the 2016 Kumamoto earthquakes, it is important to investigate the state of stress and frictional strength in and around the focal area. In this study, we estimate the spatiotemporal variation of stress orientations by analyzing focal mechanism data of small earthquakes.
In order to investigate the detailed spatial variation of stress fields, we first located hypocenters of earthquakes in and around the focal area. We compiled P- and S- wave travel time data listed in the JMA unified catalogue and the Hi-net routine catalogue for 11,154 earthquakes (M> 0.5) which occurred from 1997 to 4 May 2016. We relocated hypocenters by using the Double Difference method (Waldhauser & Ellsworth, 2000). The distribution of the relocated hypocenters shows the complicated structure composed of several sharp alignments. The M7.3 earthquake seemed to occur at the bottom of the sharp alignment of the small earthquakes formed before the M7.3 earthquake.
Second, we determined focal mechanisms of small earthquakes. We applied the HASH code (Hardebeck & Shearer, 2002) to the P-wave polarity data listed in the Hi-net routine catalogue for the earthquakes which occurred during the period from 2001 to 4 May 2016, and obtained 991 high quality (rank A or B) solutions. We also added the moment tensor solutions determined by AQUA-Hi-net and F-net to the dataset. The number of the focal mechanism data obtained here is 1104.
We investigated temporal and spatial variations of stress orientations by using the focal mechanism dataset. To investigate the spatial distribution of stress orientations, we applied the slick code (Michael, 1987) to the nearest 10 ~ 15 focal mechanisms within 5 km from each location of the focal mechanisms.

1) For the period before the M6.5 earthquake, stress fields have the different feature across the Futagawa-Hinagu fault zone. In the northern side, the stress fields with s3-axis oriented to NNW-SSE and strike-slip fault stress regime is dominant. In contrast, the stress fields with s3-axis oriented to N-S and reverse fault stress regime is dominant in the southern side. The difference of the stress fields across the fault zone can be explained by the strike-slip motion along the Futagawa-Hinagu block boundary (e.g. Nishimura & Hashimoto, 2006). In the focal area of the M6.5 earthquake, the s3-axis is oriented to N-S.
2) For the period between the 14 April after M6.5 and the 16 April before M7.3 earthquakes, the s3-axis is oriented to NNW-SSE in the focal area of the M6.5 earthquake. The s3-axis rotated from N-S to NNW-SSE by 13 degrees after the M6.5 earthquake. This is significant on the basis of the 95% confidential interval.
3) For the period after the M7.3 earthquake, the s3-axis is oriented to NNW-SSE in most of locations. However, near the hypocenter of the M7.3 earthquake, the s3-axis is oriented to NW-SE, which substantially differs from the surrounding region. This NW-SE oriented s3-axis can be

explained by the static stress change caused by the right-lateral strike-slip of the mainshock. And this suggested that the possibility of the rotation of the stress field after the M7.3 earthquake and thus we could consider that the deviatoric stress is very small in the focal area and the reduction of frictional strength may play an important role of the occurrences of the series of the earthquakes.

Keywords: stress field, frictional strength, focal mechanism, fault structure, The 2016 Kumamoto earthquake

Relationship between Distributions of Shallow Earthquakes and Gradients of Gravity Anomaly Field in and around the Focal Area of the 2016 Kumamoto Earthquake.

*Takeshi Kudo[1], Akihiko Yamamoto[2]

1.Science and Technology Section, College of Engineering, Chubu University, 2.Graduate School of Science and Engineering, Ehime University

Relationship between distributions of shallow earthquakes and gradients of gravity anomaly field in and around the focal area of the 2016 Kumamoto Earthquake is investigated. In this session, we will present Bouguer anomaly maps, Bouguer anomaly horizontal gradient maps, and some graphs showing relations between gravity anomaly gradients and spatial distributions of hypocenters related to the 2016 Kumamoto Earthquake.

Zones with steep horizontal gradient of gravity anomaly field are presumably caused by faults bounding different density structures in the crust. On the other hand, most shallow earthquakes are supposed to be caused by dislocations at faults in the crust. From both presumptions, it follows that the distribution of epicenters should be overlapped with that of the steep gravity gradient zones. Kudo and Kono (1999) verified the overlap in Southwest Japan.

In the case of the 1995 Hyogo-ken Nanbu earthquake, however, very low seismicity along the steep gradient zone of gravity anomaly was followed by the mainshock (Kudo and Kono, 1999). The preliminary report for the case of the 2016 Kumamoto Earthquake will also be presented.

Keywords: 2016 Kumamoto Earthquake, gravity anomaly, seismicity

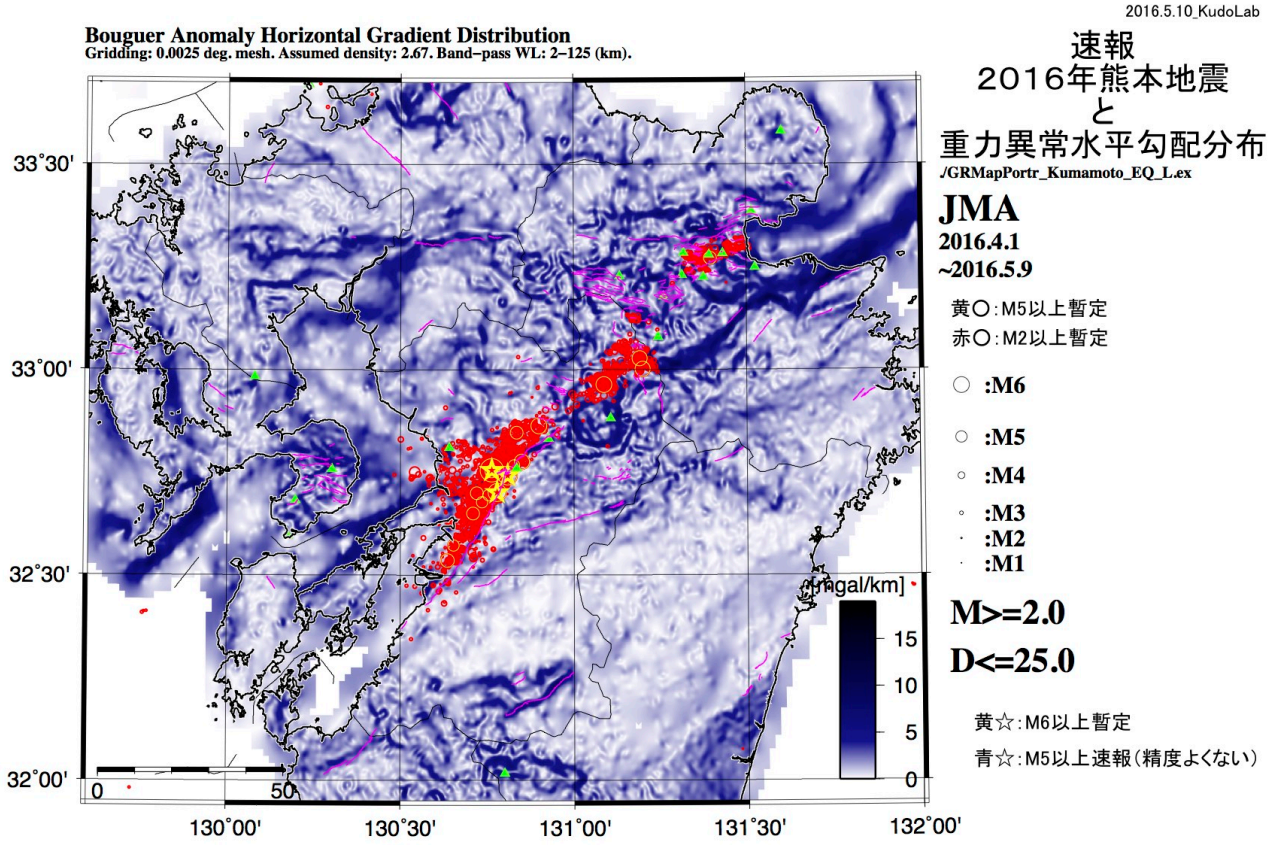

Relationship between fault structures detected from gravity anomalies and the aftershock distribution of the 2016 Kumamoto earthquake

*Nayuta Matsumoto[1], Yoshihiro Hiramatsu[2], Akihiro Sawada[2]

1.Graduate School of Natural Science and Technology, Kanazawa University, 2.Institute of Science and Engineering, Kanazawa University

In this study, we analyze gravity anomalies in/around the focal region of the 2016 Kumamoto earthquake, evaluate subsurface features of the continuity, segmentation and faulting type of the active fault zones and discuss relationships between those features and the aftershock distribution.
The gravity data published by GSI [2006], Yamamoto *et al.* [2011], Geological Survey of Japan (AIST) [2013], Gravity Research Group in Southwest Japan [2001], and Kanazawa University data are compiled in this study. We apply terrain corrections with 10 m DEM and a low-pass filter, then remove a linear trend to obtain Bouguer anomalies. We calculate the first horizontal derivative (HD), the first vertical derivative (VD) and TDX (Cooper and Cowan, 2006) to detect subsurface structural boundary and dip angle β(Beki, 2013) to infer a faulting type of active fault zones.
The obtained HD, VD and TDX indicate the existence of the continuous subsurface structural boundary along the Futagawa fault zone. This boundary extends from the Uto peninsula to the Beppu bay except Mt. ASo area. The distribution of dip angle βalong the Futagawa fault zone implies a normal faulting, which corresponds to the faulting of this fault zone estimated geologically and geomorphologically. Aftershocks are distributed along this structural boundary from the confluence of the Futagawa and the Hinagu fault zones to the east end of the Aso volcano.
The Bouguer anomalies around the southern part of the Hinagu segment of the Hinagu fault zone indicate a right lateral faulting. The VD and TDX show a structural boundary along the segment but it is not so clear. No clear structural boundaries are observed along the Takano-Shirahata segment, although the most of aftershocks occurred around this segment. TDX implies the existence of a structural boundary with a NW-SE trend around the boundary between the Hinagu and Takano-Shirahata segments. The invariant quantity I (Perdersen and Rasmussen, 1990) shows that this structure boundary has a 3D-like structure rather than a 2D-like. Geological map indicates that this structure boundary corresponds to a boundary between metamorphic rock and sedimentary rock. The active area of the aftershocks does not extend to the south beyond this structure boundary, implying that the spatial extent of the source fault is controlled by this boundary
Around the Beppu-Haneyama fault zone, circular density structures related to active volcanoes are so dominant that we cannot recognize any linear structural boundaries, which correspond to aftershock distribution.

Keywords: Gravity Anomaly, Aftershock distribution, Subsurface structural boundary

Broad-band magnetotelluric data around the focal region of the 2016 Kumamoto-Oita earthquakes

*Koki Aizawa[1], Hisafumi Asaue[2], Katsuaki Koike[3], Shinichi Takakura[4], Nobuo Matsushima[4], Maki Hata[4], Tohru yoshinaga[5], Takeshi Hashimoto[6], Mitsuru Utsugi[7], Hiroyuki Inoue[7], Taro Shiotani[13], Makoto Uyeshima[8], Takao Koyama[8], Wataru Kanda[9], Kazunari Uchida[1], Yuko Tsukashima[1], Azusa Shito[1], Shiori Fujita[12], Asuma Wakabayashi[12], Kaori Tsukamoto[12], Takeshi Matsushima[1], Ryokei Yoshimura[10], Ken'ichi Yamazaki[10], Shintaro Komatsu[10], Makoto Tamura[11], The 2016 Kumamoto earthquake research group

1.Institute of Seismology and Volcanology, Faculty of Sciences, Kyushu University, 2.Laboratory on Innovative Techniques for Infrastructures, Kyoto University, 3.Graduate School of Engineering and Faculty of Engineering, Kyoto University, 4.National Institute of Advanced Industrial Science and Technology, 5.Kumamoto University, 6.Hokkaido University, 7.Kyoto University, 8.Earthquake Research Institute, University of Tokyo, 9.Volcanic Fluid Research Center, Tokyo Institute of Technology, 10.Disaster Prevention Research Institute, Kyoto University, 11.Hokkaido Research Organization, Geological Survery of Hokkaido, 12.Department of Earth and Planetary Sciences, Kyushu University, 13.Division of Earth and Planetary Sciences, Graduate School of Science, Kyoto University

The Mj 6.5 and Mj 7.3 Kumamoto earthquakes that occurred on 14 and 16 April 2016 triggered not only the aftershocks around the epicenters, but also triggered the earthquakes 50~100 km far from the main shocks. The aftershocks and the triggered earthquakes that exceed Mj 3.5 are amounted up 230 on 8 May, 2016, and are mainly located on NE-SW lines that may correspond to the westward extension of median tectonic line (MTL). The active seismicity can be divided into three regions, (1) the Futagawa and Hinagu faults (the region around the main shocks), (2) the northern part of Aso volcano, and (3) the region around the Tsurumi and Yufu volcanoes. There are distinct seismically inactive area between these regions. We show the broad-band (200~0.0003 Hz) MT data, which were obtained 1999~2015 around these focal regions. The dataset consists of that around the main shocks (Asaue et al., 2006, 2013; Takakura et al., 2000; Hata et al., 2016), and that around the triggered seismicity (Aizawa et al., 2015, 2016; Shiotani et al., 2015). The apparent resistivity of the sum of the squared elements (ssq) invariant impedance (Rung-Arunwan et al., 2016) shows that the earthquakes occur on the electric resistive zones. The electric conductive zones correspond to the seismically inactive areas. The faults of main shock is located at the boundary between conductive and resistive zones. We will discuss the possibility that the series of earthquakes were guided by the resistivity structure.

The figures is found below.
http://www.sevo.kyushu-u.ac.jp/kumamoto2016/MT2016KumamotoOita.pdf

Acknowledgements
This work is partly supported by MEXT KAKENHI Grant Number 16H06298, MEXT under its Earthquake and Volcano Hazards Observation and Research Program, and
Earthquake Research Institute, University of Tokyo under Joint Usage Program.

References

Asaue, H., Koike, K., Yoshinaga, T., and Takakura, S., 2006, Magnetotelluric resistivity modeling for 3D characterization of geothermal reservoirs in the Western side of Mt. Aso, SW Japan: Journal of Applied Geophysics, v. 58, p. 296-312.
Asaue, H., Kubo, T., Yoshinaga, T., and Koike, K., 2012, Application of Magnetotelluric (MT)

Resistivity to Imaging of Regional Three-Dimensional Geologic Structures and Groundwater Systems: Natural Resources Research, v. 21, p. 383-393.
Rung-Arunwan, T., Siripunvaraporn, W., and Utada, H., 2016, On the Berdichevsky average: Physics of the Earth and Planetary Interiors, v. 253, p. 1-4.

Keywords: resistivity structure, magnetotelluric data, The 2016 Kumamoto earthquake

The tectonic background of the 2016 Kumamoto Earthquakes across middle Kyushu, the junction of southwest Japan Arc and the Ryukyu Arc

*Hidehisa Mashima[1]

1.Center for Obsidian and Lithic Studies, Meiji University

The 2016 Kumamoto Earthquakes have been occurring across Mid-Kyushu, the junction of the SW Japan Arc and the Ryukyu Arc. Tectonic elements of both arcs therefore should be taken in account for our understanding of the tectonic background of the earthquakes. In this study, the roles of tectonic elements of the SW Japan Arc and the Ryukyu Arc in the tectonics of Kyushu were estimated using geodesic observations (GEONET, GSI), anisotropy of Vs in the uppermost mantle (Shimizu, 1992) and geological structures of Kyushu.
Horizontal displacements of Kyushu with respect to Genkai, Saga at the back arc coast in northwest Kyushu were examined. On this projection, observation points around Kumamoto migrate west-southwestward. The migration directions rotate counterclockwise to turn southwestward at the south of Kumamoto. The directions of horizontal displacements are similar to those of major tectonic lines such as the Usuki-Yatsushiro Line and the Butsuzo Line. Anisotropy of V_s in the uppermost mantle (Shimizu, 1992) is also oriented to an NE-SW direction around Amakusa and Shimabara. The directions of horizontal migrations significantly change on a line connecting Hokusatsu, Kirishima and Nichinan, striking to the NW-SE direction. The part of Kyushu at the south of this line migrates southward. At Hokusatsu, the Butsuzo line changes its direction form NE-SW to N-S, which is called “the Hokusatsu Bend”. The horizontal displacements with respect to Genkai therefore are consistent with geological and seismological observations of Kyushu, which indicates that the projection would represent the tectonics of Kyushu. Around Kumamoto, the Futagawa Fault, one of the earthquake source faults, is oriented to an NE-SW direction, whereas horizontal displacements are oriented to west-southwestward, which would have accumulate horizontal compressive stress created by the strike-slip activity of the fault to cause the earthquakes.
The SW Japan Arc, such as the Chugoku-Shikoku district migrates northwestward. On the other hand, the Ryukyu Arc migrates southward. The southward component in horizontal displacements of Kyushu therefore represents the deformation element of the Ryukyu Arc. The conjunction of the northwestward deformation element of the SW Japan Arc and the southward deformation element of the Ryukyu Arc would create complex tectonics in Kyushu. The oblique relationship between zonal geological structures and horizontal displacements would make the tectonic of Kyushu more complicated.
The direction of horizontal displacements rotates counterclockwise at the south of Kumamoto, which indicate that not simple strike-slip tectonics but “rotation tectonics” occurs there. Nichinan in southeast Kyushu, horizontal displacements there are relatively small, is the pivot of this rotation. Bathymetric features (Okino, 2015) and seismic observations (Nishizawa et al., 2009) indicate that the subducting Kyushu-Palau Ridge would extend there and obstruct the southward migration. The subducting Kyushu-Palau Ridge therefore would be one of important factors of the rotation tectonics in Kyushu.

Keywords: The 2016 Kumamoto Earthquakes, arc junction, The Southwest Japan Arc, The Ryukyu Arc, The Kyushu-Palau Ridge, tectonics

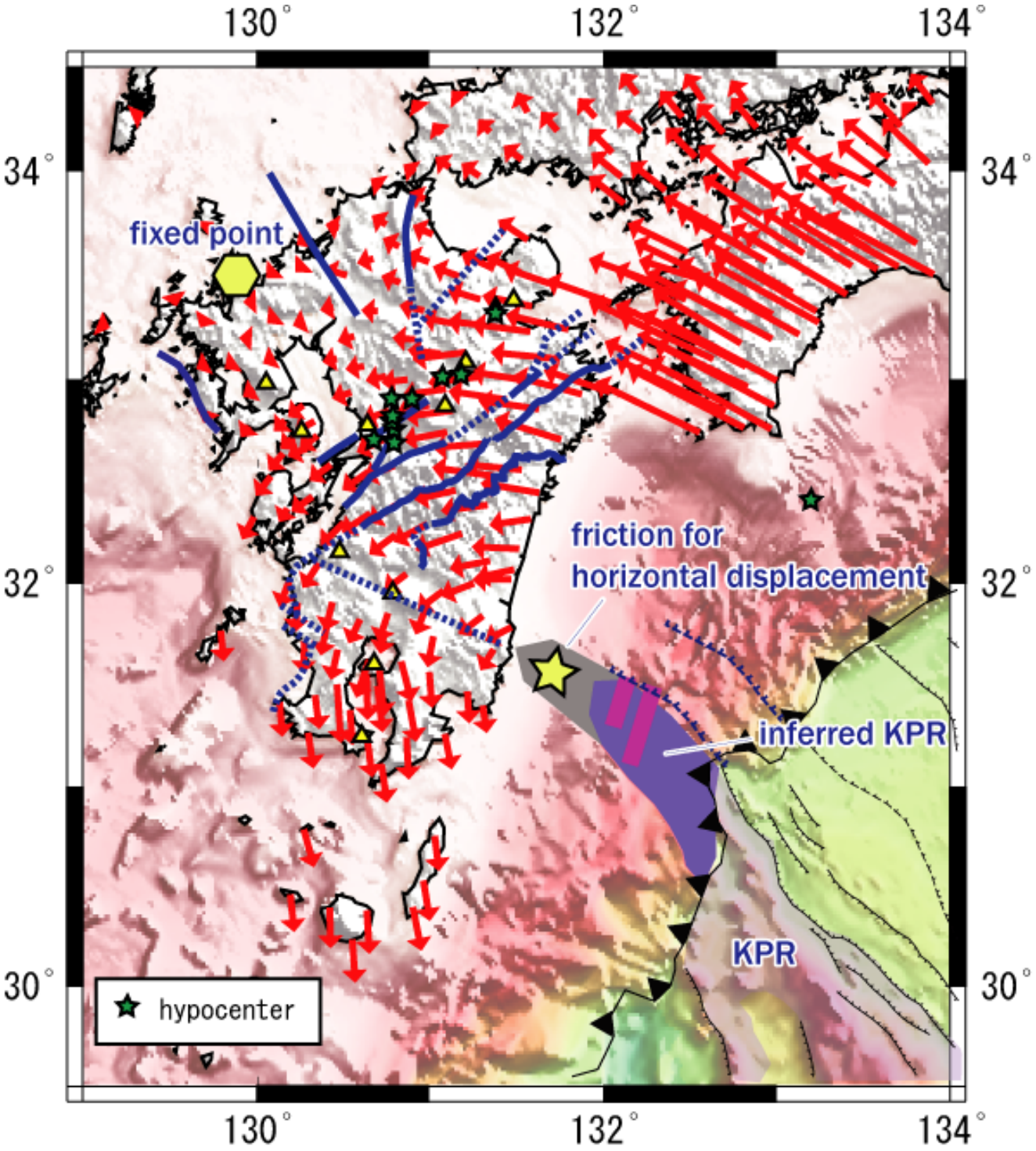

Crustal deformation at the shear zone of the southern part of Kyushu region accompanied with the 2016 Kumamoto earthquake (Preliminary report)

*Tsuyoshi Watanabe[1], Koichi Asamori[1], Koji Umeda[2], Hiroki Amamiya[1], Katsuhiro Nomura[1], Noboru Nakatsuka[1]

1.Tono Geoscience Center, Japan Atomic Energy Agency, 2.Graduate School of Science and Technology, Hirosaki University

From an estimation of strain rate using the recent GPS crustal velocities, two remarkable regions with high shear strain rate of the $1.0x10^{-7}$/yr order exist in the Kyushu district (Wallace et al., 2009). The first region spreads out from Iyo Nada to the sea of Ariake with 60 km in width and 120 km in length. The region contains major active faults such as the Beppu-Haneyama fault zone and the Futagawa fault zone, which corresponds to the northern part of the Shimabara-Beppu rift zone. The 2016 Kumamoto earthquakes seemed to be occurring at the distal area the first region with the high shear strain rate. The second region cuts through the Kyushu district along latitude 32 degrees north with 30 km in width and 120 km in length. We call this region a shear zone of the southern part of Kyushu region, where active left-lateral crustal deformation is detected by GPS observations and it is going on. Although the focal areas of the 1997 Northwest Kagoshima earthquakes (M6.6, M6.4) are included in the shear zone, the existence of active faults corresponding to those seismic activities and to the high shear strain rate is unrevealed till now. Therefore, in order to develop the numerical modeling techniques for crustal deformation, we started GNSS observation at 10 sites in February or March in 2016. Then, we investigate crustal deformation precisely and clarify the formation process of the high shear strain rate zone. On April 14 and 16, about one month after the observation started, the earthquakes with M6.5 and M7.3 continuously occurred at the Kumamoto region. We could detect the southward co-seismic displacement of approximately 6 cm accompanied with the M7.3 earthquake at a GNSS sites about 60 km away from the epicenter of the earthquake. In this study, we show the preliminary result of the GNSS observation. Then, we estimate the strain rate using the GEONET F3 solution provided by the Geospatial Information Authority of Japan and discuss spatiotemporal variation of strain rate before and after the earthquakes and the income and outgo of elastic strain in the Kyushu district. In addition, based on the result of geological strain rate using the active fault database of the National Institute of Advanced Industrial Science and Technology, we compare the strain rates in geological time scale and those in geodetic time scale and discuss the deformation process of the upper crust in the region.

Reference

Wallace et al. (2009): Enigmatic, highly active left-lateral shear zone in southwest Japan explained by aseismic ridge collision, Geology, vol.37, 2009, pp.143-146.

This study was carried out under a contract with Agency of Natural Resources and Energy (ANRE), a part of Ministry of Economy, Trade and Industry (METI) of Japan as a part of its R&D supporting program for developing technology of geological disposal of high-level radioactive waste. We used GEONET F3 solution provided by the Geospatial Information Authority of Japan, the active fault database of the National Institute of Advanced Industrial Science and Technology, and RTKLIB ver. 2.4.3 (RTKLIB: An open source program package for GNSS positioning developed by T. Takasu, Tokyo University of Marine Science and Technology) for the analysis. In addition, we hope people suffered from the 2016 Kumamoto earthquake will make a swift recovery.

Keywords: shear zone of the southern part of the Kyushu region, spatiotemporal variation of strain rate, geodetic strain rate, geological strain rate

Co- and post-seismic displacements due to the 2016 Kumamoto earthquake observed by GEONET

*Satoshi Kawamoto[1], Yohei Hiyama[1], GSI GEONET group[1]

1.Geospatial Information Authority of Japan

The 2016 Kumamoto earthquake (M 7.3) occurred at 01:25 JST on 16 April 2016, and two large foreshocks (M6.5, M6.4) occurred at 21:26 JST on 14 April and 00:03 JST on 15 April, respectively, damaging a wide area around Kumamoto prefecture. The geospatial Information Authority of Japan (GSI) operates the nationwide GNSS network GEONET, which consists of about 1,300 GNSS stations with the average spacing of 20 km. We report the preliminary estimates of co- and post-seismic displacements due to the Kumamoto earthquake using GEONET data.
The GEONET data are processed with three kinds of routine analyses: F3 (24-hour session), R3 (24-hour session), and Q3 (6-hour session). Since two foreshocks on April 14 occurred consecutively within three hours, the coseismic displacements could not be detected from the routine analyses separately. Therefore, an emergency analysis (S3) for static solutions with arbitrary session length, and GEONET real-time analysis (REGARD), which offers 1 Hz kinematic solutions, were also used to detect the coseismic deformations.
Clear coseismic displacements due to the Kumamoto earthquake were observed: NE displacement of 20 cm and subsidence of 3 cm was found at site 1071 near the Hinagu fault during the two foreshocks. NE displacement of 75 cm and subsidence of 20 cm, and SW displacement of 97 cm and uplift of 28 cm were detected just after the mainshock at sites 0465 and 0701, which are located near the Futagawa fault, respectively (Figure). Postseismic deformation up to 3 cm also has been observed, showing a roughly similar deformation pattern to those associated with the mainshock.
The results implicate that the two foreshocks occurred at the Hinagu fault, and the mainshock occurred at Futagawa fault. Especially, the observed displacements indicate that the mainshock ruptured from the epicenter to east with a lower dip angle compared to the foresocks. We plan to investigate the fault slips for the sequence of the earthquakes and continue to monitor the postseismic deformation.

Keywords: The 2016 Kumamoto earthquake, GEONET, crustal deformation, Kinematic GNSS analysis

暫定

平成28年４月16日の熊本県熊本地方の地震(M7.3)(暫定値)前後の観測データ（１）
地殻変動(水平)

基準期間:2016/04/15 03:00～2016/04/15 23:59[Q3:迅速解]
比較期間:2016/04/16 02:00～2016/04/16 05:59[S3:迅速解]

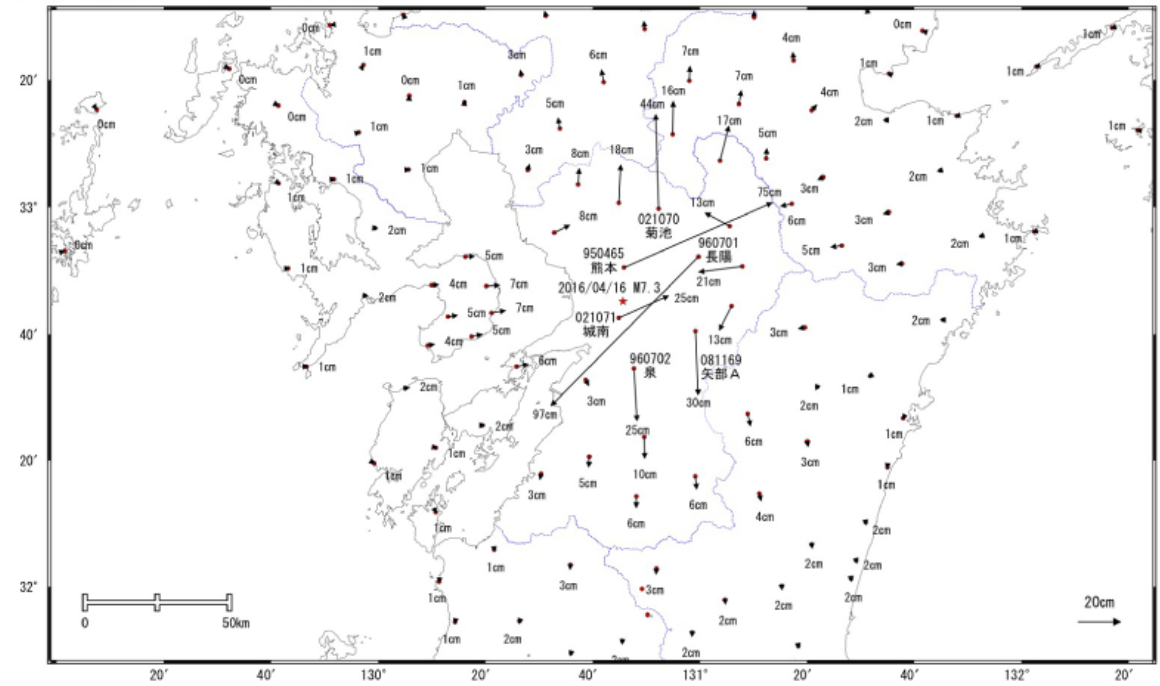

☆ 固定局:福江(950462)

国土地理院

暫定

平成28年４月16日の熊本県熊本地方の地震(M7.3)(暫定値)前後の観測データ（２）
地殻変動(上下)

基準期間:2016/04/15 03:00～2016/04/15 23:59[Q3:迅速解]
比較期間:2016/04/16 02:00～2016/04/16 05:59[S3:迅速解]

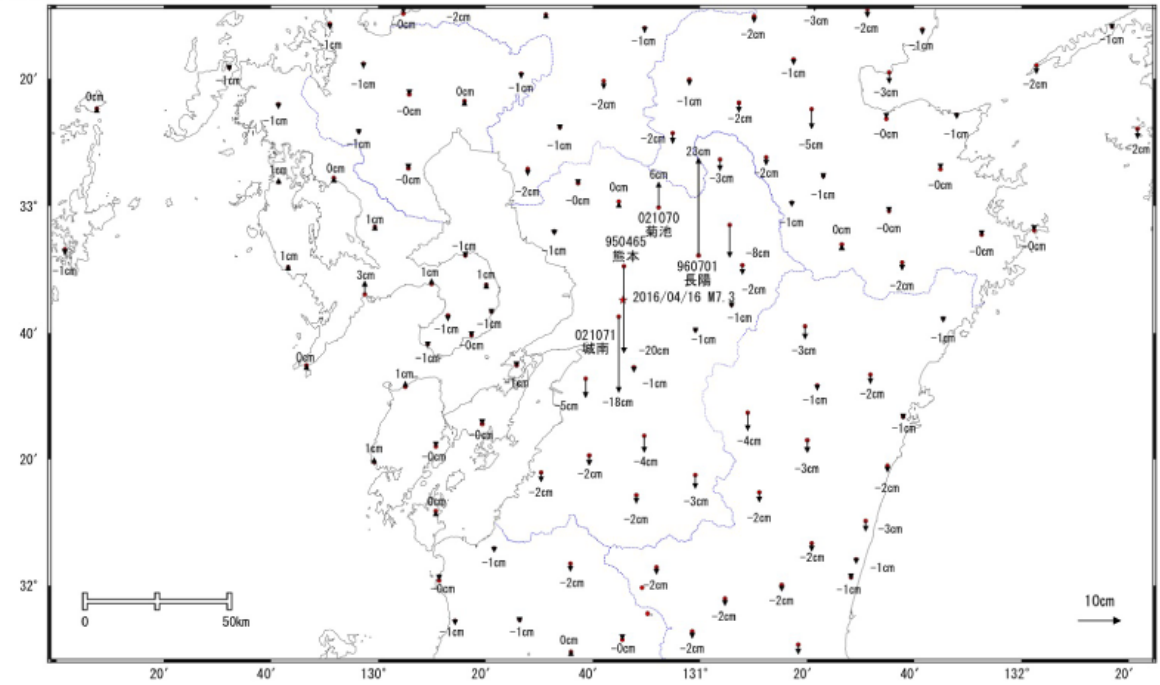

☆ 固定局:福江(950462)

国土地理院

Analysis of Crustal Defomations of Kumamoto Earthquake Obtained by JISLaD System Using GEONET Observation Data

*Seiichi Shimada[1], Yohei Shinde[2], Hirokazu Itoh[2], Kazuyuki Ukei[2], Mikio Sueno[3]

1.Graduate School of Frontier Sciences, University of Tokyo Nippo Co. Ltd., 2.Nippo Co. Ltd., 3.Cal System Co. Ltd.

Introduction

We have developed the every-day automated analyzing system of all GEONET network sites, and have been analyzing GEONET observation data (RINEX data) since 2008 in Nippo Co. Ltd., and obtained daily and weekly coordinate solutions of all GEONET sites (Shimada et al., 2008, 2009, 2013, 2015). Moreover we have developed the Japanese Information System of Land Deformations (JISLaD) applying the GEONET coordinate solutions above obtained, and monitoring time variations of baseline lengths and crustal strains of the nationwide GEONET observation network (Itoh et al., 2015; Ukei et al. 2015a, 2015b).

Applying JISLad System, we deduced crustal deformations of the largest foreshock (M6.5) occurred at 21:26, April 14, 2016 (JST) by the fault movement in the northern part of Hinagu fault system, and the main shock (M7.3) occurred at 1:25, April 16, 2016 (JST) by the fault movement in Futagawa fault system.

In our system, we analyze routinely 24-hourly GEONET RINEX data from 0:00 to 23:59 UTC and obtain daily and weekly coordinate solutions. In the Kumamoto Earthquake, the main shock occurred 28 hour after the largest foreshock, but it is not possible to obtain daily solution routinely that do not include both the largest foreshock and the main shock, thus we manually analyze 24-hourly RINEX data from 13:00, April 14 UT (22:00, April 14 JST) to 12:59, April 15 UT (21:59, April 15 JST), and obtained the daily coordinate solutions which do not include the largest foreshock nor the main shock co-seismic deformations.

Co-seismic deformation

Using the weekly coordinate solution during April 7 and 13 before the largest foreshock, the daily coordinate solution between the largest foreshock and the main shock mentioned above, and the weekly coordinate solution during April 16 and 22 after the main shock, we obtained the co-seismic horizontal and vertical movements around the epicenters of the largest foreshock and the main shock.

In the co-seismic movement of the largest foreshock, the GEONET Johnan site (021071 site) west of the Hinagu fault moves 27 cm NNE and 5mm subsidence. The Kumamoto site (950465 site) north of the fault moves 12cm NNW and 3cm uplift. Those co-seismic movements are consistent with the theoretical movements when the northern part of the Hinagu fault moves right-lateral strike-slip.

Next in the co-seismic movement of the main shock, the Choyo site (960701 site) near northeast end of the Futagawa fault moves 99 cm SW and 25cm uplift. The Kumamoto site (950465 site) north of the southwest end of the fault moves 76 cm ENE and 19cm subsidence. The Johnan site (021071 site) south of the southwest end of the fault moves 28 cm ENE and 19cm subsidence. Three sites east of the fault move 21cm –13cm WNW to SW and maximum 9cm subsidence. The other sites north of the fault move almost north, and the sites south of the faults south in general. Those movements are generally coincided with the preliminary result of the co-seismic movement of the main shock released by Geospatial Information Authority of Japan (GSI).

Dilatational strain

We reduce triangulation network of the GEONET sites that does not contain the triangle across the seism generic fault both in the largest foreshock and the main shock, and calculate the distribution of the dilatational strain.
Both for the largest foreshock and the main shock, the distribution of the dilatational strain is consistent with those expected from the right-lateral strike slip, but the pattern does not show the representative one calculated from the theoretical dislocation theory.

Discussion and conclusion
The main shock of the Kumamoto earthquake (M7.3) is one of the largest earthquakes occurred by the active faults inland Japanese Islands in the recent 100 years. Moreover the Futagawa and Hinaku fault system locates the central part of Kyushu Island and the GEONET network sites are located surrounding the seism generic faults. However the observed co-seismic motions and the dilatational strain distribution do not show the expected clean pattern of the right lateral strike slip. This is caused by the fewer in number of the network site, spacing 10km-20km interval between the sites in this region. For the advanced study of inland earthquakes applying GEONET network, densification of the network sites (at least spacing of equal or less than 10km interval between sites) is thought to be necessary.

Keywords: GEONET network, co-seismic motion, dilatational strain, JISLaD

Crustal deformation observation after occurrence of 2016 Kumamoto Earthquake by GNSS

*Shigeru Nakao[1], Takeshi Matsushima[2], Takao Tabei[3], Tadashi Yamashina[4], Takahiro Ohkura[5], Takuya NISHIMURA[6], Takuo Shibutani[6], Masahiro Teraishi[6], Takeo Ito[7], Takeshi Sagiya[8], Kenjiro Matsuhiro[7], Teruyuki Kato[9], Jun'ichi Fukuda[9], Atsushi Watanabe[9], Satoshi Miura[10], Yusaku Ohta[10], Tomotsugu Demachi[10], Hiroaki Takahashi[11], Mako Ohzono[11], Teruhiro Yamaguchi[11], Okada Kazumi[11]

1.Department of Earth and Environmental Sciences, Graduate School of Science and Engineering, Kagoshima University, 2. Institute of Seismology and Volcanology, Faculty of Sciences, Kyushu University, 3.Department of Applied Science Department, Faculty of Science, Kochi University, 4.Kochi Earthquake Observatory, Faculty of Science ,Kochi University, 5.Aso Volcanological Laboratory, Institute for Geothermal Sciences, Graduate School of Science, Kyoto University, 6.Disaster Prevention Research Institute, Kyoto University, 7.Earthquake and Volcano Research Center, Graduate School of Environmental Studies, Nagoya University, 8.Disaster Mitigation Research Center, Nagoya University, 9.Earthquake Research Institute, University of Tokyo, 10.Research Center for Prediction of Earthquakes and Volcanic Eruptions, Graduate School of Science, Tohoku University, 11.Institute of Seismology and Valcanology, Graduate School of Science, Hokkaido University

The earthquake (M 6.5) occurred on April 14, 2016. Hokkaido and Kagoshima University settled a continuous GNSS observation site. 2016 Kumamoto earthquake (M 7.1) occurred on April 16 and after the occurrence earthquake activity enlarged to northern region of Aso volcano and central part of Ohita prefecture. Our group started settlement of the continuous GNSS observation site in aftershock area of main shock, around Aso volcano and central Ohita prefecture. Our aims of observation are observation of post-seismic deformation and relationship between seismic activity and crustal deformation.

Twenty-one GNSS sites have been set up by April 28. There are nine sites in aftershock area, four sites in east area to Aso volcano, four sites in the central Ohita prefecture and three sites in southern part of Hinagu fault system. In four sites of 24 telemetering system also installed. In the other sites data are kept on a GNSS receiver or a small computer.

Bernese GNSS Software Ver. 5.2 is used for GNSS data analysis of our newly sites together with GEONET and JMA GNSS sites for volcanoes in Kyushu for the period from April 15 to May 7, 2016. We used CODE precise ephemerides and CODE Earth rotation parameters until April 30 and CODE rapid solution of ephemerides and Earth rotation parameters for the period from May 1 to 7. The coordinates of the GNSS sites are estimated respect to ITRF2008.

North-east displacement at the sites of western side of Hinagu fault and south-west displacement at the site of eastern side of Hinagu fault are observed. However, in the central part of Ohita prefecture and the southern part of Hinagu fault system it seems that no deformation related to earthquake activity.

GEONET RINEX data and RINEX data of Volcanoes' observation site of JMA are used. This study was supported by the Ministry of Education, Culture, Sports, Science and Technology (MEXT) of Japan, under its Earthquake and Volcano Hazards Observation and Research Program and Grants-in-Aid for Scientific Research (KAKENHI, Grant Number 16H06298) .

Keywords: GNSS observation, post-seismic deformation

Co-seismic displacements of the 2016 Kumamoto Earthquake derived from GNSS Campaign measurements

*Takeshi Matsushima[1], Yoshiko Teguri[1], Shigeru Nakao[2], Hiroshi Shimizu[1], Satoshi Matsumoto[1], Manami Nakamoto[1], Kazunari Uchida[1]

1.Institute of Seismology and Volcanology, Faculty of Sciences, Kyushu University, 2.Department of Earth and Environmental Sciences, Graduate School of Science and Engineering, Kagoshima University

Since October 1999, small-earthquake activity has been detected in the Futagawa and Hinagu fault zones. In particular, in June 2000 an earthquake of magnitude 4.8 occured in the northern end of Hinagu fault, and JMA intensity 5- was recorded in the surrounding area.
In order to reveale the presence or absence of a creep movement in the deeper area of Hinagu fault, and to obtain the knowledge of the loading process of the fault, we set the west-northwest to east-southeast survery line of about 30km which is perpendicular to the Futagawa fault. We set the reference point of the 11 places on the survey line. We started the Campaign observation from 2000. The reference point, the antenna was fixed using a wooden tripod, and acquires data of 2-3 days per point. The most recent measurement was February 2010, but after the 2016 Kumamoto earthquake occurred, we carried out the re-measurement hurriedly.
The Precise Point Positioning mode of GIPSY- OASIS version 6.4 and the JPL final almanac file was used in the process.
At the continuous observation point (MRTK and GEONET), the co-seismic crustal displacement of Kumamoto earthquake that occurred on April 14 to 16, 2016, the difference vector between the average value of each of the five days of the coordinates of the April 1-5 and April 23-27, 2016. For the campaign observation, the observation vector includes the secure movement for 6 years since 2010 and besides the co-seismic movement. Therefore the average value between the early April, 2010 and in early April, 2016, crustal movement vector obtained by the GEONET observation points around is assumed to be secure crustal movements in the region.
Co-seismic crustal movement vectors were show in the figure. (1) The largest vector of 50 cm was found in our observation. The small vector was found just along the active fault zone, because the rupture of Hinagu fault was not reached to the earth surface. (2) The displacement was limited tn the northern segment of the Hinagu fault. (3) The earthquake source fault of the underground was shifted to 1~2km west side of the active faults that have been traced at the surface.
Also the central and southern segment of the Hinagu fault, which lies on the south of our survey line, does not release the strain, there is a possibility that large earthquakes future occur.

Keywords: The 2016 Kumamoto Earthquake, The Futagawa and Hinagu Fault Zones, Crustal Displacement, GNSS

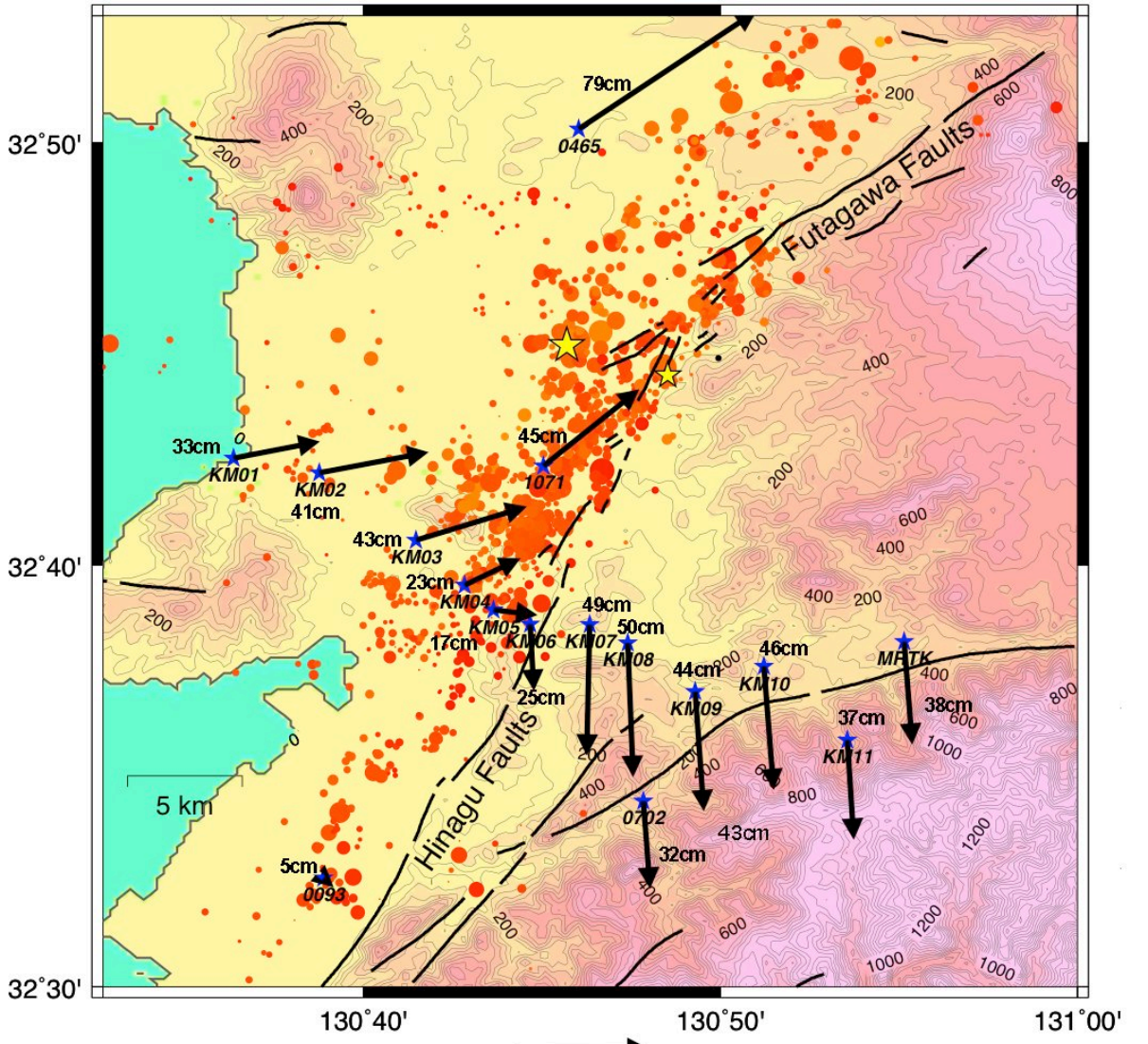

Campaign観測点（KM01- KM11)
測定1：2010年2月 7～12日
測定2：2016年4月23～27日
連続観測点(MRTK)およびGEONET
測定1：2016年4月 1～5日
測定2：2016年4月23～27日

固定点：IGS点　解析:GIPSY 6.4　暦：JPL Final

Campaign観測点については，2010年2月から2016年4月上旬の間の定常的な地殻変動を周囲のGEONET観測点から推定し，測定値から差引いている．

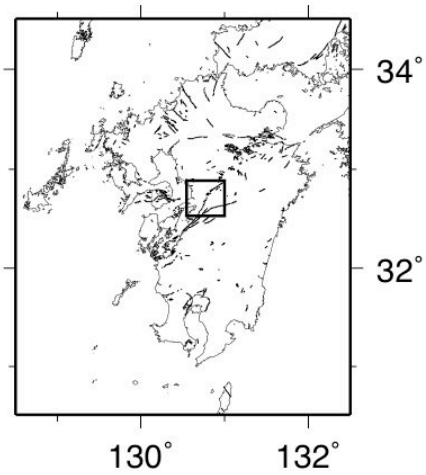

Spatio-temporal strain change around the 2016 Kumamoto earthquakes observed by GEONET data

*Mako Ohzono[1], Hiroaki Takahashi[1]

1.Institute of Seismology and Volcanology, Graduate School of Science, Hokkaido University

We analyzed GEONET data to estimate coseismic strain field induced by three large earthquakes over Mj6.0 (Mj6.5 on 14 April, Mj6.4 on 15 April, and Mj 7.3 on 16 April). First two earthquakes took place several ppm strain around the source area with a pattern of right lateral faulting along the Hinagu active fault. On the other hand, Mj 7.3 earthquake induced ~100 ppm of areal strain and ~40 ppm of right lateral maximum shear strain around the hypocenter on the Futagawa active fault. In order to explain the coseismic strain field, we estimate coseismic fault assuming a slip of simple rectangular fault in the half-space elastic media. The estimated fault corresponds to Mw6.96 with a length of 26 km and width of 10 km along the Futagawa active fault. Although the calculated strain field roughly explains observed data, residuals of several cm displacements and several ppm strains are remaining near the hypocenter. Our rectangular fault may be too simple to explain the more complex fault slip distribution. Anomaly of the coseismic strain field around the aftershock area is not appear from those residuals at this moment.

Acknowledgment: This study was supported by the Ministry of Education, Culture, Sports, Science and Technology (MEXT) of Japan, under its Earthquake and Volcano Hazards Observation and Research Program.

A crustal deformation model for central Kyushu with a graben area represented by dislocation

*Kazuma Mochizuki[1], Yuta Mitsui[1], Shunsuke Morikami[1]

1.Department of Geosciences, Shizuoka University

The 2016 Kumamoto earthquakes, including an Mw 7 earthquake on April 15 (UTC) and previous two Mw 6 earthquakes, have struck central Kyushu region, Japan. These earthquakes have been considered to occur at right-lateral strike-slip faults. First, we confirm this result by GNSS data analyses at a sampling rate of 30 seconds using a kinematic PPP method.

On the other hand, the epicenters of the 2016 Kumamoto earthquakes were located within a graben area (N-S extension), named as the Beppu-Shimabara graben. Truly the aftershocks and induced earthquakes were composed of right-lateral strike-slip earthquakes and normal-fault earthquakes. We should consider both components when discussing the sources of the crustal deformation in this area.

In this study, we estimate stationary deformation rates at GEONET stations in central Kyushu using three-direction (both horizontal and vertical) GNSS data of the F3 solution during 2000-2010. We observed stationary subsidence at several millimeters per year in the graben area.

On the basis of the observation, we set block boundaries with tracing surface faults. We assume elastic dislocations on the boundaries other than rigid motion of the blocks. We interpret the rifting zone in the graben area as a reverse of collision zone, where the collision zone can be represented by a vertical dislocation with a tensile component (Shimazaki and Zhao, 2000). In addition, we model elastic deformation due to subduction of the Philippine sea plate and magma accumulation beneath several volcanos (Mt. Aso, Kuju, Unzen).

We invert the deformation rates of the above components from the Green's function and the estimated stationary deformation rates, using a least-square method with singular value decomposition (the same method as SSS32-01 in this meeting). At present, we obtained stable solutions for all the components, for instance, back-slip rates over 1 cm/yr at the source faults of the 2016 Kumamoto earthquake and compression of the magma reservoirs about 10^6 m^3/yr beneath the volcanos.

Keywords: Kumamoto earthquake, Crustal deformation, Graben area

Fault activities and their relations to volcanoes in the 2016 Kumamoto earthquake: Insight from InSAR analysis and field observations

*Takeshi Tsuji[1], Kazuya Ishitsuka[2], Tatsunori Ikeda[1], Toshifumi Matsuoka[2]

1.Kyushu University, 2.Fukada Geological Institute

We investigate fault activities during the 2016 Kumamoto earthquake and heterogeneities at the boundary of fault segmentation (or edge of earthquake faults) from field observations, satellite data analyses and seismic data analyses. The fault activities in the Kumamoto earthquake sequence can be clearly identified on the surface deformations from Interferometric SAR (InSAR). We conducted field observations based on the surface deformation derived from InSAR. We mainly focus on the complex fault movements around the Mt Aso. In the results of InSAR analyses, the fault trace can be clearly identified as NE-SW lineament across western part of Kyushu Island (from Kumamoto to Mt Aso), but the fault ruptures are locally influenced by geologic heterogeneity, such as volcano. Before the mainshock (M7.3) on 16 April, the fault system at southwest of Mt Aso was ruptured, and the fault rupture was terminated around Mt Aso. The right lateral slip motion generated extension around Mt Aso region and compression around the Ohtsu-machi northwest of Mt Aso (northern side of the right lateral fault). Indeed, Mt Aso (inside its caldera) largely subsided. Because the large subsidence area roughly corresponds to the predicted magma chamber, the subsidence within caldera could be partially due to extension of magma. Extension of the magmatic body at active volcano was also reported in the 2011 Tohoku earthquake. In the field observations, we identified large fissures in the subsidence area maybe due to the extension. The width of fissures is ~1m, and their strike is NE-SW. On the other hand, several sequential fault movements were observed in the Ohtsu-machi, and there is a possibility that the fault mechanism was reverse motion. In the field observation, we could not identify lateral motion at the fault traces. The interpreted reverse faults could be generated due to compressional stress because the fault rupture rapidly halted at the volcanic body of Mt. Aso.
At the earthquake at Aso region (M5.6) occurred after the mainshock (3:55 on 16 April), rupture region moves to further northeast and terminated around Mt Kuju. At the southwest of Mt. Kuju, we observed linear surface deformation due to fault movement. Because the source mechanisms at Kumamoto-Aso-Kuju region (strike-slip motion) and fault system at Oita region (normal motion; M5.8) are different, the volcanic body of Mt Kuju works as the boundary of tectonic stress.
These results demonstrate that the volcanoes (Mt Aso and Kuju) could work as segmentation boundary of the earthquake rupture. The stiffness of the volcanic body or deposit is different from other regions, and the temperature anomaly influencing frictional property along the fault is abnormally high around the volcano.

Keywords: Field observations in 2016 Kumamoto earthquake, Interferometric SAR, Earthquake and volcano

Detection of crustal deformation signal and fault dislocation model associated with 2016 Kumamoto earthquake:Preliminary report by space geodesy laboratory in Hokkaido university

*Yuji Himematsu[1], Takahiro Abe[1], Takatoshi Yasuda[2], Masato Furuya[2]

1.Department of Natural History Sciences, Hokkaido University, 2.Department of Earth and Planetary Sciences, Hokkaido University

Three M>6 earthquakes occurred on 14th April (12:26:41.1 GMT, Mw 6.2 [Mj 6.5] and 15:03:50.6 GMT, Mw 6.0 [Mj 6.4]) as foreshocks and 15th April (16:25:15.7 GMT) as main shock (Mw 7.0 [Mj 7.3]) in Kumamoto prefecture along Beppu-Shimabara rift system. These focal mechanisms have been reported right-lateral with NE-SW striking. Epicenters during this event concentrated along the Beppu-Shimabara rift system dividing Kyusyu region. The Beppu-shimabara rift system is located from Beppe bay in Oita prefecture to Shimabara peninsula in Nagasaki prefecture via Yatsushiro bay in Kumamoto prefecture, and western part of the rift system is linking to the Okinawa trough. The rift system is one of the active geothermal area including Kyujyu volcanic system, Mt. Aso, Mt. Unzen. Although the mechanism of constructing the rift system is uncertain, some mechanisms are assumed to be pull apart basin, which is constructing under N-S extension field with right-lateral, and continental pull apart, which is influenced by mantle flow.
GSI (Geospatial Information Authority of Japan) group have already reported on their website that signals of crustal deformation associated with the event using InSAR and MAI. These results have indicated deformation field caused by right-lateral slip and >30 cm subsidence at Mt. Aso. We have applied PALSAR-2 data spanning 2016 Kumamoto earthquake to InSAR and offset tracking in order to obtain robust crustal deformation signal. These data are sharing with PIXEL (PALSAR interferometry consortium on study our evolving and surface) group. Our results show near-fault 3D displacement field where is lack of data in GSI results, and also show significant shape offset at the Futagawa- and Hinagu-fault belt. We present preliminary fault dislocation model to reproduce our results.

Keywords: Kumamoto earthquake, Synthetic Aperture Radar, Crustal deformation, Rifting system

DInSAR Analysis on regional distribution pattern of surface displacement caused by the 2016 Kumamoto Earthquake

*TAKUMI ONUMA[1]

1.JGI, Inc.

Regional distribution pattern of surface displacement caused by 2016 Kumamoto Earthquake has been delineated by DInSAR analysis of co-seismic Sentinel-1 C-SAR pairs. Sentinel-1 carries C-band SAR sensor of which wavelength is 5.6cm, and covers the area of 250km x 250km by 1 scene of the Interferometric Wide Swath mode with the ground range resolution of 5m and the azimuth resolution of 20m. Recurrent period of the Sentinel-1 is 12 days and the region around Japan has been observed at least once every 2 periods. Twelve days interval data are sometimes available for emergency observation cases such as huge disaster of 2016 Kumamoto earthquake. Thanks to these features the Sentinel-1 is said to be one of the most suitable satellite in broad region monitoring.
Two co-seismic pairs of the Sentinel-1 C-SAR data, acquired on 2016/4/8 and 2016/4/20 on the ascending orbit and of 2016/3/27 and 2016/4/20 on the descending orbit, are used in the study. The results of DInSAR analysis of each pair as well as 2.5-dimensional analysis combining these pairs are introduced. Adding to the Sentinel-1 C-SAR data processing, Multi Aperture Interferometry processing which treats the azimuthal offsets along the flight direction of the satellite was performed using co-seismic pair of ALOS-2 PALSAR-2 data covering the main part of the Futagawa Fault and the Mt. Aso caldera.

Keywords: Satellite SAR Differential Interferometry (DInSAR), Sentinel-1 C-SAR data, regional distribution pattern of surface displacement

Estimation of co-seismic surface displacement and ground deformation associated with the April 2016 Kumamoto Earthquake, based on differential InSAR by Sentinel-1 and differential LiDAR DEM analysis.

*Sakae Mukoyama[1], Kenichi Honda[1], Norichika Asada[1], Takumi Sato[1]

1.KOKUSAI KOGYO CO., LTD.

The 2016 Kumamoto earthquake occurred on April 14 and 15, 2016, along the Futagwa fault and Hinagu fault, in central Kyusyu Island, Japan. We try to reveal location of co-seismic displacement based on InSAR analysis using Sentinel-1 data and high-resolution differential LiDAR DEM.
We used 1 m mesh DEM (Digital Elevation Model) data measured in 2009 (pre-event), 2014 (5 days later from the event), 2015 (about 1 year later from the event), and applied the particle image velocity method to obtain 3-D vectors of coseismic deformation (Mukoyama, 2011). The precision of this method is 0.1 m.
Results show a wide area distribution of ground deformation clealy. Additionally, the result of differential coherence analysis shows distribution of damaged houses and constructions.

Keywords: the 2016 Kumamoto Earthquake, InSAR, Differential DEM Analysis, LiDAR, Image matching analysis

Groups of Surface Faults with Small Displacement of the 2016 Kumamoto Earthquake Detected by ALOS-2 SAR Interferometry

*Satoshi Fujiwara[1], Hiroshi Yarai[1], Tomokazu Kobayashi[1], Yu Morishita[1], Takayuki Nakano[1], Basara Miyahara[1], Hiroyuki Nakai[1], Yuji Miura[1], Haruka Ueshiba[1], Yasuaki kakiage[1], Hiroshi Une[1]

1.GSI of Japan

The 2016 Kumamoto earthquake in Japan caused large crustal deformation, and several exposed faults have been identified by ground survey. We mapped the displacement field on the surface associated with the earthquake using satellite radar interferometry images of ALOS-2 operated by JAXA. The Synthetic Aperture Radar (SAR) interferogram generally shows elastic motion caused by the main earthquakes but many discontinuities of fault like displacements are found.

More than 200 lineaments are found and the position of some lineaments coincides with known active faults, such as the Futagawa fault zone, the Hinagu fault zone and other minor faults, however the number of the lineaments were much more than that of the known active faults. In each area, the lineaments have similar direction and motion each other, then they can be classified into several groups of faults. Since the direction of the lineaments coincides with that of the known active faults or that of their conjugate faults, the cause of the lineaments was related with the tectonic field of this region.

The lineaments are classified into the following several categories; (a) the main earthquake faults and their branched sub-faults, (b) earthquake faults which are not directly related to the main earthquake, (c) landslides and/or creep along geologically weak surfaces caused by the strong earthquake motion.

Keywords: 2016 Kumamoto earthquake, SAR interferometry, Fault

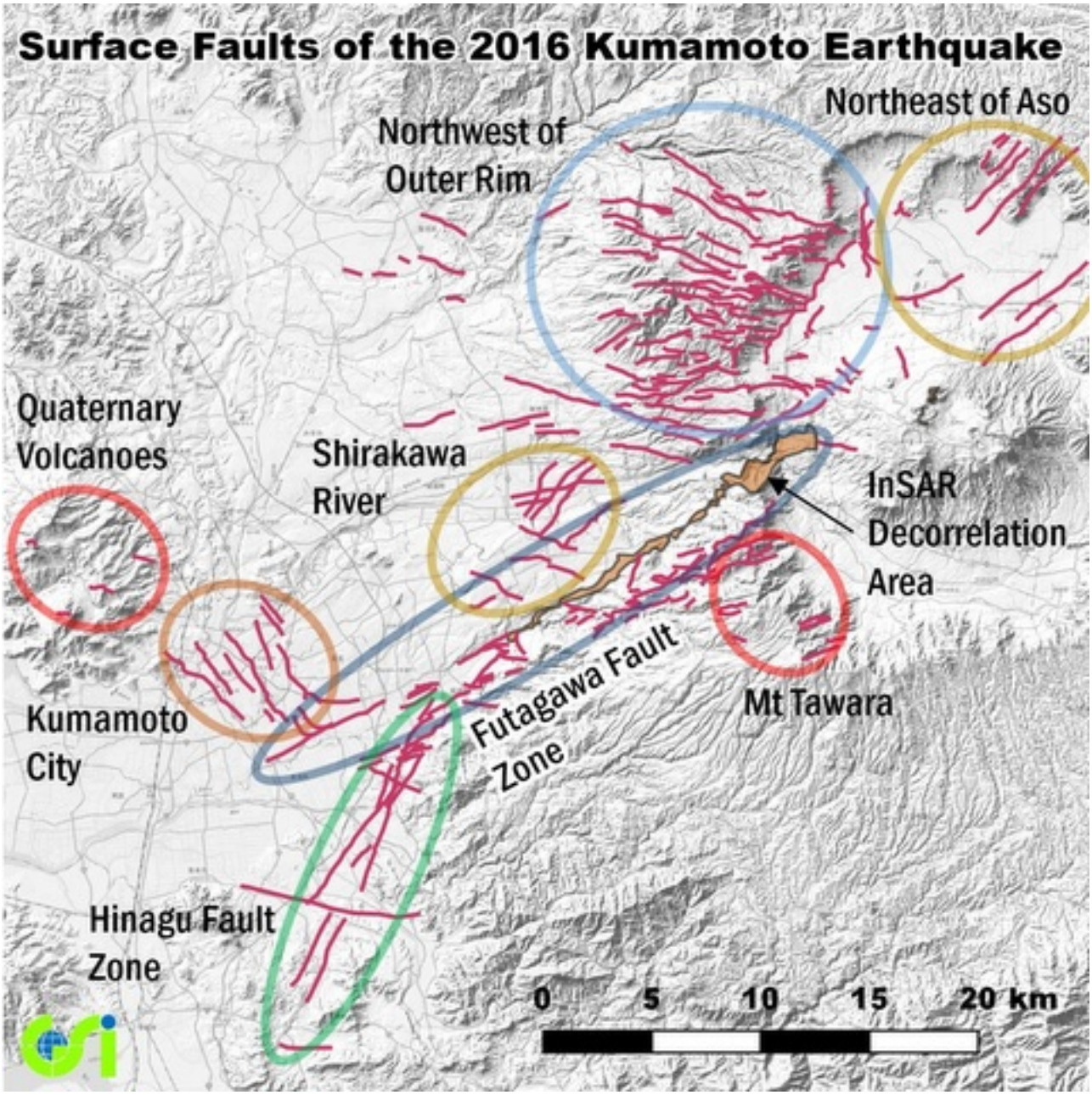

Analysis of the 2016 Kumamoto earthquakes using ALOS-2/PALSAR-2

*Shinobu Ando[1], Okuyama Satoshi[2], Akio Katsumata[1], Kenichi Fujita[1], Koji Tamaribuchi[1]

1.Seismology and Tsunami Research Department, Meteorological Research Institute, 2.Volcanology Research Department, Meteorological Research Institute

An earthquake of M6.5 occurred in Kumamoto Prefecture at 21:26 on April 14, 2016. Following this earthquake, earthquakes occurred at 00:03 on April 15 (M6.4) and at 01:25 on April 16 (M7.3). We report the analysis of such crustal deformation associated with these earthquakes including their aftershocks using the emergency observed data by ALOS-2/PALSAR-2.
There are 13 pairs of data that can be used for InSAR analyses of these earthquakes. One of them is a pair covering foreshocks that occurred on April 14 and 15. There are two pairs covering only the main shock of April 16; three pairs after the main shock; the remaining pair covering both a foreshock and the main shock.
In the image of the pair that contains foreshocks, the southwest area from the two epicenters shows crustal deformation up to 12cm away from satellite in the radar line-of-sight (LOS) direction, displacement up to 9cm toward the satellite can be seen in the northwest area from the epicenter. The simulation pattern of the interferometry fringe, calculated based on source processes of JMA, indicated relatively smaller dip angle fault of NW-dip.
The image of the pair that contains main shock suggests the right-lateral strike-slip fault along the Futagawa fault zone and Hinagu fault zone. Furthermore, more complex phase changes are recognized in the vicinity of the fault zone in the LOS direction.
For some of the pair, we also tried analysis of the intensity image and correlation image. As a result, areas that are assumed to have been heavily damage were detected along the Futagawa fault zone. Details of these analyses are reported together in this poster.
Some of PALSAR-2 data were prepared by the Japan Aerospace Exploration Agency (JAXA) via Geospatial Information Authority of Japan (GSI) as part of the project ‘ALOS-2 Domestic Demonstration on Disaster Management Application’ of the SAR analysis of earthquake Working Group. Also, we used some of PALSAR-2 data that are shared within PALSAR Interferometry Consortium to Study our Evolving Land surface (PIXEL). PALSAR-2 data belongs to JAXA. We would like to thank Dr. Ozawa (NIED) for the use of his RINC software. In the process of the InSAR, we used Digital Ellipsoidal Height Model (DEHM) based on ‘the digital elevation map 10m-mesh’ provided by GSI, and Generic Mapping Tools (P.Wessel and W.H.F.Smith, 1999) to prepare illustrations.

Keywords: the 2016 Kumamoto earthquake, ALOS-2/PALSAR-2, InSAR

Relataion between the 2016 Kumamoto earthquake-induced landslide distribution and surface deformation detected by ALOS-2/PALSAR-2 data

*Hiroshi, P. Sato[1]

1.College of Humanities and Sciences, Nihon University

In the 2016 Kumamoto earthquake, Japan, preshock (M6.5, on 14 April) and mainshock (M7.3, on 16 April) jolted not only the Kumamoto Plain but also mountain areas. Especially, mainshock induced many landsldie in mountain area of the western part of Aso Volcano. This study focused on the mainshock and tried to find the relation between earthquake-induced surface deformation and landslide distribution. I used ALOS-2/PALSAR-2 ascending and descending orbits data, observed on 15 and 29 April. Both data were observed left side from the orbit, and both are observed in Stripmap mode 1). Specifications of ascending data are beam U1-4, off-nadir angle 21.9 degree; specifications of descending data are beam U2-6, off-nadir angle 29.1 degree, according to JAXA. I produced images of SAR interferometry for both orbits data, and performed 2.5D analysis (Geospatial Information Authority of Japan, 2016) to detect surface deformation using both images of SAR interferometry. Then I overlayed landslide inventory data (Chigira and Matsushi, 2016) on the EW (east-west) and UD (up-down) components of surface deformation data. I found that the area where surface was remarkablly deformed was coincident with the area where landslides occurred.

References
Chigira M and Matsushi U (2016): Condition of slope failures by the 2016 Kumamoto earthquake (Report No.2).
http://www.slope.dpri.kyoto-u.ac.jp/disaster_reports/2016KumamotoEq/2016KumamotoEq2.html
Geospatial Information Authority of Japan (2016) : Result of 2.5D analysis for surface deformation triggered by the 2016 Kumamoto earthauake.
http://www.gsi.go.jp

Keywords: earthquake, landslide, slope, Kumamoto, SAR, PALSAR-2

Crustal deformation associated with the 2016 Kumamoto Earthquake and its effect on the magma chamber of Aso volcano

*Taku Ozawa[1], Eisuke Fujita[1], Hideki Ueda[1]

1.National Research Institute for Earth Science and Disasters

The Mj6.5 earthquake (foreshock) struck the Kumamoto Prefecture on 14 Apr. 2016, and the Mj7.3 earthquake (mainshock) followed it on 16 Apr. 2016. Aso volcano which is recently active is located to east of their epicenters, and then it is concerned that the earthquake affects its volcanic activity. In this study, we derived fault models from crustal deformations obtained by InSAR analysis and estimated the effect of crustal deformation on the magma chamber of Aso volcano based on their models.

To detect crustal deformation, we used InSAR analysis with ALOS-2/PALSAR-2 data. In the period between the foreshock and the mainshock, a left-looking observation from descending orbit (observation from west sky) was carried out. We analyzed it with data observed before the earthquake and detected slant-range shortening and extension area to the west of the Hinagu Fault. This slant-range change distribution could be explained by 1m right-lateral slip in the fault with the strike which is the same to that of the Hinagu Fault. After the mainshock occurrence, several PALSAR-2 observations were carried out from various directions, and we analyzed PALSAR-2 data observed from six orbit tracks for the mainshock investigation. In all results, discontinuity of slant-range change along the Futagawa Fault was identified, indicating the main fault for this earthquake. Furthermore, steep gradient of slant-range change was also identified along the Hinagu Fault and east extension of the Futagawa Fault. Especially, it seems that the strike of east extension of the Futagawa Fault changes to northeast direction. Analysis of observed SAR data from east sky derived slant-range shortening in north of the Futagawa Fault and slant-range extension in south. On the other hand, results of SAR data from west sky showed opposite results. Such deformation can be roughly explained by right-lateral slip of the fault. However, slant-range change distribution is more complex; for example, slant-range extension was obtained in both sides of the fault around Nishihara village. We found that their slant-range changes could be reasonably explained by a model with four faults (F1-F4). F1 and F2 are along the Hinagu and the Futagawa Faults, and F3 corresponds to extension from the east end of the Futagawa Fault. Their faults have almost right-lateral slip. F4 was estimated under the Nishihara village and its rake angle was about 250 deg., including normal dip-slip component. From analysis of InSAR pair which didn't include mainshock occurrence time, local deformation along the fault was obtained, but obvious deformation associated with volcanic activity was not identified. At the time of this paper submission, the observation data of the volcano observation network (V-net) of NIED do not show significant change in volcanic activity of Aso Volcano.

Based on the revealed seismic fault models, we calculated the displacement and stress field around Aso volcano by FEM method to evaluate the effects on Aso magma plumbing system. Disturbances due to seismic faults are categorized into three types, i.e., static, quasi-static and dynamic effects, here we consider only static ones as a preliminary analysis. Suto (2006) suggested a magmatic reservoir at the 6km depth beneath Kusasenri region, in addition, Abe et al. (2010) implicated the sill source at 15km depth. In this evaluation, the estimated fault depths are about 0~10km, therefore, we only assume the shallower magma reservoir. The result shows complex distributions of displacements and stresses, but we can notice the following significant points: 1) the western part of magma reservoir experiences tensional stress about 10MPa toward southwest, 2) the magma reservoir deforms to an ellipsoid elongated to west-east. Displacement around the western part is

about 60cm westward, and the top of reservoir and Aso surface is downward about 10cm.

Keywords: Kumamoto Earthquake, Aso volcano, crustal deformation, Magma chamber

Active fault in Aso area formed at the Kumamoto Earthquake and its relationship with neotectonics in the Southwestern Japan

*hisashi Oiwane[1]

1.Mishimamura Village, Kagoshima Prefecture

I conducted geological survey in the Aso area about the faults that appear at the Kumamoto Earthquakes. I found 10 grabens in Akamizu - Uchinomaki area, which are bounded by ENE-WSW trending normal faults. Lengths of faults are about 100 m and the maximum displacement is ca. 2 m. These grabens compose NNE-SSW trending two segments with en echelon arrangement. Also, ENE-WSW trending grabens are found between the segments.
The arrangement of these grabens shows typical right-lateral strike slip displacement as a whole. It is most likely that these grabens are active fault that activated on the Earthquake. In this presentation, I discuss tectonic background of these a series of fault activities.

Keywords: Kumamoto Earthquake, Okinawa Trough, Beepu-Shimabara graben

Surface Fault Ruptures of the 2016 Kumamoto Earthquake

*Hideaki Goto[1], Yasuhiro Kumahara[1], Takashi Nakata[1], Satoshi Ishiguro[2], Daisuke Ishimura[3], Tatsuya Ishiyama[4], Shinsuke Okada[5], Kyoko Kagohara[6], kashihara shintaro[7], Heitaro Kaneda[7], Nobuhiko Sugito[8], Yasuhiro Suzuki[9], Daishi Takenami[10], Kei Tanaka[11], Tomoki Tanaka[7], Hiroyuki Tsutsumi[12], Shinji Toda[5], Daisuke Hirouchi[13], Nobuhisa Matsuta[10], Hikaru Moriki[10], Haruka Yoshida[14], Mitsuhisa Watanabe[15]

1.Hiroshima University, 2.Aichi Institute of Technology, 3.Tokyo Metropolitan University, 4.University of Tokyo, 5.Tohoku University, 6.Yamaguchi University, 7.Chiba University, 8.Hosei University, 9.Nagoya University, 10.Okayama University, 11.Japan Map Center, 12.Kyoto University, 13.Shinshu University, 14.Fukuoka Prefectural Yame High School, 15.Toyo University

A Mj 6.5 earthquake hit Kumamoto prefecture, central Kyushu, southwest Japan at 21:26 JST on April 14th. 28 hours after, another Mj 7.3 at 01:25 JST on April 16 generated severe shaking in the same region (JMA, 2016). It is well know previously mapped the ~100-km-long active fault called Futagawa-Hinagu fault zone (FHFZ) (Watanabe et al., 1979; RGATK, 1989; Ikeda et al., 2001; Nakata and Imaizumi ed, 2002) runs in the epicentral area, we considered the northeastern portion of the FHFZ could be responsible to two earthquakes and started to do a field reconnaissance along the fault zone after the Mj 6.5 event.

According to 3 weeks field survey by our team, we found the 31-km-length successive surface rupture close to the traces of the northeastern portion of the FHFZ and another the 5-km-length rupture on a part of Denokuchi fault and some possible surface ruptures in the epicentral area. The rupture along the FHFZ shows right-lateral strike-slip mainly (~ 2 m in maximum between Dozon in Mashiki city and Nishihara village) with down-thrown to northwest. The rupture on the Denokuchi fault, far from 1 to 2km east of the FHFZ, is normal component with down to northwest. These coseismic ruptures of the Mj 7.3 earthquake represented a characteristic movement of the northeastern portion of the FHFZ.

A series of the open cracks with NW-SE-trending were traceable for a distance of 5.4 km from Kengun to Shirakawa River in Kumamoto city. Those features followed on tectonic landform by possible active fault and on the line of the fringe abnormal in InSAR image, and may represent minor surface rupture.

The local eyewitness and our observation revealed that the coseismic minor rupture of the Mj 6.5 earthquake prior to the Mj 7.3 earthquake were emerged on the some trace of the rupture of the Mj 7.3 earthquake in Mifune town and South of Mashiki town.

Keywords: 2018 Kumamoto Earthquake, earthquake fault, active fault

Characteristics of the surface ruptures associated with the 2016 Kumamoto earthquake sequence, Kyushu, southwestern Japan

*Yoshiki Shirahama[1], Masayuki Yoshimi[1], Yasuo Awata[1], Tadashi Maruyama[1], Takashi AZUMA[1], Yukari Miyashita[1], Hiroshi Mori[1], Kazutoshi Imanishi[1], Naoto Takeda[1], Tadafumi Ochi[1], Makoto Otsubo[1], Daisuke Asahina[1], Ayumu Miyakawa[1]

1.Geological Survey of Japan, AIST

The Kumamoto earthquake sequence that culminated in the Mj 7.3 event on April 16, 2016, produced the *ca*. 30 km long complex surface ruptures having a predominantly dextral with subordinately normal or reverse slip component along the eastern section of the Futagawa fault zone, the northern section of the Hinagu fault zone and previously unmapped faults including those across the Kiyama plain and across the western caldera rim of the Aso volcano, central Kyushu, Japan. Geological Survey of Japan, AIST, carried out urgent field investigation to explore and measure the surficial deformation associated with the Kumamoto earthquake during two weeks since the day of the mainshock. Our intensive field mapping revealed nature of the surface rupture in detail, including location, geometry, temporal growth and slip distribution of the complex ruptures. The remarkable features of the surface faulting were summarized as follows; i) the rupture zone is generally composed of a series of left-stepping *en echelon* array of discontinuous fault trace with various size; ii) the maximum dextral slip of *ca*. 2.2 m was measured at central part of the rupture zone, whose location and amount is consistent with InSAR analysis; iii) large slip (>1 m) occurred on the previously unrecognized fault traces that extend across the alluvial lowland; iv) slip is accommodated by complex rupture style, such as zigzag-shaped ruptures with ESE-trending dextral slip and NW-trending sinistral slip, slip partitioning that resolves oblique slip into dextral component and vertical component on sub-parallel traces, and widely developed grabens; v) accounts by eyewitnesses and repeated measurements show that part of the surface slip along the Hinagu fault has grown not only between the 14 April earthquake (Mj6.5) and mainshock (16 April) but also after the mainshock.

Keywords: 2016 Kumamoto earthquake, Futagawa fault zone, Hinagu fault zone, surface rupture

Source process of 2016 Kumamoto earthquake viewed from surface fault rupture

*Takashi Nakata[1]

1.Professor Emeritus, Hiroshima University

Source process of 2016 Kumamoto earthquake is discussed based on location and geometry of surface fault rupture. Kumahara et al. (2016) showed branching of fault traces toward north and south around Dozon, Mashiki town, suggesting the source fault ruptures bilateral while the hypocenter of the earthquake locates near-by southwest terminal of the surface fault ruptures. Observation of fallen objects close to the surface fault rupture suggests that surface rupture initiated between Sugidou and Tjijigamine park, Mashiki town, and propagated bilaterally toward northeast and southwest.

Keywords: 2016 Kumamoto earthquake, surface fault rupture, source process

A preliminary report on outcrops of the Futagawa fault, which moved with the 2016 Kumamoto earthquakes

*Kiyokazu Oohashi[1], Tomonori Tamura[1]

1.Graduate School of Sciences and Technology for Innovation, Yamaguchi University

During a rapid survey after the 2016 Kumamoto earthquakes, we found three major fault outcrops (the Kamijin, the Kawahara, and the Kuwazuru outcrop) along the Futagawa fault, which considered to moved with the earthquakes. The Kamijin outcrop is located between the places where surface ruptures of 1-2 m (dextral movement) are found. The sharp fault plane, which trends N66°E and dips 90°, juxtaposes the Aso-4 pyroclastic rock and latery formed colluvial soil. The fault displaces modern ground surface and shows dextral displacement of 2 m in maximum due to the 2016 Kumamoto earthquakes. Based on the spatial distribution of the Aso-4 pyroclastic rock and the colluvial soil, we estimate that the accumulated displacement of ~10 m after the formation of the Aso-4 pyroclastic rock.
At the Kawahara outcrop, we found a faut breccia zone of 20 cm thickness which trends N90°E and dips 72°N.

Keywords: The 2016 Kumamoto earthquakes, Fault outcrop, Striation, Fault rocks

Slip-partitioned surface ruptures for the Mw 7.0 2016 Kumamoto, Japan, earthquake

*Shinji Toda[1], Heitaro Kaneda[2], Shinsuke Okada[1], Daisuke Ishimura[3]

1.International Research Institute of Disaster Science, Tohoku University, 2.Graduate School of Science, Chiba University, 3.Tokyo Metropolitan University

An ENE-trending ~30-km-long significant surface ruptures emerged along the previously mapped Futagawa and northern Hinagu fault zones at the Mw 7.0 2016 Kumamoto earthquake (Kumahara et al., 2016, in this JpGU meeting). The rupture zone is mostly composed of right-lateral slip fault sections that has max. 2 m coseismic slip. But we also found ~6-km-long normal faulting rupture zone on the western foothill of Mt. Tawarayama, parallel to the right-lateral fault zone. The maximum amount of throw on the normal fault is about 2 m, which is equivalent to the one on the strike-slip fault. We suppose the simultaneous dip-slip and strike-slip motion on parallel faults occurred during the slip partitioning process near the surface from an NW-dipping oblique slip at seismogenic depth. The slip partitioning section may also correspond to the section relatively fewer aftershocks have been occurring. Understanding the slip partition on parallel faults leads to the proper fault grouping and identifying seismogenic fault zone.

Keywords: active fault, surface rupture, slip partition

The surface rupture of the 2016 Kumamoto Earthquake Kumamoto prefecture, central Kyusyu, Japan

*Yorihide KOHRIYA[1], Masashi Omata[1], Kaoru Taniguchi[1]

1.PASCO CORPORATION

The 2016 Kumamoto Earthquake occurred on 14 April 2016 (Mj = 6.5) 16 April (Mj = 7.3). The surface rupture due to the earthquake appeared along the Futagawa fault zone and Hinagu fault zone (Ikeda et al., 2001; Nakata and Imaizumi, 2002).
To reveal features of the surface ruptures, we carried out field exploration from 15 April to 18. In this survey, we observed ground deformations, recorded location data of fault traces with handy GPS, and carried out simple measurement of vertical and horizontal displacement. In addition, it was interpretated the fault traces by using aerialphotographs taken after the earthquake.
As a result, we confirmed 14-km-long surface ruptures and ground deformations along the Futagawa fault zone and the Hinagu fault zone. Many of sites showed a right-lateral slip. However, there was the surface ruptures that does not match the known active faults. The left-lateral surface ruptures is continuous over 300m in NW-SE direction at Ishikawa. The right-lateral surface ruptures is continuous over 1.5km from Shimoda to Teradomari. This fault traces is to run parallel to the position of about 500 - 800m northwest of Futagawa fault.
In Terai site, damage to the road and lateral displacement of the canal that occurred in the earthquake of April 14 had been expanded after the earthquake of April 16.

Keywords: active fault, surface rupture, The 2016 Kumamoto Earthquake, Futagawa fault zone, Hinagu fault zone

Multiple active faults triggered the 2016 M_w 7.1 Kumamoto earthquakes

*Aiming Lin[1], Takako Satsukawa[1], Maomao Wang[1], Zahra Mohammadi Asl[1], Ryoushi Fueta[1], Fumiki Nakajima[2]

1.Department of Geophysics, Graduate School of Science, Kyoto University, 2.CTI Engineering International Co., Ltd.

The M_w 7.1 (Mj7.3) Kumamoto earthquake occurred on 16 April 2015 in Kyushu Island, west Japan, resulting in extensive damage in the Kyushu Island, Japan. The M_w 7.1 (Mj7.3) Kumamoto earthquake occurred on 16 April 2016 in Kyushu Island, west Japan, with **three large foreshocks of M> 5.5,** M_w 6.2 (Mj6.5) and M_w 5.5 (M5.7) **on**14 April, and M_w 6.0 (Mj6.4) on15 April, respectively. There are also four large aftershocks of M>5.0, M_w 5.8 (Mj6.0), two M_w 5.6 (Mj5.8) and M_w 5.2 (Mj5.3) occurred immediately within 6 hours after the main shock on 16 April (Japan Meteorological Agency, 2016). These foreshocks and aftershocks show a migration from the southwest to the northeast, mostly along the pre-existing active faults. To determine the motion of seismogenic fault, ground deformation features, and the relationship between the co-seismic rupturing process and crustal structure of the Aso volcano cluster, our survey group went to the epicentral area one day after the event and worked for 10 days.
Field investigations, seismic data, and analysis of high-resolution Google earth images acquired before and after the earthquake, reveal that a ~40-km-long surface rupture zone occurred mostly along the NE-SW-striking Hinagu-Futagawa fault zone, with dominantly right-lateral strike-slipping displacement in the central-southwest segment and multiple newly-identified faults in northeast segment that formed a graben structure and crosscut throughout the western side of the Aso caldera. In this presentation, we will report the detail distribution patterns of co-seismic ruptures and offset amounts, and the structural features of the newly found active faults along which the co-seismic surface ruptures occurred.

Keywords: 2016 Mw 7.1 Kumamoto earthquake, co-seismic surface rupture, Hinagu-Futagawa Fault Zone, Aso caldera, co-seismic graben, strike-slip fault

Geometry and kinematics of surface fault ruptures produced by the 2016 Mw 7.0 Kumamoto earthquake: Computerized X-ray tomography analysis of three dimensional fault geometries in basement-induced oblique-slip faulting

*Keiichi Ueta[1], Kazuo Mizoguchi[1], Keitaro Komura[1], Shiro Tanaka[1], Toshinori Sasaki[1], Koutarou Aiyama[1], Yasuhira Aoyagi[1]

1.Central Research Institute of Electric Power Industry

The 2016 Mw 7.0 Kumamoto earthquake produced surface ruptures along the Futagawa and Hinagu fault zones. The surface ruptures consist of ENE-WSW trending right-lateral faults, WNW-ESE trending left-lateral faults and ENE-WSW trending normal faults. We perform sandbox experiments by using X ray CT scanner to analyze the kinematic evolution, as well as the three –dimensional geometry, of faults in basement-controlled oblique-slip faulting. The geometry of the shear bands (Riedel shear and antithetic Riedel shear) in the experimental model shows a strong resemblance to the surface ruptures along the Futagawa fault zone. These complex surface ruptures may result from the effect of thick overburden consisting of Quaternary sediments and pyroclastic- flows.

Discussion on the ground ruptures appeared in alluvial plain in Aso caldera and earthquake fault based on field investigation and low-altitude aerial photogrammetry.

*Kei Tanaka[1], Takashi Nakata[2], Nobuhisa Matsuta[3], Kyoko Kagohara[4], Daishi Takenami[5], Takashi Kumamoto[3], Hikaru Moriki[5]

1.Japan Map Center, 2.Prof. Emeritus, Hiroshima Univ. , 3.Okayama Univ., 4.Yamaguchi Univ., 5.Graduate Student, Okayama Univ.

We examined ground ruptures appeared in alluvial plain in Aso caldera based on field investigation and low-altitude aerial photogrammetry, in order to discuss their origin. Ground ruptures are extended from north of Aso-Nishi primary school in the south to Uchinomaki hot spring in the north. They are aligned in ENE-WSW direction forming elongated depressions bounded by parallel running steep scarps with maximum height of 2m. They are, in places, are associated right-lateral fault slips of several decimeters. Therefore we suggest that some of the ground ruptures are probably triggered by surface faulting and resulted in extensive ground ruptures.

Keywords: Kumamoto Earthquake, surface fault, ground rupture, Aso caldera

Detection of surface ruptures associated with the 2016 Kumamoto earthquake with ALOS-2/PALSAR-2

*Manabu Hashimoto[1]

1.Disaster Prevention Research Institute, Kyoto University

The Japan Aerospace Exploration Agency conducted urgent observations of ALOS-2/PALSAR-2 after the occurrence of the Mjma 6.5 earthquake of April 14, 2016, in Kumamoto. ALOS-2/PALSAR-2 gives us high resolution and quality images of the ground and its changes associated with this earthquake sequence.

There are several methods to detect changes of the ground surface. Interferometry and offset tracking are most often used to detect displacements, while changes in intensity and coherence is exploited for the detection of structural damages, landslides and surface ruptures. In this study, we look closer at interferograms and associated coherence images and discuss the distribution of surface ruptures.

In the interferogram spanning the Mjma 7.3 shock of April 16, we recognize many discontinuities in phase accompanied by low coherence (< 0.6), while coherence is almost perfect (~ 1.0) in other interferograms. They are distributed mainly along the strands of the Futagawa –Hinagu fault system and on the western frank of the Aso caldera. The former is related to the coseismic surface ruptures of the source fault. Several strands of low coherence zone (< 0.8) are recognized in the coherence image. One is along the Futagawa fault in the west and the other is consistent with the Mifune segment of the Hinagu fault. These two strands join near the central part of the Mashiki city. East of the junction, the low coherence zone extends toward ENE and finally reaches the Aso caldera. In the Aso caldera, low coherence zone is separated to ENE trend and E-W swarm. Low coherence zone is not a simple line but a belt of short and thin lines of low coherence. Since surface deformation due to other factors such as liquefaction also decreases coherence, all discontinuities cannot be regarded as coseismic fault. However, it is reasonable to consider that these low coherence zones include the surface ruptures of the coseismic source fault on the basis of their feature and location.

The discontinuities on the frank of the caldera are located off the trend of coseismic surface rupture and have a different strike of nearly E-W. Some discontinuities have phase jump of about 10 rad (~ 19 cm) and several hundred to thousand meters long. However the width of low coherence and associated deformation is small. Therefore the source of these discontinuities may be shallow. This area is covered with pyroclastic deposits. Unconsolidated material moved differentially due to the strong ground motion.

The ALOS-2/PALSAR-2 images were provided by JAXA through SAR earthquake WG (Secretariart: GSI).

Keywords: ALOS-2/PALSAR-2, surface deformation, coherence, interferometry, active fault

Surface rupture associated with the 14 April 2016, Mj 6.5 earthquake in the Mashiki and Kashima area, Kumamoto Prefecture, Kyushu, Japan

*Nobuhiko Sugito[1], Hideaki Goto[2], Yasuhiro Kumahara[3], Takashi Nakata[4], Kyoko Kagohara[5], Hiroyuki Tsutsumi[6], Nobuhisa Matsuta[7], Haruka Yoshida[8]

1.Faculty of Humanity and Environment, Hosei University, 2.Graduate School of Letters, Hiroshima University, 3.Graduate School of Education, Hiroshima University, 4.Professor Emeritus, Hiroshima University, 5.Yamaguchi University, 6.Department of Geophysics, Graduate School of Science, Kyoto University, 7.Graduate School of Education, Okayama University, 8.Fukuoka Prefectural Yame High School

We conducted aerial observations and field surveys for the 14 April 2016, Mj 6.5 earthquake, which occurred in Kumamoto Prefecture, Kyushu, Japan, and found surface ruptures in the Mashiki and Kashima area on 15 April. Part of those ruptures were enlarged in their offset amounts and extended in their lengths during the 16 April, Mj 7.3 earthquake. In this presentation, we report distributions, geometries, and offset amounts of the surface ruptures associated with the 14 and 16 April earthquakes. [Acknowledgement] We thank research members for their cooperation during the field surveys, as well as the Asahi Shimbun Company for the helicopter flight. We also thank the Geospatial Information Authority of Japan for providing us with post-earthquake aerial photographs. This work was supported by 1) JSPS KAKENHI Grant Number 16H06298, and 2) MEXT of Japan, under its Earthquake and Volcano Hazards Observation and Research Program.

Keywords: Active fault, Tectonic geomorphology, Paleoseismology

Distribution of surface cracks caused by the 2016 Kumamoto Earthquake interpreted from aerial photos

*Takayuki Nakano[1], Hiroshi Une[1], Tatsuo Sekiguchi[1], Hisato Sakai[1], Kazuki Yoshida[1]

1.GSI of Japan

The 2016 Kumamoto Earthquake on 14 and 16 April 2016 caused serious damage such as house collapse and slope collapse in Kumamoto Prefecture. Surface earthquake faults were emerged along Futagawa active faults and Hinagu active faults by the earthquake of M7.3 on 16 April, and unknown active faults were emerged around Kawayo area, Minamiaso Village.
Geospatial Information Authority (GSI) of Japan have conducted on aerial photographing for disaster area since 15 April 2016. A lot of surface cracks were identified from Aso City to Mifune Town on the aerial photos after 16 April 2016. Therefore, we interpreted and mapped those cracks. Some of those cracks were already announced on the homepage of GSI of Japan. In this presentation, we will display the wider distribution of surface cracks interpreted from aerial photos from 16 April to 20 April 2016. These surface cracks were caused by surface earthquake fault, gravity deformation of slope, land liquefaction and ground motion etc. All detail cracks on the road and around slope collapse were not extracted. This interpretation work was carry out by the presenters and Geographic Department members of GSI of Japan.

Keywords: the 2016 Kumamoto Earthquake, crack, surface earthquake fault, active fault, gravity deformation

Deformation analysys of Pre- and post earthquake DATA set of airborne LiDAR 50cm DSM , Kumamoto 2016 earthquake.

*Tatsuro Chiba[1], Kazuo Oda[1], TOKO TAKAYAMA TAKATO[1], Kenichi Arai[1], Koji Fujita[1], Kazuya Funakoshi[1], Yoshiaki Kashiwabara[1], Naoki Ogawa[1], Baator Has[1], sonoka tsukuda[1]

1.Asia Air Survey Co., Ltd.

Estimation of distribution and displacement of such a dislocation is helpful for understanding and disaster prevention measures of the mechanism of the earthquake. In-SAR is suitable for detection of deformation of wide area, but cannot detect detail movement along fault zones. Ground survey can measure dislocation along linear structure like roads, etc., but hardly detect flexures without cracks. Differential Lidar is expected to detect such cases of dislocation along fault zones if Lidar data before movement is available.
We had measured airborne LiDAR just before (April 15) and after (April 23) of the main shock of the Kumamoto earthquake. The acquisition area of the both data is from Kashima-town to Nishihara-village, and acquisition density of the first data is one point per square meter, and four points per square meter for the second data. DSM of the 50cm mesh had been processed from the both LiDAR data and converted to Red Relief Image Maps(RRIM). The analysis of these data results that the quantity of biggest deflation was -2.3m in Fuda district of Nishihara-town. Horizontal displacement is clearly readable with the RRIM and aerial photos. For example, right-lateral strike-slip fault can be found at the north and south edge of Kiyama River low land, and the left-lateral strike-slip fault lies in the crossing direction (figure 1).
Movement between two point clouds before / after the main shock on 4/16 had been calculated automatically by point cloud registration with CCICP (Classification and Combined Iterative Closest Point) , where iteratively calculates rigid transformation in iterative process which first classifies point cloud into linear / planar / scatter points and minimizes point-to-plane and point-to-point distances between matching points of the same categories. The results of calculation with point clouds of about 50cm resolution shows precisely the tendencies of horizontal and vertical movement around the faults.

Reference
Oskin,M.E., et al.(2012),Near-field deformation from El MayorCucapah earthquake ewvealed by defferential LIDAR, Sciences,335,702-705,doi:10.1126/science.1213778.
Nissen et al.(2014),Coseismic failt zone deformation revealed with differential Lidar:examples from Japanese Mw~8 intraplete earthquakes,Earth and Planetary Science Letters,405,244-256.

Keywords: Airbone LiDAR, Aerial photograph, earthquake fault, defferencing of DEM

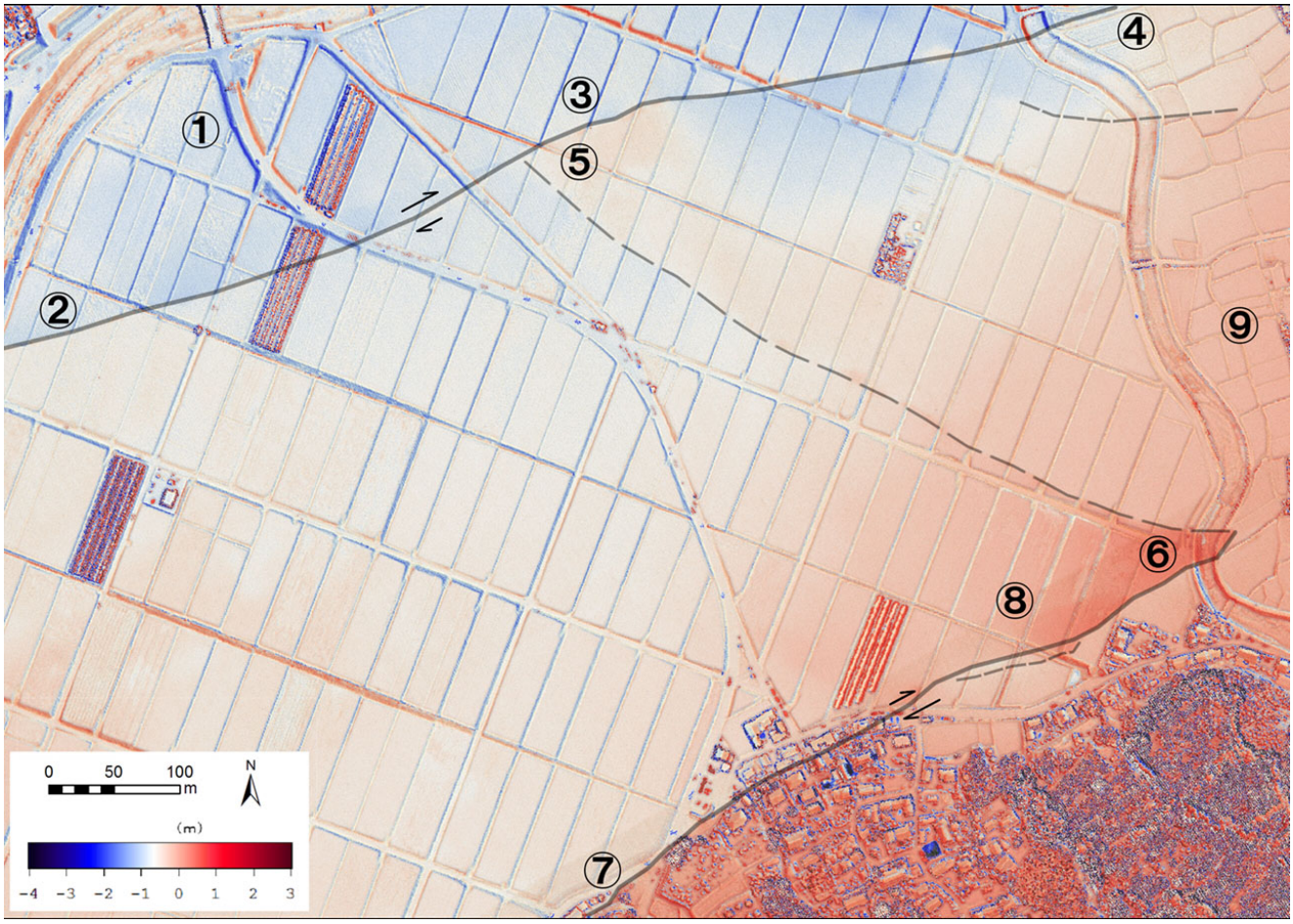

3D model of the surface deformation associate with the 2016 Kumamoto Earthquake ,Kumamoto prefecture, central Kyusyu, Japan

*Masashi Omata[1], Tsuneki Sakakibara[1], Shuuichirou Tonda[1], Yorihide Kohriya[1], Kaoru Taniguchi[1]

1.PASCO CORPORATION

The 2016 Kumamoto Earthquake occurred on 14 April 2016 (Mj=6.5), 16 April (Mj=7.3). The surface rupture associate with the earthquake appeared along the Futagawa fault zone and Hinagu fault zone (Ikeda et al., 2001; Nakata and Imaizumi., 2002). To reveal features of the surface deformation, we carried out surface exploration from 15 April to 18. And we took aerial photo from 15 April to 22. As a result of these investigations, we found surface deformation trace at besides the active fault trace of the past report.We used PALS (Portable Aerialphotography and Locator System) of in-house development by photograph taking from the airplane. Simultaneously with taking a photograph PALS is the system to acquire a coordinate in the photography location and the subject location by a GPS. 3D model was generated using SfM (Structure from Motion) software from the photographs of which we took aerial photographs. SfM software is using Smart 3D Capture (made by Acute3D company). To make 3D model can confirm the local circumstances which can be observed only from one-way from the various angles with a single aerial photograph. We can observe while scaling it freely from the topography situation of the wide range to the in-depth structure of the surface deformation. We can use much times, we can study the surface deformation more than we observe from the sky on airplane. As the correct distribution location of the surface deformation can be done clearly, it’s suitable for in-depth mapping.In Matoishi area at Aso-city, we can observe the surface deformations of straight line in the northeast-southwest direction, parallel more than one. The surface deformation made graben with Normal faults. We can’t say a definite thing about an origin of this surface deformation by this stage.In Mitake area at Mashiki-town, there was the surface rupture that does not match the known active faults. This surface rupture made right lateral offset at roads and R-shear by the right lateral shear. Between two dextral faults, we found the sinistral fault. This sinistral fault is conjugate fault of main faults.

Keywords: 2016 Kumamoto Earthquake, active fault, 3D model, surface rupture, Futagawa fault zone and Hinagu fault zone, SfM

Practical evaluation of small drone's survey for active faults, Kumamoto

*Motomaro Shirao[1], Shoichi Kiyokawa[2]

1.none, 2.Earth and Planetary Science, Kyushu Univ.

Active faults appeared Kumamoto Earthquake 16, April, 2016 are the first active faults in Japan since practical small drones have been available commercially. We carried a small drone, DJI Phantom4 by air as carry-on baggage from Tokyo. We surveyed the active faults and accompanied small cracks by Phantom4 at Kamijin of Mashiki-Town and Kurokawa of Minami-Aso-Villiage on 1st and 2nd May. Total duration of flight was 108 minutes at an altitude less than 65m.
Diagonal FOV of Phantom4 camera is 94°, image size is 4000x3000 pixels at still mode, and 3840x2160 pixels (4K) at video mode. Spatial resolution is about 1cm at an altitude of 10 m. Although vertical FOV is 72% at video mode compared with at still mode, information is much larger owing to 30 fps, and quality of capture image is good. Bird’s-eye 4K video is very impressive, and useful for research, education and public information.
At September 2016, a part of Civil Aeronautics Low has changed, a new flight rule of Unmanned Aerial Vehicles such as drones put into effect on 10th December 2016. As flight areas are near Kumamoto Airport, there is a possibility we need permission from Kumamoto Airport or MLIT. We will discuss this problem.

Keywords: Kumamoto Earthquake, active fault, drone, 4K video, Civil Aeronautics Low

Utilization of remote sensing of The 2016 Kumamoto Earthquake

*Akihiko Itou[1], Yuuji Sakuno[2], Yuji Kuwahara[3]

1.Space Engineering Development Co.,Ltd, 2.Hiroshima University, 3.Ibaraki University

The remote sensing is a technique to measure an object from remoteness, and to grasp a state, and there is a method using a satellite, airplane and drone.
Because the remote sensing can measure the wide area at the same time, it is the technique that is useful for the situation grasp at the time of the disaster.
For Kumamoto disasters, I introduce an observation example of the remote sensing and arrange usefulness of the remote sensing.

Keywords: Satellite, Remote Sensing, Drone

Hypocenter distribution and source process of the 2016 Kumamoto earthquake

Akio Katsumata[1], Kenichi Fujita[1], *Koji Tamaribuchi[1], Shinobu Ando[1]

1.Meteorological Research Institute, Japan Meteorological Agency

An earthquake of M6.5 occurred in Kumamoto Prefecture at 21:26 on April 14, 2016. Following this earthquake, earthquakes occurred at 00:03 on April 15 (M6.4) and at 01:25 on April 16 (M7.3). We report the hypocenter distribution and source processes of these earthquakes including their aftershocks.
The earthquake on April 14 of M6.5 occurred with a focal depth of 11 km, and was strike-slip type with a tension axis of NNW-SSE (JMA). According to a result of relocation by the double difference method with cross-correlated data, the seismic cluster including the one of M6.5 on April 14 is distributed along a nearly-vertical plane with SE-dip. Source process analysis with KiK-net record indicated a large slip area in the NE of the hypocenter. Although source process was analyzed also with assumption of NW-dip, we could get better fitting between observed and synthetic records for the case of SE-dip, especially at nearby stations (KMMH16 and KMMH14) to the assumed fault. In the case of SE-dip, normal fault slip component of SE-side down was estimated.
The earthquake of M6.4 on April 15 occurred with a focal depth of 7 km and with a similar focal mechanism as the one of M6.5 on April 14 (JMA). The epicenter was located in the SE of that of M6.5 event on April 14. The focal depth was estimated at 2 km when a 3D-inhomogeneous velocity structure (3D-vel.) was assumed. The source process analysis indicated a SE-dip fault with a large slip in the SW of the hypocenter, that was a different area of the large slip on April 14. Analysis of interferometric SAR indicated relatively smaller dip angle fault of NW-dip as the total effects of April 14 and April 15 events. In contrast with NE part, the double difference location presented a NW-dipping nearly-vertical plate in the SW part.
The event of M7.3 on April 16 occurred with a focal depth of 11 km and with a NS tension axis (JMA). The CMT solution of JMA had some normal fault component. Double difference locations presented a distribution along a NW-dipping plane. Whereas the focal depth of the event was estimate at 11 km also with the 3D-vel., the focal depth of the cluster was shallower by 2-3 km with the 3D-vel compared with the result with the JMA2001 velocity structure, and hypocenter distributing in the NE of the main cluster was estimated at depths shallower than 5 km by the 3D-vel. After this event, the seismic activity with SE-dip ceased. The result of source process analysis indicated a large slip at the shallow part in the NE of the epicenter. The result of interferometric SAR also indicated crustal deformation distribution up to the area around Mt. Aso that is located in the NE of the epicenter of the M7.3 event.
Seismic activity is observed also in Oita Prefecture. A few clusters were recognized in the activity in Oita Prefecture.

We used data from the National Research Institute for Earth Science and Disaster Prevention, Hokkaido University, Hirosaki University, Tohoku University, the University of Tokyo, Nagoya University, Kyoto University, Kochi University, Kyushu University, Kagoshima University, the National Institute of Advanced Industrial Science and Technology, the Japan Marine Science and Technology Center, Geospatial Information Authority of Japan, the Tokyo metropolitan government, the Shizuoka prefectural government, the Kanagawa prefectural government, and the Japan Meteorological Agency.

Keywords: the 2016 Kumamoto earthquake, hypocenter distribution, source process

Source Rupture Processes of the 2016 Kumamoto Earthquake Sequence from Strong Motion Data

*Kimiyuki Asano[1], Tomotaka Iwata[1]

1.Disaster Prevention Research Institute, Kyoto University

The 2016 Kumamoto earthquake sequence started with an M_J 6.5 foreshock at 21:26 on 14 April, 2016, and another M_J 7.3 mainshock occurred at 01:25 on 16 April, just 28 hours after the foreshock. We estimated the source rupture processes of the foreshock and the mainshock of this earthquake sequence by the multiple time window linear waveform inversion technique using strong motion data (e.g., Hartzell and Heaton, 1983; Sekiguchi et al., 2000).
For the analysis of the foreshock, we assumed a nearly vertical planar fault plane (strike 212, dip 89, length 14 km, and width 13 km) along the northern part of the Hinagu fault considering the aftershock distribution and the moment tensor solution by F-net project of NIED. We analyzed velocity waveforms in 0.05-1 Hz recorded at 13 strong motion stations of K-NET, KiK-net, and F-net. The obtained source model has a large slip area near the rupture starting point at a depth of 11.4 km. Another large slip area is found close to the northern edge of the fault at a depth of approximately 5 km. That is, the rupture of the foreshock mainly propagated northeastward with almost pure right-lateral strike-slip, and it would be a reason why severely strong ground motion was observed in Mashiki town, which is located northeast of the epicenter. The total seismic moment is 2.04×10^{18} Nm (Mw6.1), and the average and maximum slip amount is 0.36 m and 1.2 m, respectively. The best estimate of the first time-window front triggering velocity is 2.2 km/s.
For the mainshock, northwestward dipping fault plane along the Futagawa fault is expected by the spatial distribution of the aftershocks and the coseismic crustal deformation analyzed by the Geospatial Information Authority of Japan. The aftershocks occurring along the Hinagu fault also appear to align on a northwestward dipping fault plane. The several emergency field survey teams dispatched from the Geological Survey of Japan, Tohoku University, and other institutes reported the surface breaks along both of Futagawa and Hinagu fault zones. Thus, we assumed a source model consisting of two planar fault planes; one along the northern part of the Hinagu fault (strike 205, dip 72, length 14 km, and width 18 km), and the other along the Futagawa fault (strike 235, dip 65, length 28 km, and width 18 km). We analyzed velocity waveforms in 0.05-0.5 Hz recorded at 15 strong motion stations of K-NET, KiK-net, F-net, and JMA. The slip on the Futagawa fault initiated from the deep portion of the fault, and propagated northeastward and to the ground surface. The largest slip is observed at depth approximately 8-10 km, and the slip amount of the shallowest subfault approximately ranges from 1 to 3 m. The subfaults in the shallow part close to the northern end of the Hinagu fault also has relatively large slips, and these slips corresponds to the emergence of the surface breaks. By comparing the temporal slip progression on the fault estimated by this study with the observed displacement waveforms without filter at two strong motion stations nearby the surface fault, which are not used in the inversion analysis, we could confirm that the large fault parallel displacements at these two stations coincide with the rupture of the fault in front of the stations. The total seismic moment is 4.67×10^{19} Nm (Mw7.0), and the average and maximum slip amount is 1.9 m and 5.3 m, respectively. The best estimate of the first time-window front triggering velocity is 2.4 km/s.
From above analysis, we conclude that the rupture of the 2016 Kumamoto mainshock continuously propagated from the northern part of the Hinagu fault to the Futagawa fault. This earthquake scenario is quite similar to the old long-term evaluation of the Futagawa-Hinagu fault system published in May 2002 by the Headquarter of Earthquake Research Promotion.
Acknowledgements: We used strong motion data from K-NET, KiK-net, and F-net of NIED, JMA, and

Kumamoto Prefecture.

Keywords: the 2016 Kumamoto earthquake, source rupture process, strong motion data

Source rupture process of the 2016 Kumamoto earthquake derived from strong motion data

*Hisahiko Kubo[1], Wataru Suzuki[1], Shin Aoi[1], Haruko Sekiguchi[2]

1.National Research Institute for Earth Science and Disaster Prevention, 2.Disaster Prevention Research Institute, Kyoto University

A series of earthquakes in Kumamoto and Oita Prefectures from April 14, 2016, which are collectively called the 2016 Kumamoto earthquake, caused destructive damages by their strong ground motions. In this study, we estimate the source processes of two major events using strong motion data; One occurred at 21:26 on April 14 with Mj 6.5 (which we will call “the M6.5 event”) and the other occurred at 1:25 on April 16 with Mj 7.3 (which we will call “the M7.3 event”).
The multi-time-window linear waveform inversion method (Olson and Apsel 1982; Hartzell and Heaton 1983) is used in this study. For the fault plane model of the M6.5 event, we assume a 22 km x 12 km rectangle with a strike of 212 degree and a dip of 89 degree referring to the F-net moment tensor solution. For the fault plane model of the M7.3 event, we assume a 56 km x 24 km rectangle with a strike of 226 degree referring on the F-net moment tensor solution. The dip angle is set to 65 degree based on the hypocenter distribution of aftershocks after the M7.3 event and the surface-rupture distribution, and the static coseismic displacements inferred by InSAR and GNSS. These fault planes are discretized with 2 km x 2 km subfaults. The rupture starting point of each event is set to the hypocenters determined by Yano et al. (2016) with the double-difference method. The slip time history of each subfault is represented by 5 time windows of 0.8 s for the M6.5 event and 13 time windows for the M 7.3event. The triggering velocity of first time window is set to 2.4 km/s for the M6.5 event and 2.8 km/s for the M7.3 event to minimize the data-fit residual.
We use three components of velocity waveforms at the 16 stations of K-NET and KiK-net, F-net of NIED for the M6.5 event and the 27 stations for the M7.3 event. The waveforms for the analysis of the M6.5 event are band-pass filtered between 0.1 and 1.0 Hz, resampled to 10 Hz, and windowed from 1 s before S-wave arrival for 7-10 s. The waveforms for the analysis of the M7.3 event are band-pass filtered between 0.05 and 1.0 Hz, resampled to 5 Hz, and windowed from 1 s before S-wave arrival for 30 s.
Green's functions are calculated with the discrete wavenumber method (Bouchon 1981) and the reflection/transmission matrix method (Kennett and Kerry 1979) assuming a 1-D velocity structure model. The structure model is obtained for each station from the 3-D structure model (Fujiwara et al. 2009). Logging information is also used for the KiK-net station. To consider the rupture propagation effect, 25 point-sources are uniformly distributed over each subfault in the calculation of Green’s functions.
Two orthogonal slips of each time window at each subfault is derived by minimizing the difference between the observed and synthetic waveforms using the non-negative least-squares scheme (Lawson and Hanson 1974). The slip angle is allowed to vary within ±45 around the F-net rake angle (-164 degree for the M6.5 event and -142 degree for the M7.3 event). In addition, the spatiotemporal slip smoothing constraint (Sekiguchi et al. 2000) is imposed in the inversion and its weight is determined based on ABIC (Akaike 1980).
In the estimated source model of the M 6.5event, the seismic moment and maximum slip are 1.8×10^{19} Nm (Mw 6.1) and 0.7 m, respectively. Two large slip areas are found in the region around the rupture staring point and the shallow region north-northeast of the rupture starting point.
In the estimated source model of the M7.3 event, the seismic moment and maximum slip are 5.3×10^{19} Nm (Mw 7.1) and 4.6m, respectively. The large slips are found from 10km to 30km northeast of the rupture starting point. The rupture mainly propagated to the northeast, developed into the large

moment release between 5 s and 15 s, and almost ceased after 20 s. The slip distribution in the shallow part is consistent the observed surface-rupture distribution. In addition, the large slip area does not overlap with the active aftershock area after the M7.3 event.

Keywords: The 2016 Kumamoto earthquake, Source process, Strong ground motion

Preliminary results of rupture processes of the 2016 Kumamoto Earthquake inferred from strong motion waveform

*Kazuhito Hikima[1]

1.Tokyo Electric Power Company Holdings Inc.

INTRODUCTION

In the 2016 Kumamoto Earthquake sequence, high acceleration records were observed and those are important to considering the relations between the source process and ground motions. I performed the inversion analyses to reveal the source processes of the main shock (4/16 1:25) and foreshock (4/14 21:26) using the strong motion records. The information of these events is limited and is updated daily, however, the results of this study are tentative. I will continue the analysis necessary to reveal detail source processes.

OUTLINE of ANALYSES

The hypocenters of these events, including the maximum foreshock, the main shock, were relocated using double-difference method (Waldhauser and Ellsworth, 2000). These parameters were used to configure the fault planes.
The strong motion records observed KiK-net stations (about 15 stations) were used for the inversion analyses. The horizontally stratified velocity models, used in calculating Green's functions, were tuned using the waveform inversion method (Hikima and Koketsu, 2005).
The source processes were inverted by the multi time window analysis (Yoshida et al., 1996, Hikima, 2012). The velocity waveforms obtained by KiK-net, filtered between 0.03 and 0.8 Hz (for the main shock), between 0.03 and 0.5 Hz (for the foreshock) were used.

RESULT of the main shock

The fault plane were configured as 227 degree for strike angle and 75 degree for dip angle, considering preliminary results and aftershock distribution. The rupture propagated toward north-east direction almost uni-laterally. The dimension of fault plane is about 40 km for strike and 16 km for dip direction. The large slip areas (asperity) are located deep northern of the hypocenter and shallow part between Mashiki and Aso. Right lateral strike slip component is dominant, but significant amount of normal fault component is contained in the shallow slip. The total seismic moment of this result was about 4.6×10^{19} Nm (Mw 7.0).

RESULT of the foreshock

Because two wave packets, those interval is about 5 seconds, are recognized on the waveforms at several stations, it seems that the foreshock is multiple shock event. The preliminary analysis was performed using the fault plane referring the F-net mechanism solution. A dominant slip was determined near the hypocenter and another large slip was recovered slightly shallow from those part after a few seconds. The result is unstable, however, I will continue source process analysis furthermore.

Keywords: 2016 Kumamoto earthquake, Source process, Strong motion, Near fault

Source Processes of three large events of the 2016 Kumamoto Earthquakes Inferred from Waveform Inversion with Strong-Motion Records

*Kunikazu Yoshida[1], Ken Miyakoshi[1], Kazuhiro Somei[1]

1.Geo-Research Institute

We have investigated the source processes of three earthquakes in the 2016 Kumamoto earthquake sequence by the multi-time-window linear waveform inversion method using the strong-ground motion data. We analyzed the three largest earthquakes of Mj6.5 (21:26 on 14 Apr., JST), Mj6.4 (00:03 on 15 Apr., JST) and Mj7.3 (01:25 on 16 Apr., JST) in the sequence.
We used the strong-motion data obtained from K-NET and KiK-net. The data were windowed for 10-25 s, starting at P-wave arrival time, and band-pass-filtered between 0.05 to 0.8 Hz (period of 1.25-20 s) for waveform inversion. The accelerograms were integrated into ground velocities. Theoretical Green's functions are calculated using the discrete wavenumber method (Bouchon, 1981) and the Reflection/Transmission coefficient matrix method (Kennett and Kerry, 1979) using a stratified medium. We assumed individual one-dimensional velocity structure model for each station, which is made from PS-logging, J-SHIS, and the seismic refraction models. We use multi-time-window linear waveform inversion procedure (e.g., Hartzell and Heaton, 1983) in which the moment-release distribution is discretized in both space and time. The relative strength of the smoothing constraint and the first time-window front triggering velocity (V_{FT}) were determined to minimize Akaike's Baysian Information Criteria.
For Mj6.5 (Apr. 14) earthquake, a fault model along the Hinagu fault striking N211°E and dipping 88° is assumed. The total length and width of the fault plane is 14 km and 14 km. The fault plane is divided into subfaults of 2 km x2 km. The moment function of each subfault is represented by a series of three smoothed ramp functions. The estimated source model has two asperities; one is located near the rupture starting point and another at the northern margin of the fault. Its largest slip is 0.8 m. The total seismic moment is 1.6×10^{18} Nm (Mw 6.1).
For Mj6.4 (Apr. 15) earthquake, a fault model along the Hinagu fault striking N211°E and dipping 86° is assumed. The total length and width of the fault plane is 12 km and 9.6 km. The fault plane is divided into subfaults of 1.2 km x1.2 km. The moment function of each subfault is represented by a series of three smoothed ramp functions. The estimated source model has one asperity located near the rupture starting point. Its largest slip is 0.9 m. The total seismic moment is 1.0×10^{18} Nm (Mw 5.9).
For Mj7.3 (Apr. 16) earthquake, a fault model along the Futagawa fault striking N236°E and dipping 86° is assumed. The total length and width of the fault plane is 34 km and 18 km. The fault plane is divided into subfaults of 2 km x2 km. The moment function of each subfault is represented by a series of six smoothed ramp functions. The estimated source model has one asperity located on approximately 10 km east to the rupture starting point. Its largest slip is 4.5 m. The total seismic moment is 3.6×10^{19} Nm (Mw 7.0). The average slip is 1.8 m.
Relationships of the estimated three earthquakes between average slip and seismic moment corresponds to the scaling law determined from previous earthquakes (Somerville et al., 1999). For Mj6.5 and Mj6.4 earthquakes, relation between the combined area of asperities and seismic moment corresponds to the scaling by Somerville et al. (1999), although the area of the asperity for the Mj7.3 earthquake is relatively small to the seismic moment.
Acknowledgements: We use the hypocentral information catalog of JMA, the moment tensor catalog by F-net, and the strong motion data from K-NET and KiK-net provided by NIED. This study was based on the 2016 research project 'Examination for uncertainty of strong ground motion prediction' by the

Nuclear Regulation Authority (NRA), Japan.

Keywords: 2016 Kumamoto earthquake, source process, asperity

Rupture processes of the 2016 Kumamoto earthquakes derived from joint inversion of strong-motion, teleseismic, and geodetic data

*Hiroaki Kobayashi[1], Kazuki Koketsu[1], Hiroe Miyake[1,2]

1.Earthquake Research Institute, The University of Tokyo, 2.Interfaculty Initiative in Information Studies, The University of Tokyo

Two earthquakes respectively occurred on April 14, 2016 at 21:26 (JST) and on April 16, 2016 at 1:25 (JST). These earthquake and aftershocks caused heavy damage to the Kumamoto Prefecture and surrounding region. Especially for the earthquake on April 16, at a strong-motion station in the Nishihara village, Kumamoto Prefecture, the observed maximum velocity of EW component was over 250 cm/s. It is essential to perform source inversion to understand the cause of such waveform observed near to source fault. Therefore, we perform joint source inversion of the earthquake on April 16 using strong-motion, teleseismic, and geodetic data. We obtained strong-motion data from K-NET, KiK-net and JMA stations, teleseismic data from IRIS-DMC, and geodetic data from GEONET. We construct a fault model with three segments because observed surface fault traces, aftershock distributions, and SAR analyses by GSI cannot be represented by single plane fault model. We bend the fault model at the junction of the Hinagu and Futagawa fault zones, and the entrance of the Aso caldera. The results show that rupture propagated to northeast shallow part from the hypocenter and total rupture duration was about 20 s. Maximum slip was obtained at the northeast shallow part near to the Nishihara village. The data fitting was largely well, but some data fitting were not enough, suggesting that further adjustments of the assumed fault model and the velocity structure model are needed. For future study, we will perform the joint source inversion of the earthquake on April 14 or others.

Keywords: 2016 Kumamoto earthquake, rupture process, joint inversion

Source inversion using empirical Green's functions for the 2016 Kumamoto main shock (M 7.3) and two large foreshocks (M 6.5, M 6.4)

*Yoshiaki Shiba[1]

1.Central Research Institute of Electric Power Industry

On April 14, 2016, inland earthquake of M 6.5 occurred at Kumamoto prefecture and seismic intensity scale 7 were recorded near the epicenter (Mashiki town). After that another event of M 6.4 and the main shock of M 7.3 have successively occurred on 15 and 16 April. During the main shock Mashiki town and Nishihara village suffered intensity 7 again. Here we call the first M 6.5 event and second M 6.4 event as foreshock 1 and 2 respectively, and the rupture process of these three events are estimated by using simulated annealing with empirical Green's function.
Foreshocks 1 and 2 are considered to rupture along the northern part of Hinagu fault according to the estimated fault mechanisms by F-net and aftershock distribution. On the other hand the main shock ruptured Futagawa fault. All events show the right-lateral strike-slip faulting with almost vertical dip. Based on these information we assume each fault plane model. For empirical Green's functions aftershock records from the M 4.8 and M 4.9 events are adopted, both of which occurred near the Hinagu fault since suitable data from the aftershocks at Futagawa fault were not available. Strong-motion records of K-NET and KiK-net stations located within about 50 km from the epicenters of the events are utilized for the inversion analysis. Observed acceleration records are band-pass-filtered in the frequency range from 0.1 or 0.2 Hz to 2 Hz, and numerically integrated to derive velocity motions. Then two horizontal S-wave portions are inverted to obtain the source models.
Consequently the estimated source model of the foreshock 2 shows a main slip on the southern part of the fault plane, which implies the spatially complemental relation with the slip distribution of the foreshock 1. Foreshock 1 also shows rather large slip just beneath the Mashiki-town area, where the seismic intensity 7 was reported. For the main shock we see the relatively large slip on the shallow part along the Futagawa fault where surface deformation was observed. The largest slip area beneath the west part of the outer rim of Mt. Aso is consistent with the aftershock gap area.

Keywords: the 2016 Kumamoto earthquake, source inversion, empirical Green's function

Source models for the 2016 Kumamoto earthquakes of April 14 (M_{JMA}6.5) and April 16 (M_{JMA} 7.3) estimated by the empirical Green's function method

*Kazuhiro Somei[1], Ken Miyakoshi[1], Kunikazu Yoshida[1], Toshimitsu Nishimura[1]

1.Geo-Research Institute

Two large inland crustal earthquakes, which occurred in the Kumamoto prefecture, Japan, excited the strong ground motions with seismic intensity 7 (upper limit value) of Japan Meteorological Agency scale. One of them occurred at 21:26 (JST=UT+9) on April 14, 2016, with M_{JMA} 6.5 (hereafter we call "the largest foreshock") and the other occurred at 1:25 on April 16, 2016, with M_{JMA} 7.3 (hereafter we call "mainshock"). The large ground motions from these events were densely observed by K-NET and KiK-net stations in and around the epicentral areas. In particular, extremely large ground motions with peak ground acceleration greater than 1000 cm/s^2 were observed at KiK-net KMMH16 (Mashiki) during both the largest foreshock and mainshock. For understanding the physical mechanisms of strong motion generation processes during these events, reliable source models to explain the observed strong motion records need to be constructed.
In this study, we estimate the source models composed of strong motion generation areas (SMGA) by the broadband strong motion simulations (0.3-10 Hz) using the empirical Green's function method. For an objective estimation of corner frequencies for the target and element events, we apply the Source Spectral Ratio Fitting Method (Miyake *et al.*, 1999). From the obtained corner frequencies, scaling parameters N and C, which required for the empirical Green's function method of Irikura (1986), are determined. Then, the parameters of each SMGA (e.g., the size, rupture starting point, rise time, rupture velocity, and relative location from the hypocenter) are estimated by trial and error method.
For the largest foreshock, 16 stations of K-NET and KiK-net (downhole) in Kumamoto prefecture are the target in the strong motion simulation. The observed ground motion records of M_w 4.4 event (element event) occurring at 7:46 on April 15, 2016, are used as the empirical Green's functions. The obtained source model is composed of two SMGAs with same size of 16 km^2. The stress drop of SMGA is estimated to be 13.3 MPa. The rupture within SMGA1 mainly propagates northeastward from the hypocenter. The rupture of SMGA2 located northeast of the SMGA1 also propagates in northeast direction. The obtained source model simulates the observed acceleration, velocity, and displacement waveforms fairly well. The each forward directivity effect by SMGA1 and SMGA2 contribute to the two pulsive wave packets observed in the northeast area along the source fault (e.g., KMM005, KMMH16).
For the mainshock, we also use the same 16 stations as in the case of the largest foreshock. The observed ground motion records of M_w 5.4 event occurring at 22:07 on April 14, 2016, are used as the empirical Green's functions. The obtained source model is composed of one SMGA of 100 km^2 located on the northeast from the hypocenter. The stress drop of SMGA is estimated to be 19.8 MPa. The main characteristics of observations near the source area could be simulated by the obtained source model, although some discrepancies between the observation and simulation still remain. In order to improve the reproducibility of observed ground motions, the parameters of SMGA for the mainshock need to be examined in more detail.

Acknowledgements: We use the hypocentral information catalog of JMA, the moment tensor catalog by F-net, and the strong motion data from K-NET, KiK-net, and F-net provided by NIED. This study was based on the 2016 research project 'Examination for uncertainty of strong ground motion prediction' by the Nuclear Regulation Authority (NRA), Japan.

Keywords: The 2016 Kumamoto earthquake, Strong motion generation area, Emprical Green's function method

Rupture process of the April 16, 2016 Kumamoto earthquake (Mjma7.3) using Seismic Back-Projection and K-NET/KiKnet waveforms

*Nelson Pulido[1]

1.National Research Institute for Earth Science and Disaster Resilience

I investigated the rupture process of the April 16, 2016 Kumamoto earthquake (Mjma7.3) using a seismic back-projection methodology and K-NET/KiKnet waveforms. The method is based on mapping amplitudes of seismogram envelopes observed around the source region, into a temporal and spatial image of the earthquake rupture (Pulido et al. 2008, Suzuki et al. 2016). The main target of this study is to understand the evolution of the rupture velocity during fault rupture propagation. For this purpose we set a horizontal grid mesh of 32 by 118km covering the regions around the Hinagu and Futagawa fault traces and beyond, as the target region for back-projection. Back-projection is calculated without any constraint on the starting point of rupture or rupture speed. We selected all the KNET/KiKnet stations that recorded the earthquake within 100 km (112 stations). The envelopes of acceleration waveforms used for back-projection were calculated as a vectorial summation of the acceleration waveforms band-pass filtered between 5Hz and 10Hz with their Hilbert transform. They start from the origin time of the earthquake and have a duration of 100 s.
Our results are consistent with a fault rupture starting exactly at the Hinet epicenter. The rupture progressed to the SW for approximately 3 s and then to the NE for 7s. The significant grid energy was released in a narrow region of 30km length (rupture zone), along the Futagawa fault. The average rupture velocity for the first 6 sec was very slow (~1.5s) and after 7 sec abruptly increased to a value significantly above the average shear wave velocity. Assuming a continuous rupture propagation this would imply a super shear rupture propagation. Further tests are required to confirm our initial results.

Keywords: strong motion, source process, High frequency

Dynamic rupture simulation for the 2016 Kumamoto, Japan, Earthquake

*Ryosuke Ando[1], Yosuke Aoki[2], Takahiko Uchide[3], Kazutoshi Imanishi[3]

1.Graduate School of Science, University of Tokyo, 2.Earthquake Research Institute, University of Tokyo, 3.National Institute of Advanced Industrial Science and Technology

The earthquake generation is the fracture along subsurface fault planes driven by the concentrated stress fields, however, these geometrical and physical parameters are hidden in the depth, leading to difficulties to understand the underlying physics of the phenomena. The ongoing sequence of the Kumamoto, Japan, earthquake including the April 15, 2016, M_w 7.0, earthquake and precursory multiple M6-class earthquakes as well as the prolonged seismic activity, provides a unique opportunity to investigate into the mechanism of the earthquake generation with its unique tectonic conditions and well-observed patterns of the sequence. In this study, we conducted a set of fully dynamic simulations and show that the dynamic rupture sequence is mainly controlled by the irregularity of the fault geometry in the subjected regional stress field. We also show that the dynamic triggering of M-6 class earthquakes occurred along the Yufuin fault (located 50 km away) because of the strong stress transient up to a few hundreds of kPa due to the rupture directivity effect of the M-7 event, and the susceptible condition developed by the high geothermal condition. We further show that the rupture growth of M-7 event into SW (to the direction of the Uto segment of the Futagawa fault) is supressed by that the Takano-Shirahata segment of the Hinagu fault slipped again while it has been rupture associated with the precursory events. We compared the simulation results with the surface displacement obtained by InSAR analysis and the observed seismograph. In addition, this dynamic rupture simulation is made possible even on a PC cluster system by the newly developed numerical method called the Fast Domain Partitioning Method (FDPM) for the elastodynamic boundary integral equation method (BIEM).

Keywords: Dynamic rupture simulation, 2016 Kumamoto earthquake, 3D Nonplanar fault geometry

Source spectra and nonlinear site factors based on the spectral inversion methods

*kenichi Nakano[1], Hiroshi Kawase[2]

1.HAZAMA ANDO CORPORATION, 2.DPRI, Kyoto University

The first earthquake occurred in Kumamoto prefecture at April 14 in 2016. The JMA magnitude (M_{JMA}) of this earthquake is 6.5, and Kumamoto Prefecture's shindokei-network recorded the instrumental JMA seismic intensity of 7 at Mashikimachi in Kumamoto prefecture ("JMA" is abbreviation of Japan Meteorological Agency). After the occurrence of the earthquake, another earthquake with M_{JMA}7.3 occurred at April 16 in 2016. We called the former the foreshock, and the latter the mainshock here. These earthquakes and subsequent aftershocks named as the 2016 Kumamoto earthquake sequence. In the mainshock, Kumamoto Prefecture's shindokei-network recorded also the instrumental JMA seismic intensity of 7 at Mashikimachi as well as Nishihara village. If we confirm the distribution of aftershocks, we can see that the aftershocks are on the Futagawa-Hinagu fault zone.

The strong ground motions of the 2016 Kumamoto earthquake sequence were observed by K-NET and KiK-net of NIED (The National Research Institute for Earthquake Science and Disaster Prevention) and also by JMA shindkei-network. These waveforms are published at the webpage of NIED or JMA, and are used for inversion analysis to estimate rupture process. According to the field survey report, we can see the damage of building due to ground deformation a lot. On the other hand, the damaged buildings caused by strong ground motions are also seen. It suggests the necessity of careful discussions to investigate the correlation of damaged buildings, strong ground motions, and ground deformations. Here, we perform spectral inversion analysis on the 2016 Kumamoto earthquake to investigate the properties of source spectra and site amplifications.

We selected the strong ground motions provided by K-NET, KiK-net, and JMA, based on the conditions of Nakano et al. (2015). The main conditions are; events with M_{JMA}4.5 or larger, sites within the hypocentral-distance of 200km, events with the hypocenter depth shallower than 30km in the case of crustal earthquake. We used the hypocenter locations estimated by the Hi-net and seismic moments M_0 estimated by the F-net. For more information on the analysis conditions, please see Nakano et al. (2015). As a result of the selection, we found 25 events usable from the 2016 Kumamoto earthquake sequence in total. From the separated source spectra, we evaluated that the corner frequency fc of the foreshock and the mainshock are 0.19Hz and 0.06Hz, respectively. We also estimated that the stress drop of the foreshock was about 2.2MPa, while that of the mainshock was about 1.8MPa. The stress drops of aftershocks are equal to or lower than the mainshock and the foreshock. This trend is consistent with the relationships of the mainshock-aftershock sequences presented in Nakano et al. (2015) for moderate-size earthquakes. We also calculate short-period levels A to find that the mainshock's A is slightly lower than the average scaling law. Also the short-period levels A of the foreshock, the mainshock, and all the aftershocks are lower than the regression line of Dan et al. (2001) or Sato (2010). Instead, the short-period levels A of the aftershocks are consistent with the regression lines of Sato (2003) or Nakano et al. (2015). Further, the nonlinear site effects clearly seen in the site amplification factors for strong motions such as KMMH16, which are calculated by dividing the Fourier spectrum by the product of source characteristics and damping characteristics estimated in the linear region.

In short, it can be said that the 2016 Kumamoto earthquake is not extraordinary event considering the scaling law, since the stress drop of the mainshock and the foreshock are lower than the

average of previous events with similar magnitude In the foreshock and the mainshock, pervasive emergence of non-linear effects can be found in the site amplification for strong motions such as KMMH16. Note that we used only strong ground motions equal to or lower than 200gal for spectral inversion analysis here to avoid nonlinear site effects. To account for site-specific near fault ground motions we need to consider both a complex rupture process on the fault and a three-dimensional nonlinear site response, which will be our future tasks.

Acknowledgement
We used the strong ground motions provided by NIED and JMA in this study. We are grateful for this.

Keywords: Spectral inversion method, Source spectra, Nonlinear site factors

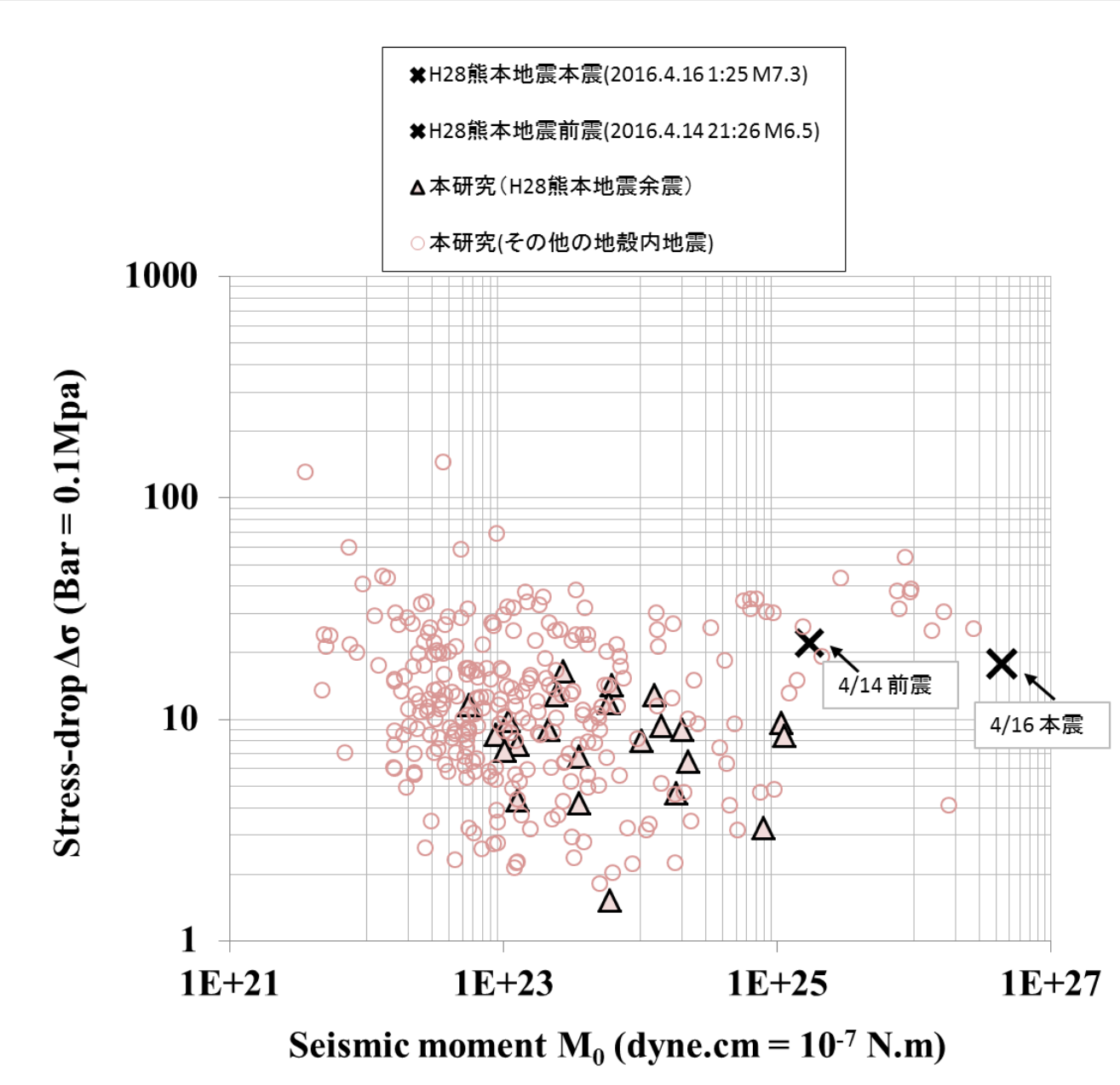

Source, path and site effects of the 2016 Kumamoto earthquake, the foreshocks and aftershocks using the spectral inversion method

*Toshimi Satoh[1]

1.Shimizu Corporation

We estimate source, path and site effects of the 2016 Kumamoto earthquake, the foreshocks and aftershocks using the spectral inversion method. We use 37 events with M_J larger than 4.0 and the focal depth < 20 km around the 2016 Kumamoto earthquake in 1997 to April 19, 2016.
The spectral inversion method and the data selection criteria are basically same to those by Satoh (2010), but we use JMA-95 type records and KiK-net records at the borehole as well as K-NET and KiK-net records at the surface. The used data are Fourier spectra of S wave parts of horizontal components with PGA < 200 cm/s^2 and the hypocentral distance < 60 km at the strong motion stations in the fore arc. We remove the data with hypocentral distance < 30 km for the main shock because we assume the point source. For the main shock the data around OIT009 which are contaminated by an aftershock just after the main shock are removed by above criteria.
The estimated frequency (f) dependent Q is modeled to $Q=62f^{0.87}$, which agrees with that estimated using the moderate earthquakes around Kumamoto by Satoh (2010). The short period spectral level A is estimated to fit the estimated source spectra to omega squared model in the frequency of 0.2 to 5 Hz. Figure compares the M_0-A relations of three largest strike-slip earthquakes estimated in this study with those of previous crustal earthquakes. M_0 by F-net is used. The A of the main shock is almost the same to the relation for crustal earthquakes by Dan et al.(2001). The A of the largest foreshock (M_J6.5) is a litter larger than the relation by Dan et al.(2001). The A of the two earthquakes are the largest among previous strike-slip earthquakes but smaller than the relation for dip-slip earthquakes by Satoh (2010). The A of the second largest foreshock (M_J6.4) is smaller than the relation by Dan et al.(2001) and almost the same to the relation for strike-slip earthquakes by Satoh(2010). There are no clear differences of M_0-A relations between strike-slip and normal-slip earthquakes among 37 earthquakes.
The observed PGVs of the main shock and the largest foreshock are compared with GMPEs. We assume the fault plane and Mw based on Koketsu et al.(2016). The GMPE by Satoh(2008) is derived from data observed in the fore arc of crustal earthquakes from Niigata prefecture to western Japan by considering the difference between strike-slip and dip-slip earthquakes. The attenuation of Satoh's GMPE is different near and far from the fault distance of 70km. The attenuation of Satoh's GMPE almost reproduces the observed PGVs, but the absolute values of observed PGVs of the main shock (Mw7.0) are a little larger and those of the largest foreshock (Mw6.1) are obviously larger than the GMPE within the fault distance of 60 km. This result is consistent with the A estimated in this study.
Although KMMH16(Mashiki), KMM006(Kumamoto) and EEB(JMA Kumamoto) are located within 10km, the seismic intensity is 6.4, 6.0, and 6.0 during the main shock and 6.4, 5.9, and 5.9 during the largest foreshock, respectively. The empirical amplification factors at three stations have the peaks at 4Hz and are almost the same less than 5Hz. The surface-to-borehole spectral ratios and H/V of strong motions at KMMH16 during the main shock and the largest foreshock are obviously different from weak motions. At KMM006 and EEB the differences of H/Vs between strong and weak motions are smaller than those at KMMH16. Therefore causes of the difference of the seismic intensity at three stations are thought to be source effects and the nonlinear site effects depending on nature of soil, but not the 1-D effects due to deep structures.
Acknowledgments: We use K-NET, KiK-net records and F-net CMT solutions by NIED and JMA-95 type

records and the hypocenters by JMA. This research is supported by the Ministry of Education, Science, Sports and Culture, Grant-in-Aid for Scientific Research (A), 26242034 (P.I. Prof. Hiroshi Kawase).

Keywords: The 2016 Kumamoto earthquake, Spectral inversion, Short period spectral level, Attenuation, Empirical amplification factors, Nonlinearity of soil

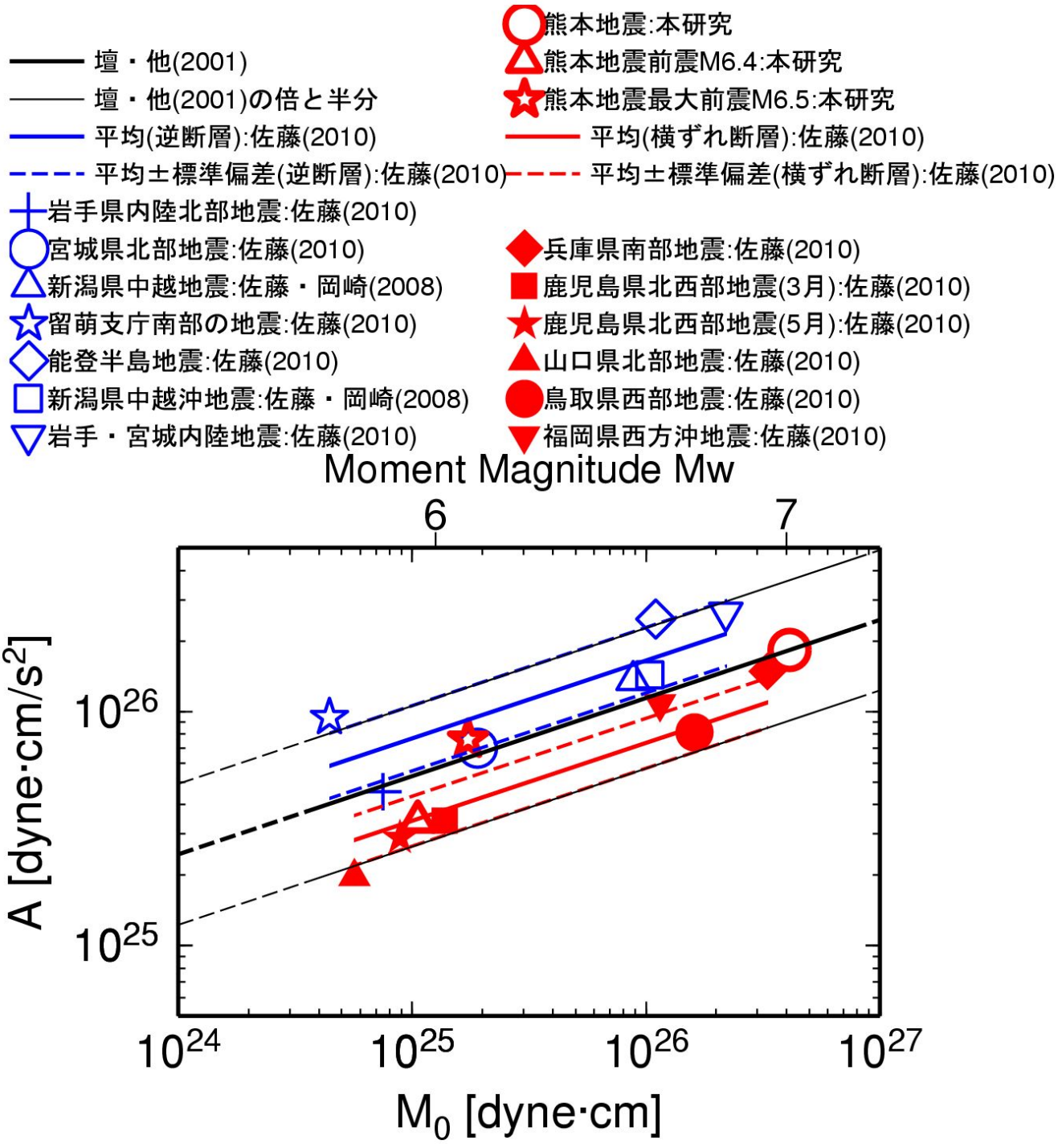

Attenuation Characteristics of Strong Motions during the 2016 Kumamoto Earthquake

*Hongjun Si[1], Kazuki Koketsu[1], Hiroe Miyake[1], Rami Ibrahim[1]

1.Earthquake Research Institute, The University of Tokyo

Two major earthquakes occurred near the Mashiki-machi, Kumamoto, at 21:26 on 14 April, 2016 (M_w 6.2, GCMT), and at 1:25 on 16 April, 2016 (M_w 7.0, GCMT). Serious casualties and damages are reported during the earthquakes. A large number of strong ground motions were recorded during these two earthquakes. In order to understand the correlation between damages and the strong ground motion, we discuss the attenuation characteristics of the strong ground motions observed during the earthquakes.

The data used in this study are observed by K-NET and KiK-net. The 5% damped acceleration response spectra (GMRotI50) are calculated based on the method proposed by Boore et al. (2006). PGA and PGV is defined as the larger one among the PGAs and PGVs of two horizontal components. The PGA, PGV, and GMRotI50 data were corrected to the bedrock with Vs of 1.5km/s based on the method proposed by Si et al. (2013) using the average S wave velocity (Vs30) and the thickness of sediments over the bedrock. The thickness is estimated based on the velocity structure model provided by J-SHIS. We use a source model derived based on the waveform inversion by Koketsu et al. (2016). Based on the source model, we calculated the median distance (MED) which defined as the closest distance from a station to the middle line of the fault plane.

We compared the observed PGAs, PGVs, and GMRotI50 with the GMPEs developed in Japan using MED (Si et al., 2014). The predictions by the GMPEs are generally consistent with the observations during the two Kumamoto earthquakes. The results of the comparison also indicated that, (1) strong motion records from the earthquake on April 14th are generally consistent with the predictions by GMPE, however, at the periods of 0.5 to 2 seconds, four or three records closest to the fault plane greatly exceeds the predictions by GMPE. KiK-net station Mashiki (KMMH16) is included in these stations. (2) for the earthquake on April 16, the PGAs and GMRotI50 at periods from 0.1s to 0.4s with short distance from the fault plane are slightly smaller than the predictions by GMPE. On the other hand, for the PGVs and GMRotI50s at periods longer than 2.5s with MED larger than about 100 km, the observations are generally larger than the prediction by GMPE, showing smaller attenuation.

Reference: Asano (2016): Private communication; Boore et al.(2006), BSSA; Koketsu et al.(2016):Private communication; Si et al.(2014), Proceedings of the 14th JEES.

Acknowledgement: We thank NIED to provide strong motion data by K-NET and KiK-net.

Keywords: The 2016 Kumamoto Earthquake, Attenuation Characteristics, GMRotI50

Characterized source model for estimating strong ground motions during 2016 Kumamoto earthquake

*Susumu Kurahashi[1], Kojiro Irikura[1]

1.Aichi Institute of Technology

1. Introduction
Strong ground motions from the 2016 Kumamoto earthquake (Mw7.3) strikeed in and around Kumamoto city, Kyushu, Japan, on April 16, 2016. The maximum seismic intensity 7 was observed at Mashiki and Nishihara near earthquake fault. PGA and PGV of 825 gal and 171 cm/s, respectively, were observed at the Mashikisite. Coseismic surface rupture is also identified along the Futagawa fault. We estimated the characterized source model, which explain broad-band strong motions, during this earthquake using the results of the waveform inversion using the strong motion data and the empirical Green's function method.
2. Source model inferred from the wavefrom inversion results
We analyzed the slip distribution during this earthquake using the multi-time window linear waveform inversion method (Sekiguchi et al., 2000). The data sets used for an analysis were velocity waveforms of S-waves parts in the frequency range 0.05-0.5Hz at 16 stations (KiK-net, K-NET, JMA and Seismic intensity network). The Green's functions were calculated using the one-dimensional velocity structure model by the discrete wavenumber method (Bouchon, 1981) with the reflection and transmission matrix method (Kennett and Kerry, 1979) at each station. A fault plane was assumed referring to the aftershock distribution and moment tensor solution determined by F-net. The fault plane is decided into 184 subfaults of 2km x2km. The temporal moment release history from each subfault is modeled by a series of 6 smoothed ramp function with a rise time of 1 second each separated by 0.5 second. The characterized source model is constructed based on slip and slip-velocity distributions from the waveform inversion.

3. Conclusion
Large slip areas were constructed about 15km eastward from the hypocenter. Especially, very large fault-slip was obtained at two places on the assumed fault plane, one at about 2 km depth and 8 km eastward away from the hypocenter and the other at about 2 km beneath Mashiki and Nishihara eastward from hypocenter. Seismic moment of the estimated model is 4.6×10^19Nm. The calculated waveform from the estimated model agrees rather well with the observed one at KMMH16 (KiK-net:Mashiki). However, the synthesized waveform of EW component at Mashiki-site of the seismic-intensity-network was clearly underestimated, although that of NS component agrees well with the observed one. The distance between two stations is about 200m away from each other.
One of the reasons why the EW component of ground motions at the site might be that fling step are not correctly simulated in our calculation. We will improve the source model to be able to explain the ground motions observed extremely near the earthquake fault.

Keywords: 2016 Kumamoto earthquake, strong ground motion, characterized source model

Along-Strike Ground Motion Variation for the 2016 Kumamoto Earthquake Sequence

*Hiroe Miyake[1], Kosuke Chimoto[2], Hiroaki Yamanaka[2], Seiji Tsuno[3], Masahiro Korenaga[3], Nobuyuki Yamada[4], Takeshi Matsushima[5]

1.The University of Tokyo, 2.Interdisciplinary Graduate School of Science and Engineering, Tokyo institute of Technology, 3.Railway Technical Research Institute, 4.Fukuoka University of Education, 5.Institute of Seismology and Volcanology, Faculty of Science, Kyushu University

Several earthquakes mainly with strike-slip faulting occurred during the 2016 Kumamoto earthquake sequence. Ground motions are observed by nationwide seismic networks installed after the 1995 Kobe earthquake. Especially, long-period ground motion pulse with a dominant period of around 3 s is observed along-strike stations as seen at NIED/KiK-net KMMH16 (downhole), Nishihara village station of the Kumamoto prefecture, KiK-net KMMH04 (ground surface). Fault parallel components are larger between the Mashiki town and the Nishihara village, on the other hand, fault normal components are larger inside the caldera of the Aso volcano. The former indicates rupture passed through along-strike stations, and the latter stations located at the forward rupture direction (e.g., Miyatake, 1999). We here investigate ground motion characteristics of the fault normal, fault parallel, and vertical components. In addition to the along-strike stations, ground motions at the rock site stations as KMP1 (Kyushu University) and NIED/F-net well constrain pulse width and arrival times for short-period and long-period components. However, current density of permanent stations is not enough to capture overall ground motion characteristics for M7-class inland crustal earthquakes. To overcome this issue, temporary strong motion observation along strike direction is deployed just after the 2016 Kumamoto earthquake sequence. The temporary stations record small-to-moderate size earthquakes. We introduce ground motion characteristics of some along-strike stations (Kumamoto Techno Research Park and Toriko in the Nishihara village) from azimuth dependency of source locations.

Acknowledgement: We used observation data by JMA, Kumamoto prefecture, NIED K-NET/KiK-net/F-net, and Kyushu University as well as the JMA unified hypocenter catalog. This work is partly supported by the Grant-in-Aid for Special Purposes (16H06298: P.I. Hiroshi Shimizu). Temporary strong motion observation is based on the research collaboration led by Tokyo Tech, Railway Technical Research Institute, ERI UTokyo, and Fukuoka University of Education.

Keywords: 2016 Kumamoto earthquake, strong ground motion, temporary strong motion observation

Quick report of aftershock and microtremor observations in disaster area due to the 2016 Kumamoto Earthquake
- From points of view of surface faulting and geographic transition in Mashiki town -

*Takao Kagawa[1], Shohei Yoshida[1], Hiroshi Ueno[1]

1.Tottori University Graduate School of Engineering

Aftershock and microtremor observations were conducted in Mashiki town where severe damage spreads over due to the 2016 Kumamoto Earthquake. Two targets are set for the observations. One is searching out the difference of ground motion between surface faulting areas without severe damage and severely damaged areas without surface faulting. Another is assessing the effect of surface geology and geographic transition on spotted damage distribution in downtown area. Using the observed records, productive discussions about causes of disaster are expected.
We express our appreciation to the local people who kindly showed their favoritism to our observations.

Keywords: Mashiki town, Aftershock observation, Microtremor observation, Surface faulting, Geographic transition

Strong motion observation of aftershocks of the 2016 Kumamoto Earthquake at temporary stations

*Kosuke Chimoto[1], Hiroaki Yamanaka[1], Seiji Tsuno[2], Hiroe Miyake[3], Nobuyuki Yamada[4]

1.Tokyo Institute of Technology, 2.Railway Technical Research Institute, 3.The University of Tokyo, 4.Fukuoka University of Education

The Japanese seismic intensity scale of 7 was observed in Mashiki and Nishihara, Kumamoto Prefecture, Japan during the 2016 Kumamoto Earthquake which caused heavy damages to many buildings and huge landslides. JMA reported that ground motion with the intensity above 1 has been observed more than 1,000 times due to the many aftershocks. We then have begun to perform temporary strong motion observation in Mashiki town, Nishihara village, Kumamoto city and Minami-Aso village to investigate the cause of the heavy damages.

We have installed a temporary strong motion network since 2016 April 16. We have deployed accelerometers at the town office of Mashiki where the intensity of 7 was observed, and near the strong motion station of the KiK-net Mashiki, operated by NIED. We also deployed stations in heavily damaged area along route 28, southern and northern part of the route, and also, perpendicular to the fault. In addition to the stations in Mashiki town, we installed the instruments at village office of Nishihara and Kurokawa-district in Minami-Aso village, etc. The instruments have also been deployed along a line from the east to the west in Kumamoto city. We used the accelerometer JEP-6A3 with sensitivities of 10V/G or 2V/G by Mitutoyo Corp. and the data loggers of LS7000XT or LS8800 manufactured by Hakusan Corp. The acceleration records are continuously obtained with a sampling of 100 Hz.

For the moment, we have collected the aftershock records from the temporary network in Mashiki town, including records due to events with the JMA Magnitudes of above 5 and seismic intensity of about 4. We observed high spatial variation of ground motion features in Mashiki town. The ground motion observed at the town office exhibits higher value than that observed at KiK-net Mashiki. The peak ground acceleration and peak ground velocity observed at the southern part of route 28 show larger values than those at the town office. The ground motion in agricultural field zone in the center of Mashiki town or the northern part of the town shows same level or smaller level to that at town office. We found a dominant peak at a period of about 0.5 seconds in the 5% damping velocity response spectra at the Mashiki town office, the site along route 28 and the southern part of the route.

The collection and the analysis of all records in the temporary network is remind work. We continue to investigate the spatial variety of ground motions by using those records. We are also planning to estimate S-wave velocity profiles using microtermor exploration to discuss about the ground motion characteristics of observed records.

Keywords: The 2016 Kumamoto Earthquake, Temporaray Strong Motion Observation, Aftershock

Characteristics of earthquake ground motions in the Kumamoto City, using the aftershock observation data of the 2016 Kumamoto Earthquake

*Seiji Tsuno[1], Masahiro Korenaga[1], Kazunori Wada[1], Kimitoshi Sakai[1]

1.Railway Technical Research Institute

During the 2016 Kumamoto earthquake occurred on 4/14 and 4/16, strong ground motions were observed in Kumamoto Prefecture, for examples, Mashiki recorded the Japanese seismic intensity scale of 7 and Kumamoto City recorded the scale of more than 6. The Kumamoto Plain spreading the northeastern area of Kumamoto Prefecture is consist of diluvial plateau in the west slope of the outer rim of Aso and alluvial lowland formed by Shirakawa and Midorikawa and therefore; it is pointed out that the earthquake ground motions are amplified largely in Kumamoto City due to the soft-soil sediments. To evaluate the characteristics of earthquake ground motions in the north-south cross-section in Kumamoto City, we performed the aftershock observation at 6 temporary stations (full length of 6km) along the railway line installed after the date of 4/15, 2016. We installed the accelerometer of JEP-6A3 (the sensitivity of 10V/G) by Mitutoyo Corp. and the data logger of LS8800 by Hakusan Corp. with the continuous recording at 2 stations on 4/15 and at 4 stations on 4/16, 2016.

Accelerations at 6 stations for an earthquake occurred at Aso were variety in the phase and the amplitude at the southern site was larger by a factor of 2 than one at the northern site. The earthquake ground motion at the southern site were amplified by a factor of 3 for a period of 0.5 second and by a factor of 2 for a period of 1 second, comparing to the earthquake ground motion at the northern site. The various levels of ground motions from small to large earthquakes, including the earthquake (Mj 7.3) occurred on 4/16/1:25, were recorded at 2 stations in the southern sites. In those velocity responses, the dominant period of 0.8 and 1.2 seconds were appeared at velocity response of 0.1 cm/s and 30 cm/s, respectively. In case of the large earthquake (Mj7.3), the nonlinearity of soft-soil was suggested by the dominant period of 2.2 seconds at velocity response of 120 cm/s. The earthquake records at 2 southern sites which are 600m far had a large difference for a period of 1 to 2 seconds. In the future, we will investigate the characteristics of earthquake ground motions at those 2 sites.

Keywords: Aftershock observation, 2016 Kumamoto earthquake, Kumamoto City

Attenuation Structure around Kumamoto Region.

*Shutaro Sekine[1]

1.Associatinon for the Development of Earthquake Prediction (ADEP)

Introduction
The seismic attenuation implies inelasticity or scattering of the structure. In this study, we estimate the 3-D attenuation structure beneath the Japanese islands by tomographic method. And we show the Kumamoto Region.

Data and Method
Vertical amplitude data of the JMA Catalog from January 1994 to December 2014. The data is represented by the indices Qp and Qs, which are dependent on the frequencies of ground motion. We estimate each earthquake mechanism, and the effect of the radiation pattern is also applied. The study area of the inversion is whole Japanese island, a grid with interval of 0.25 degree in horizontal is applied to this region at depth of every 5km to 50 km, and then 10km to 100km.

Result
The target area of the Kumamoto Earthquake region, is shallow, so the resolution of the checker board test is almost good. Most of earthquakes are occurred in the high-Q region. Between Kuju region to Yufu, the low-Q area is laid, and earthquakes don’t occur in this series of the earthquakes.

Acknowledgement
The earthquake catalog used in this study is produced by the Japan Meteorological Agency, in cooperation with the Ministry of Education, Culture, Sports, Science and Technology. The catalog is based on seismic data provided by the National Research Institute for Earth Science and Disaster Prevention, the Japan Meteorological Agency, Hokkaido University, Hirosaki University, Tohoku University, the University of Tokyo, Nagoya University, Kyoto University, Kochi University, Kyushu University, Kagoshima University, the National Institute of Advanced Industrial Science and Technology, the Geographical Survey Institute, Tokyo Metropolis, Shizuoka Prefecture, Hot Springs Research Institute of Kanagawa Prefecture.

Reference
S.Sekine (2005): Tomographic Inversion of Ground Motion Amplitudes for the 3-D Attenuation Structure beneath the Japanese Islands, Report of the National Research Institute for Earth Science and Disaster Prevention, 68, 137-174

Keywords: attenuation structure, Q

130.76481 32.75389 224

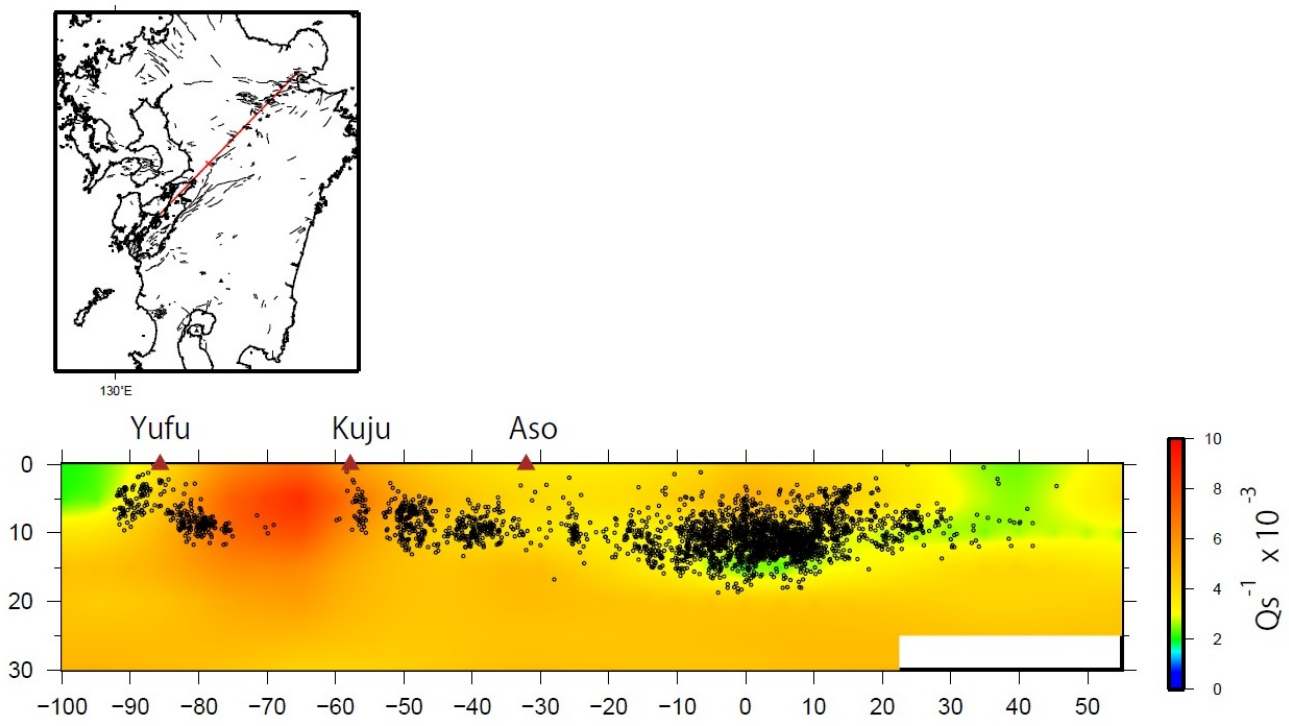

Site amplification at strong-motion stations in the Kumamoto prefecture and identification of underground velocity structures at Mashiki

*Hao Wu[1], Susumu Kurahashi[2], Kazuaki Masaki[1], Kojiro Irikura[1]

1.Disaster Prevention Research Center, Aichi Institute of Technology, 2.Department of Civil Engineering, Aichi Institute of Technology

We made a field survey near ten strong-motion stations to confirm the damage of buildings after the mainshock of the 2016 Kumamoto Earthquake. The JMA seismic intensity was as large as 6-upper at six stations. We measured microtremors at two K-NET stations, three KiK-net stations and five Seismic Intensity Information Network (SIIN) stations. We found that the microtremor H/V of spectral ratios at most of the stations have a predominant period around 1.0 sec. We examined the reliability of PS logging data at three KiK-net stations, i.e., KMMH03, KMMH14 and KMMH16 by comparing the theoretical H/V spectral ratio based on diffuse field approach (Sanchez-Sesma, et al. 2011, GJI) with the observed one. The shape and amplitude of the theoretical H/V spectral ratios around the fundamental predominant period are almost the same as those of the observed counterpart at these three KiK-net stations. It suggests that the PS logging data under these stations are reliable. However, the PS logging data at the KMMH16 station (Mashiki) are not adequate to explain the peak at about 2.5 sec of the observed microtremor H/V spectral ratio.

We attempt to identify the underground velocity structures in the deep layer at KMMH16 station from the microtremor H/V spectral ratio of surface waves based on the diffuse field approach (DFA). The initial underground velocity model in the deep layer is referred to the J-SHIS. We obtain the best underground velocity structures after confirming the good coincidence between the theoretical and observed H/V spectral ratios. The identified underground velocity structures are used to evaluate the transfer functions at KMMH16. We make a comparison of the transfer functions at these three KiK-net stations. We find that the site amplification as large as about 8 at 0.2 sec and 1.0 sec is almost the same at the KMMH03 and KMMH14 stations. The site amplification at the KMMH16 station is as large as 10 from 0.2 sec to 1.0 sec, and as large as 5 from 2.0 sec to 3.0 sec which is affected by the deep layers.

Keywords: site amplification, microtremor H/V spectral ratio, underground velocity structures

Earthquake Early Warning for the 2016 Kumamoto earthquakes: on overview of how warnings and forecasts were issued and expected improvements that come from introducing new methods

*Yuki Kodera[1], Jun Saitou[2], Naoki Hayashimoto[2], Shinpei Adachi[2], Masahiko Morimoto[2], Yuji Nishimae[2], Mitsuyuki Hoshiba[1]

1.Meteorological Research Institute, Japan Meteorological Agency, 2.Seismology and Volcanology Department, Japan Meteorological Agency

During the period from 14 to 30 April 2016, the Japan Meteorological Agency (JMA) issued 175 forecasts and 19 warnings of Earthquake Early Warning (EEW) whose estimated hypocenters were located around the Kyushu district. For an earthquake in the Kumamoto prefecture at 21:26 (JST) in 14 April (M6.5), JMA issued a warning about 3.8 sec. after detecting the seismic wave. For an earthquake in the Kumamoto prefecture at 01:25 (JST) in 16 April (M7.3), JMA issued two warnings about 3.8 and 8.6 sec. after the detection. Scores of seismic intensity prediction(*) in the warning for the M6.5 earthquake in 14 April and the second warning for the M7.3 earthquake in 16 April were 100.0% and 97.4% respectively. During the period, there were 18 earthquakes where the maximum observed JMA seismic intensity was 5-lower or more. JMA disseminated warnings or forecasts that predicted the maximum intensity of 4 for all of them, which means the EEW system did not miss strong motions in large earthquake events. After the M7.3 earthquake in 16 April, zones of earthquake occurrence expanded and simultaneous multiple earthquakes happened frequently with a distance of about 50 to 100 km away. Since the 2011 off the Pacific coast of Tohoku earthquake, JMA has continued to improve the process of grouping trigger data when simultaneous multiple earthquakes happen (e.g. JMA implemented a strict range limitation of stations targeted for comparing trigger data based on a station network configuration). However, in the Kumamoto earthquakes, distances of simultaneous multiple earthquakes were too short for the system to correctly discriminate each of them. There were some cases that it over-predicted seismic intensities by wrongly processing trigger data from multiple earthquakes, assuming that the data came from a single earthquake. During the period, JMA issued four incorrect warnings whose score of seismic intensity prediction was less than 10% due to simultaneous multiple earthquakes.

JMA plans to introduce new methods: Integrated Particle Filter (IPF) method, expected to be a measure for over-prediction with simultaneous multiple earthquakes, and Propagation of Local Undamped Motion (PLUM) method, for under-prediction with huge earthquakes. Simulations for the incorrect warnings mentioned above show IPF method avoids issuing incorrect warnings in three cases and reduces the number of areas affected by a warning in the remaining case. Simulations with PLUM method reveal that it makes the system issue the first warnings for the M6.5 earthquake in 14 April and the M7.3 earthquake in 16 April about 2.6-3.6 and 3.0-4.0 sec. faster than the current method, which resulted from denser observation network in PLUM method.

(*) “Score of seismic intensity prediction” is defined as a percentage of areas where an error of seismic intensity prediction is within one degree on the JMA scale among areas where observed or predicted seismic intensity is 4 or more.

Keywords: Earthquake Early Warning, the 2016 Kumamoto earthquakes

Real-time Damage Estimations for the 2016 Kumamoto Earthquakes by J-RISQ

*Hiromitsu Nakamura[1], Hiroyuki Fujiwara[1], Yoshinori Homma[2]

1.National Research Institute for Earth Science and Disaster Resilience, 2.Mitsubishi Space Software Corporation

The National Research Institute for Earth Science and Disaster Resilience (NIED) is developing a real-time earthquake information system for damage estimation and situation assessment (J-RISQ) as a Cross-ministerial Strategic Innovation Promotion Program (SIP).J-RISQ is able to immediately estimate earthquake damage by combining methods for predicting ground motion using amplification characteristic data for subsurface ground, basic information on population and buildings, damage assessment methods for buildings using fragility functions, and observation data such as real-time strong motion data obtained by K-NET, KiK-net, local governments, and JMA. A part of J-RISQ information (including the estimated distribution of seismic intensity and the population exposed to each seismic intensity level) is published as a “J-RISQ Report” on http://www.j-risq.bosai.go.jp/ immediately after the occurrence of an earthquake. In this study, we describe the estimations by J-RISQ for the 2016 Kumamoto earthquakes (M6.5 event and M7.3 event) with maximum seismic intensity of 7 caused great damage to human beings, buildings, and infrastructures.
J-RISQ issued the first report 29 seconds after the M6.5 event occurred and a total of seven reports for about 10 minutes. The first report using data from 5 stations showed that population exposed to seismic intensity 6 lower or larger was 7,800. Finally the system estimated that population exposed to seismic intensity of 6 lower or larger was 620,000 and that of 6 higher or larger was 290,000 by using 1091 strong motion data. The estimated results of building damage showed that completely destroyed buildings were between 6,000 and 14,000 and partly destroyed were between 7,000 and 33,000. The distribution of estimated completely destroyed buildings spread 7 km long by 1 km wide in Mashiki town.
For the M7.3 event occurred about 28 hours after the M6.5 event, the system distributed the first report 29 seconds after the M7.3 event occurred and a total of eight reports for about 11 minutes. Finally the system estimated that population exposed to seismic intensity of 6 lower or larger was 1,130,000 and that of 6 higher or larger was 670,000 by using 2391 strong motion data. The estimated results of building damage showed that completely destroyed buildings were between 16,000 and 38,000 and partly destroyed were between 18,000 and 88,000. The distribution of estimated completely destroyed buildings spread in Mashiki town similar to the result of the M6.5 event and Kumamoto city. However, this result of damage building is out of consideration of the effect of the earthquakes including M6.5 event before M7.3 event. At this time, we are not able to compare these results with real damage because the whole picture of real damage has not been grasped yet. A detailed analysis of real damage is to be desired.

Acknowledgements
This work was supported by the Council for Science, Technology and Innovation (CSTI) through the Cross-ministerial Strategic Innovation Promotion Program (SIP), titled ``Enhancement of societal resiliency against natural disasters'' (Funding agency: JST). The seismic intensity data from local governments and JMA that were used in the real-time system were provided by JMA.

Keywords: Kumamoto earthquake, J-RISQ, real-time damage estimation

Building Damage in the Mashiki-town for the foreshock and mainshock of the 2016 Kumamoto earthquake

*Masumi Yamada[1], Junzo Ohmura[2], Hiroyuki Goto[1]

1.Disaster Prevention Research Institute, Kyoto University, 2.Bukkyo University

The 2016 Kumamoto earthquake caused serious building damages in the near-source regions. The Mashiki-town, about 10km northeast from the epicenter, was located less than 1km from the fault line and subjected to the two strong shakings of level 7 in the JMA seismic intensity scale. The first earthquake (foreshock, Mj6.5) occurred at 21:26, April 14 and the second one (mainshock, Mj7.3) occurred at 1:25, April 16. Since there was only 28 hours interval, it is difficult to classify the damage of two earthquakes.

We analyzed the aerial photos taken by the Geospatial Information Authority of Japan on 15th and 16th of April (http://www.gsi.go.jp/BOUSAI/H27-kumamoto-earthquake-index.html). The photos cover the damaged area in Mashiki-town, and two sets of photos taken before and after the mainshock help classifying the damage due to the foreshock and mainshock. We defined the following houses as collapsed building: 1) edge of the building is distorted 2) roof tiles are completely fallen down 3) center line of the roof is tilted 4) debris is observed around the building. We excluded public reinforced concrete structures.

We observed 130 totally collapsed buildings after the foreshock, but the number increased to 350 after the mainshock. The damaged buildings after the foreshock distributed between route 28 and Akitsu river, but the distribution expanded to the north of the route 28 after the mainshock. There are two strong motion stations in the surveyed area (Mashiki LGV and KiK-net KKMH16). Both stations recorded seismic intensity 7 for the mainshock, but the damage distribution was very different. 21 buildings were collapsed within 200m of the Mashiki LGV, whereas only 4 building collapsed within 200m of the KiK-net KKMH16.

The distribution of the damaged buildings after the mainshock has a good correlation with the distribution of the village 100 years ago . The region around the village was originally floodplain and river terrace of Akitsu river. The village was developed at the edge of the river terrace, and the floodplain was used as a rice field. In 1970s, the village was expanded to the upper river terrace and floodplain. The floodplain is in general considered to be softer soil condition, but for this particular area, damage on the floodplain was much less than that on the river terrace. We need further survey to classify the effect of the subsurface soil structure and seismic performance of the buildings for the better understanding of the damage distribution.

Figure: Damage distribution after the mainshock and aerial photo in 1964.

Keywords: 2016 Kumamoto Earthquake, Building Damage

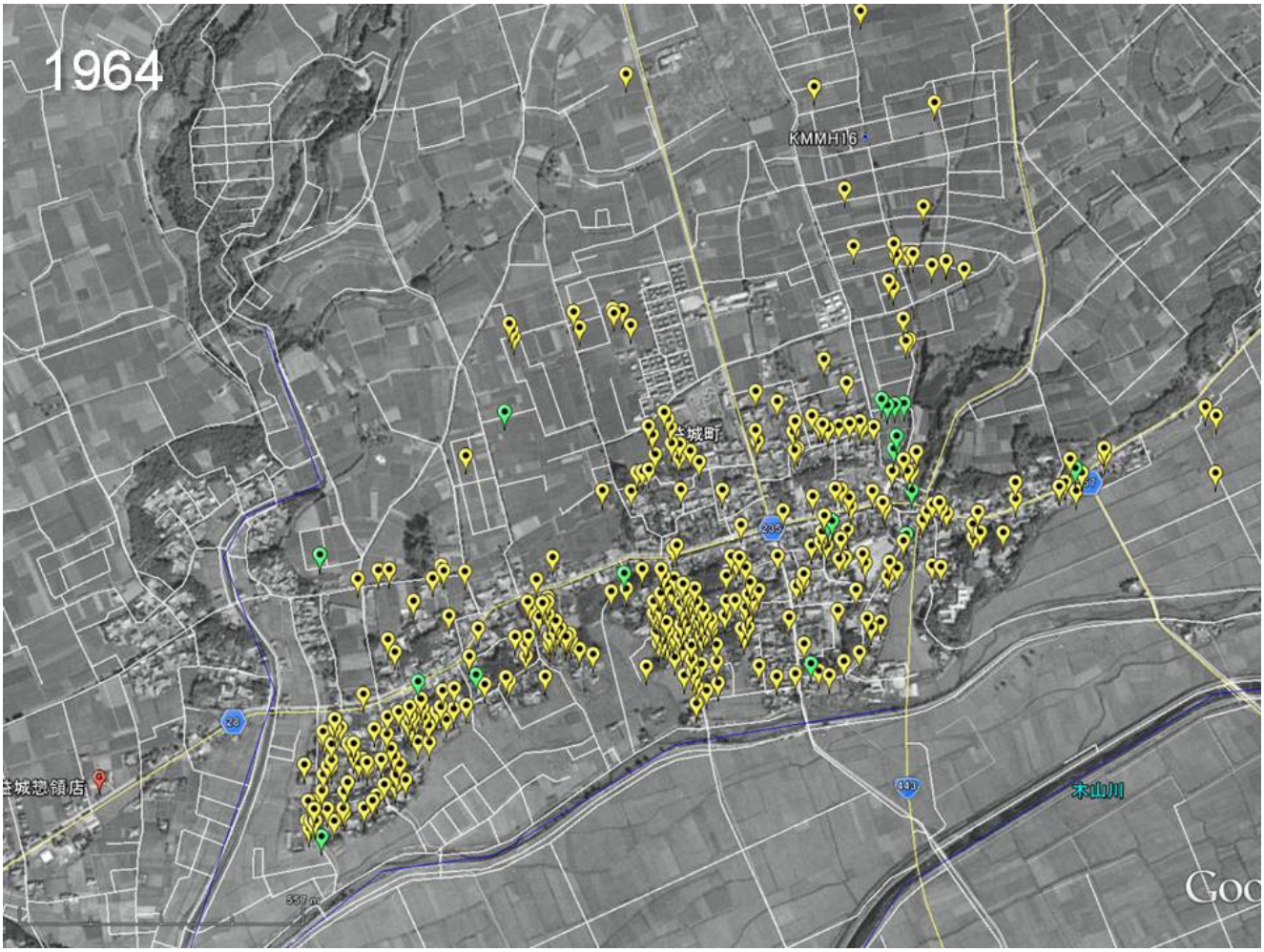

Distribution patterns of house damages in the central part of Mashiki Town caused by the 2016 Kumamoto Earthquake: Geological and geomorphological implications

*Tsutomu Nakazawa[1], Atsushi Urabe[2], Yoshiki Sato[1]

1.Geological Survey of Japan, AIST, 2.Research Institute for Natural Hazards and Disaster Recovery, Niigata University

Serious house damages were caused by the 2016 Kumamoto Earthquake in the central part of Mashiki Town, Kumamoto Prefecture. Our detailed investigation on the damage distribution reveals that the houses were most seriously damaged in the lower part of the gentle-slope areas along the margin of the uplands and less damaged in the lowland along the Akitsu-gawa River. Lateral movements and/or failures of the embankment caused the collapse of houses only in the steep slope areas along the small incised valleys.
Although the uplands in the study area are composed mainly of pyroclastic-flow deposits derived from the Aso volcano, they are covered by soft tuffaceous muddy sediments with various thickness. Consequently, the margin of the uplands, in which the house damages were most serious, would be underlain by the thick soft muddy sediments or ones with different (rather soft) physical properties.

Keywords: earthquake disaster, house damage, geologic setting

Damages of museums suffered from the 2016 Kumamoto Earthquake

*Akihisa Kitamura[1], Naoki Ikegami[2], Haruyoshi Maeda[3], Makoto Manabe[4]

1.Institute of Geosciences, Faculty of Science, Shizuoka University, 2.Mifune Dinosaur Museum, 3.The Kyushu University Museum, 4.National Museum of Nature and Science

We report damages of Mifune Dinosaur Museum suffered from the 2016 Kumamoto Earthquake.

Keywords: 2016 Kumamoto Earthquake, Kumamoto prefecture, museums, damages

Preliminary report of liquefaction damage and distribution of liquefied sites caused by the 2016 Kumamoto Earthquake

*Koki Teshirogi[1], Takushi Koyama[2], Haruhiro Doi[2]

1.Research Institute for Humanity and Nature, 2.Oita Univ.

Kumamoto city was affected by the liquefaction due to the 2016 Kumamoto Earthquake. This preliminary report shows overview of the liquefaction damage and the distribution of liquefied sites at the Nishi and Minami Wards, Kumamoto city by field observation and interpretation of satellite images.

Keywords: Liquefaction damage, Topographic conditions, The 2016 Kumamoto Earthquake, Liquefaction site map

Distribution and land conditions of the liquefied sites caused by the 2016 Kumamoto Earthquake

*Masafumi Aoyama[1]

1.Faculty of Education, Gunma University

Distribution and land conditions of the Liquefied sites caused by the 2016 Kumamoto Earthquake were investigated by the field survey and aerial photo interpretation. A large number of the liquefaction damages were concentrated on the zonal area located on the natural levee between the Shirakawa River and Kasegawa River. A number of the liquefied sites were observed on the former river channels and natural levees along the Shirakawa River, Midorikawa River and Kasegawa River. Sand boils were also observed at the refilled lot of gravel pits along the Midorikawa River.

Keywords: liquefaction, former river channel, natural levee, refilled gravel pit, land condition

Liquefied sites during the 2016 Kumamoto Earthquake

*Shigeki Senna[1], Wakamatsu Kazue[2], Kyoko Ozawa[1], Hiroyuki Fujiwara[1]

1.National Research Institute for Earth Science and Disaster Prevention, 2. Kanto Gakuin Univ

This paper summarizes reconnaissance surveys of liquefaction and its damage to structures during the 2016 Kumamoto Earthquake. The principal findings include: 1) Sand boils observed in eight cities and towns in Kumamoto City and the surrounding areas where seismic intensity 6 minor in the Japan Meteorological Agency Scale was observed during the foreshock, main shock or aftershocks; 2) Geomorphologic units of liquefied sites are reclaimed land, natural levee, back marsh, former river channel and delta along the major rivers in the affected areas including Shirakawa, Midorikawa and their tributaries; 3) Repeated liquefaction was observed at Akitsu, Kumamoto City and Syouwa-doujin-machi, Yatsushiro City where liquefaction took place during the 1889 Kumamoto and 1968 Hyuganada earthquakes, respectively.

Keywords: liquefaction, seismic intensity, geomorphologic land classification

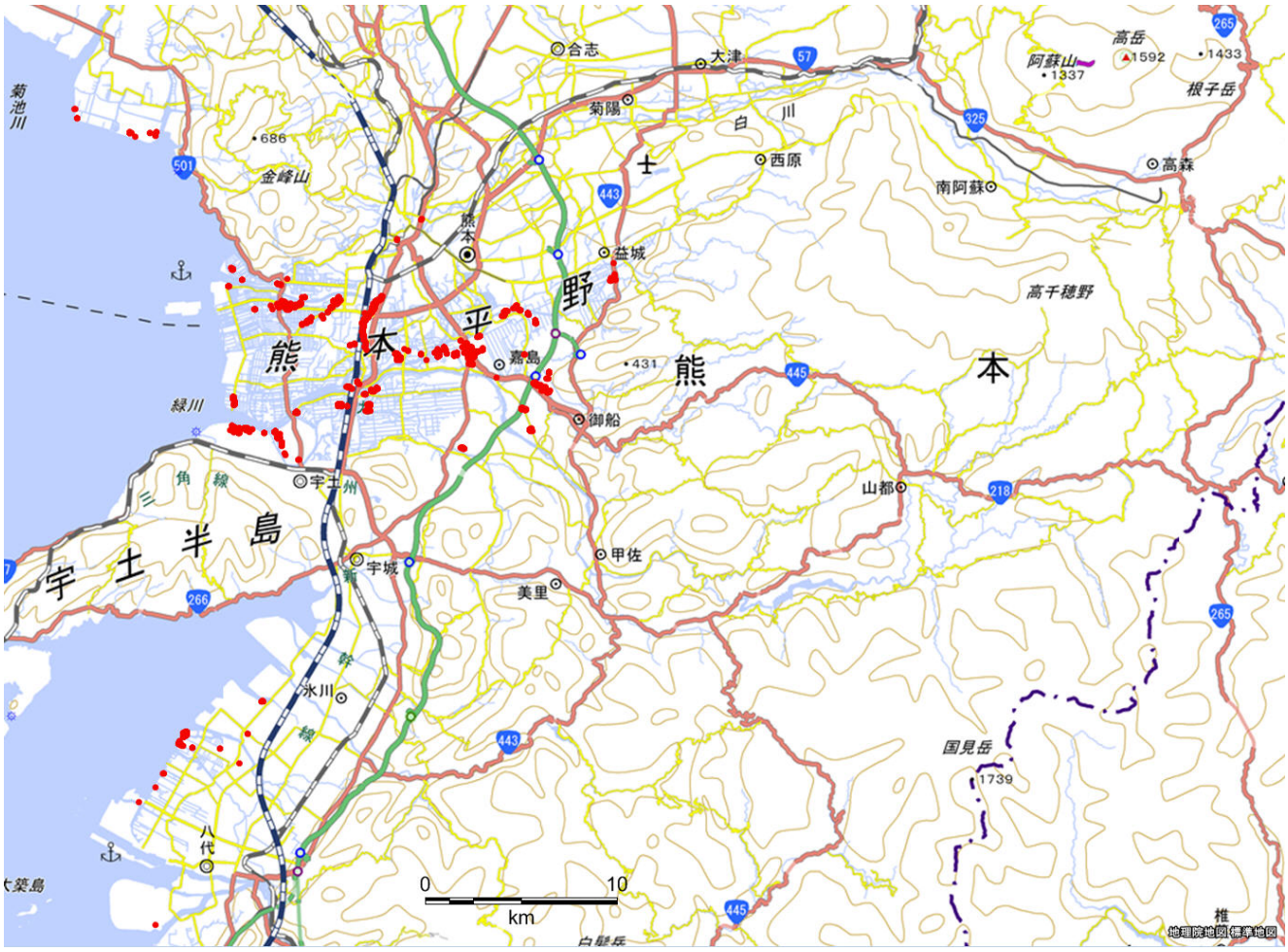

Distribution of liquefactions and sand volcanoes in Aso Caldera, associated with the 2016 Kumamoto earthquake

*Daisuke Ishimura[1], Shinji Toda[2]

1.Department of Geography, Tokyo Metropolitan University, 2.International Research Institute of Disaster Science, Tohoku University

In this study, I report distribution of liquefactions and sand volcanoes in Aso Caldera, associated with the 2016 Kumamoto earthquake. Surface rupture associated with the M7.3 earthquake on 16 April (Japan Meteorological Agency, 2016) was identified along the Futagawa and Hinagu faults. The easternmost point of the identified surface ruptures was at the western part of the Aso Caldera. However, liquefactions and sand volcanoes were widely distributed on lowlands in the northern part of the Aso Caldera. On the other hand, they were not identified in the southern part of the caldera. In order to reveal this difference, I mapped liquefactions and sand volcanoes based on aerial photos taken by Geospatial Information Authority of Japan. I will report their features and comparison with InSAR images (Geospatial Information Authority of Japan, 2016) on the presentation.

This study was supported by a special emergency grant from the International Research Institute of Disaster Science (IRIDeS), Tohoku University.

Geospatial Information Authority of Japan (2016) The 2016 Kumamoto Earthquake
http://www.gsi.go.jp/BOUSAI/H27-kumamoto-earthquake-index.html
Japan Meteorological Agency, 2016, The 2016 Kumamoto Earthquake -Portal-.
http://www.jma.go.jp/jma/en/2016_Kumamoto_Earthquake/2016_Kumamoto_Earthquake.html

Keywords: 2016 Kumamoto earthquake, liquefaction, sand volcano, lateral spreading

Co-seismic pore pressure/groundwater level changes associated with the 2016 Kumamoto Earthquake(Mj7.3)

*Yasuhiro Asai[1], Hiroshi Ishii[1], Osamu Murakami[1]

1.Tono Research Institute of Earthquake Science, Association for the Depvelopment of Earthquake Prediction

Clear pore pressure/groundwater level changes associated with the 2016 Kumamoto Earthquake (Mj7.3) were observed at borehole observation sites (STG200, STG200N, and TGR350), Tono region, central Japan (Hypocentral Distances are approximately 665km). Amount of pore pressure changes in STG200 and STG200N are approximately 25kPa-rise, and groundwater level in TGR350 is approximately 2m-rise. We will present the details of these pore pressure/groundwater level changes, and attempt to clarify the qualitative/quantitative model for the co-seismic pore pressure/groundwater level changes.

Keywords: The 2016 Kumamoto Earthquake (Mj7.3), Co-seismic pore pressure/groundwater level changes

Earthquake fault and "severely damaged zone" in Mashiki Town and Minami-Aso Village.

*Mitsuhisa Watanabe[1], Yasuhiro Suzuki[2], Takashi Nakata[3]

1.Faculty of Sociology, Toyo University, 2.Nagoya University, 3.Hiroshima University

The 2016 Kumamoto earthquake occurred by rejuvenation of the Futakawa-Hinagu fault. In the vicinity of the Futagawa-Hinagu fault, severe damage was concentrated. In Makishi Town, where high seismic intensities were recorded on April 14th and 16th, numerous buildings collapsed during the earthquake on April 16th. The “severely damaged zone” approximately less than 1 km in width, trended in the east-west direction. In Minami-Aso village, several earthquake faults were discovered, and almost all of the buildings located on these faults collapsed. At least five cars overturned onto their sides in the north to northward direction. Such phenomenon had not been observed before in Japan. It is very important to specify the area where the seismic intensity could reach 7 for disaster prevention. The location and the characteristics of active faults are the most important and indispensable informations.

Keywords: Active fault, Earthquake fault, Earthquake disaster, Concentration of damage

Investigation on earthquake damage in the Near-Surface-Fault area during the 2016 M_w7.0 Kumamoto earthquake

*Hongjun Si[1], Tetsuro Sasaki[2]

1.Seismological Research Institute Inc., 2.The Japan Atomic Power Company

On 16 April, 2016, an earthquake of M_{JMA}7.3 (M_w7.0) occurred in Mashiki-machi, Kumamoto Prefecture. During the earthquake, traces of surface fault are observed in the source region along the Futagawa and Hinagu faults, and heavy building damages are report in Mashiki machi, South Aso village, and other area.
In this study, in order to study the damages in the near field area, we carried out an investigation for the damage in the near-surface-fault-area, from 6th to 8th, May, 2016, 20 days after the earthquake. The main methods used in the investigation are interviews and photography. The investigation is carried out along the Futagawa faults at Fukuhara, Shimochin, Kamichin, sugidou, and Miyazono in Mashiki machi, Ohkirihata dam in Nishihara village, and Kawayo and Kurokawa area in South Aso village. The preliminary results of the investigation indicate that, (1) The surface faults are a little distant from the center of the Mashiki machi, the most damaged area; (2) in Mashiki machi, the damaged buildings just near the surface faults tend to be older buildings, rather than newer and well-constructed ones. (3) in the South Aso village, relatively new buildings just on the fault were damaged due to large deformation, but keep not collapsed, though an old temple building was totally collapsed.
Based on our preliminary results, a Future detailed investigation is considered necessary for better understanding the damages during the Kumamoto earthquake.

Keywords: Surface fault, Damage, Kumamoto earthquake

Trial of detection for damaged urban area and landslide area from wide range of image obtained by L-ban SAR (PALSAR-2)

*Manabu Watanabe[1], chinatsu Yonezawa[2], Jun Sonoda[3], Masato Ohki[4], Naoya Tomii[4], Masanobu Shimada[1]

1.Tokyo denki Univ., 2.Tohoku Univ., 3.National Institute of Technology, Sendai College, 4.JAXA

PALSAR-2 (Phased Array type L-band Synthetic Aperture Radar 2), L-band SAR on-board Advanced Land Observing Satellite-2 (ALOS-2), data were used to detect disaster areas caused by the 2016 Kumamoto earthquake.
1. Coherence change technique with coherence filter [1] was used to detect damaged urban areas.
2. Alpha angle [2] and HH-VV coherence [3] change techniques were used to detect landslide areas.
The coherence change technique with coherence filter identifies candidates of severely damaged urban areas located along a fault, which induces the earthquake. The detected damaged areas are Mashiro town, Koyo area in Minamiaso village, which incudes Aso campus of Tokai university, Aso Ohashi bridge, and some of landside areas.
Some landslides occurred in a forest area before the disasters were detected by using the alpha angle and HH-VV coherence change techniques. But miss-identification were often observed. Additional forest mask was produced from the image taken before the disaster, and tested to reduce the miss-identification. It is confirmed that the forest mask works well to reduce the miss-identification of landslide area.

[1] M. Watanabe, R. Natsuaki, H. Nagai, T. Motohka, T. Tadono, M. Ohki, R. B. Thapa, C. Yonezawa, M. Shimada, S. Suzuki, Damaged area detection caused by 2015 Nepal earthquake with coherence difference obtained by PALSAR-2 three observations, JpGU 2015, May 24-28, 2015, Makuhari Messe/Chiba
[2] Pi-SAR-L2 observation of the landslide caused by Typhoon Wipha on Izu Oshima Island, M. Watanabe, R. B. Thapa, M. Shimada, Remote Sensing, 8(4), 282, 2016
[3] M. Shimada, M. Watanabe, N. Kawano, M. Ohki, T. Motooka, W. Wada, Detecting mountainous landslides by SAR polarimetry: A comparative study using Pi-SAR-L2 and X band SARs. Trans. Jpn. Soc. Aeronaut. Space Sci., Aerosp. Technol. Jpn. 2014, 12, 9–15.

Keywords: The 2016 Kumamoto earthquake, Coherence, Polarimetry

Emergency response of earth observation satellites for the Kumamoto earthquake 2016

*Hiroto Nagai[1], Ryo Natsuaki[1], Mitsunori Ishihara[1], Masato Ohki[1], Takeo Tadono[1], Takeshi Motohka[1], Shinichi Suzuki[1]

1.Japan Aerospace Exploration Agency

The Japan Aerospace Exploration Agency carried out emergency observation by means of PALSAR-2 onboard ALOS-2, corresponding to the Kumamoto earthquakes started from April 16, 2016. Acquired PALSAR-2 images and several other images observed by international satellites were analyzed for hazard recognition since its early stage. This presentation shows multiple methods which were used for this activity.

Keywords: the Kumamoto earthquake, PALSAR-2, ALOS-2

How quickly can topographic data are acquired after earthquake? A case study for the landslide in Minami-Aso, Kumamoto, Japa

*Yuichi S. Hayakawa[1]

1.Center for Spatial Information Science, The University of Tokyo

A large earthquake can drastically deform the land surface including buildings, roads and slopes, therefore prompt topographic mapping of damaged areas is crucial for identification of those changes just after the earthquake. Photographs or videos taken either on ground or from air often provide great amount of information, but more can be obtained, including three dimensional data, from those datasets. Structure-from-Motion Multi-View Stereo (SfM-MVS) photogrammetry enables to generate three-dimensional topographic data from multiple photographs or video images. Here the author demonstrates prompt 3D mapping of the earthquake-triggered landslide occurred in Minami-Aso, Kumamoto. Several data sources are utilized for the photogrammetric processing, including oblique aerial photographs taken from a manned aircraft, and video images taken by either a manned or unmanned aircraft. The data processing can be carried out remotely, without the necessity to visit the field site if the data sources are provided online. Topographic data, with accuracies on the order of meters, were obtained within tens of minutes after these data sources became available. An example is shown in the figure attached, which was generated from oblique aerial photographs provided by Geospatial Authority of Japan (GSI). During the data processing, setting ground control points (GCPs) was the most time consuming because it requires manual reading of the images. The images of the mapped data (topographic contour lines, hillshade image, and orthorectified photographs) were promptly shared over online social networks including twitter and facebook, as visible jpg or animation gif files, and the data itself including point cloud, digital elevation model and orthorectified image were published in an online data storage system (Hayakawa, 2016). Three-dimensional models (point cloud or TIN) were also shared online to enhance the visibility of the data. These data helped some people particularly in remote places (e.g., university students and overseas researchers) to understand the situation of the landslide area, although limitations exist for the on-site use. For the purpose of enhancing the use of prompt and accurate 3D mapping, the speed of such data processing should be further improved. The exported products should also be in other formats, not only digital ones but also printed paper maps, if they are to be used for on-site rescue purposes. This study is supported by JSPS KAKENHI Grants (25702014).
Hayakawa, Yuichi (2016),"Topographic data generated from oblique aerial photos in Minami-Aso, Kumamoto, Japan just after the April 2016 earthquake", Mendeley Data, v1. doi:10.17632/sbxkzhy7h6.1

Keywords: structure-from-motion multi-view stereo photogrammetry, point cloud, digital elevation model, data sharing, landslides, topographic mapping

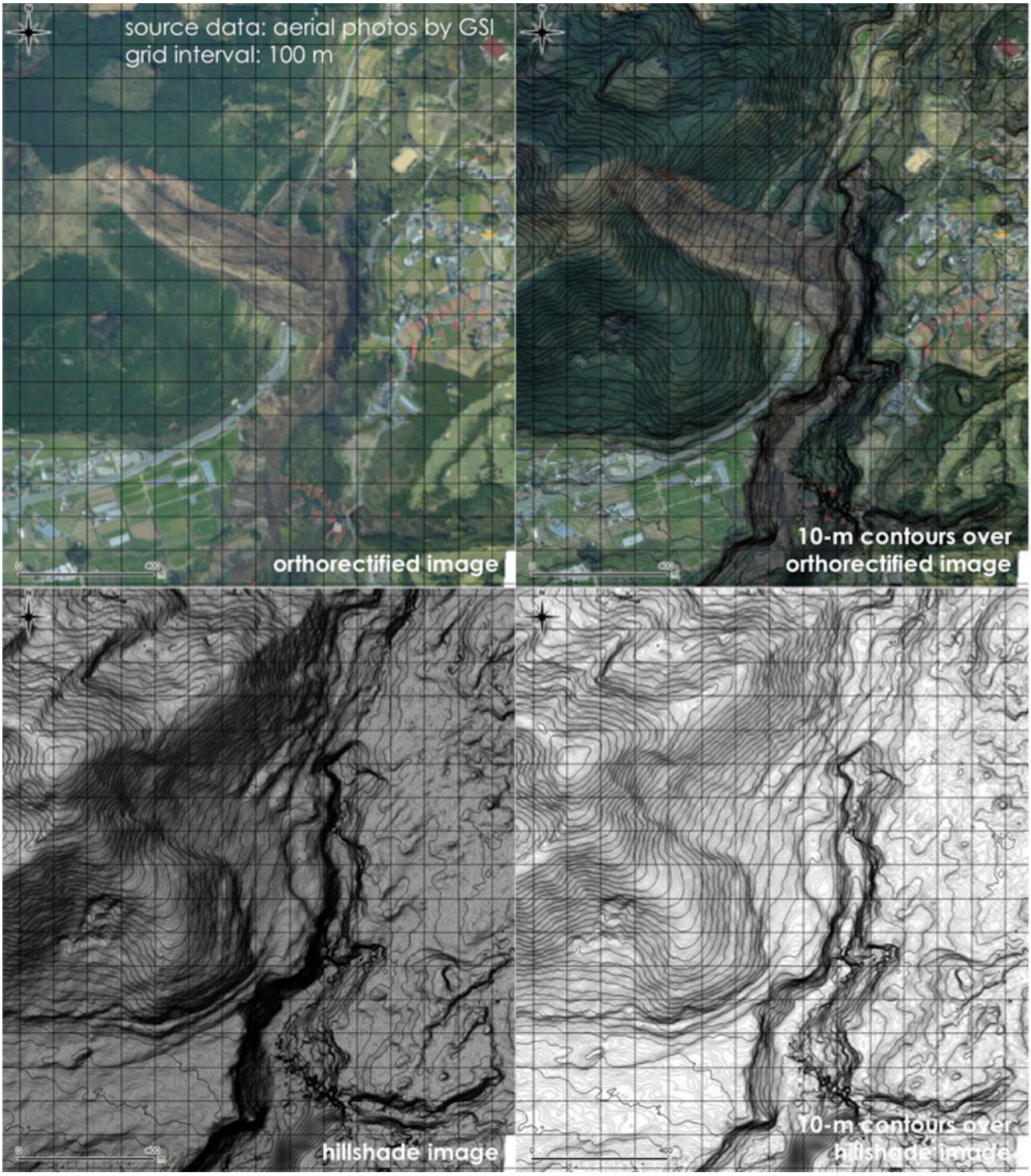

Surveillance of the Damage Inflicted by the Kumamoto Earthquake Using the Airborne X-band SAR System (Pi-SAR2)

*Minoru Kubota[1], Seiho Uratsuka[1], Syoichiro Kojima[1], Jyunpei Uemoto[1], Akitsugu Nadai[1], Toshihiko Umehara[1], Takeshi Matsuoka[1], Tatsuharu Kobayashi[1], Maiko Mitsumori[1]

1.National Institute of Information and Communications Technology

The second generation airborne synthetic aperture radar system, called as Pi-SAR2, has been developed by NICT (National Institute of Information and Communications Technology) in 2009. The system provides high-resolution, X-band, polarimetric and interferometric data. The spatial resolution is 0.3 m in the azimuth and the slant range directions. Using this equipment, areas of over 7 km wide, flying distances of over 50 km can be observed in a single pass from an altitude of about 9,000 m.
NICT conducted urgent Pi-SAR2 observations to survey the damage inflicted by the Kumamoto earthquake the day after the earthquake of M 7.3 occurred on 16 April. The observation areas (flight-paths) and Pi-SAR2 images of the area around Aso-ohashi-bridge are shown in Figure 1. SAR images were processed in flight using the onboard processor, transmitted to NICT via satellite, distributed to headquarters for disaster control, and uploaded onto the website within 10 minutes after the observation. In this paper, we present methods of the Pi-SAR2 observation and results of analyses. We also discuss how airborne SARs should be utilized in times of disaster.

Keywords: Kumamoto Earthquake, synthetic aperture radar, SAR

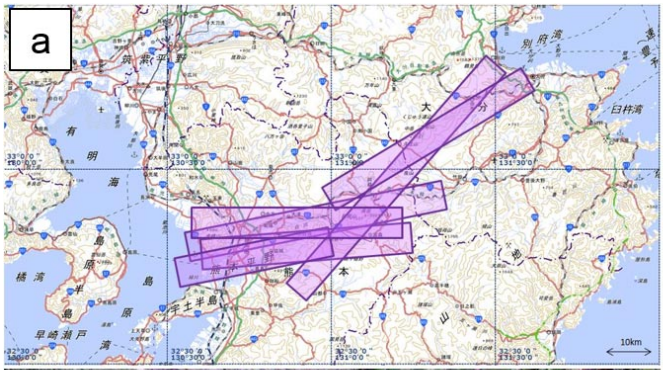

a) Pi-SAR2による熊本地震緊急観測（2016年4月17日）のフライトパス

b) 南阿蘇村阿蘇大橋付近の観測画像拡大図

c) 同じ領域の被災前（2015年12月5日）の観測画像

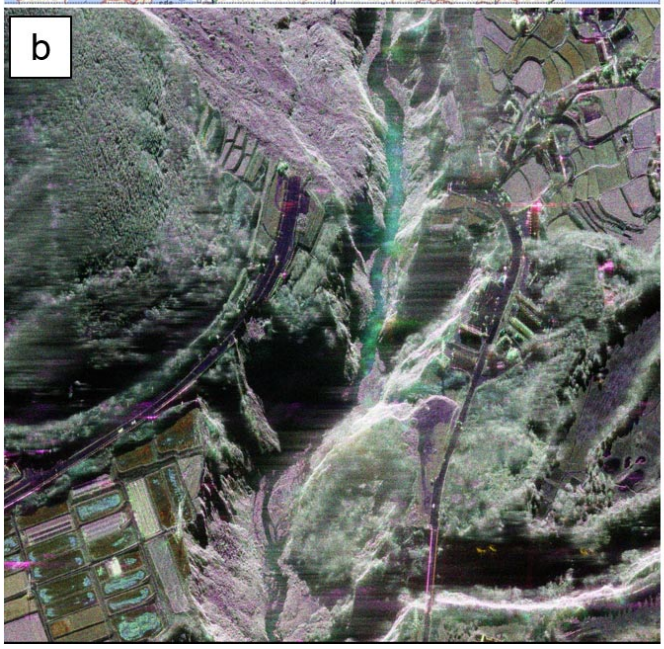

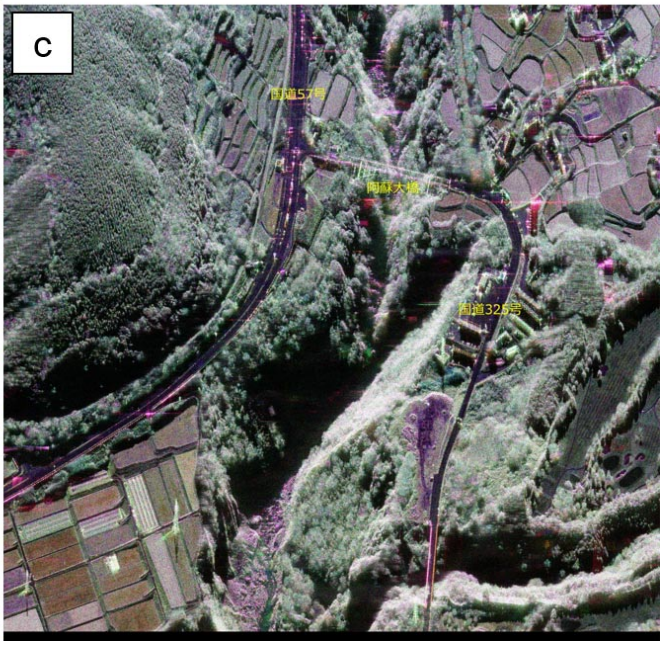

Detection of morphological changes around post-caldera central cones of Aso Volcano caused by the 2016 Kumamoto Earthquake using aerial photos and 3D model

*Hisashi Sasaki[1], Yasuyuki Hirakawa[1], Kazuya Yamaguchi[1], Kenichi Arai[1], Koji Fujita[1], Shino Naruke[1], Tatsuro Chiba[1], Kazuya Funakoshi[1]

1.Asia Air Survey Co., Ltd.

This is a preliminary report about morphological changes around post-caldera central cones of Aso Volcano caused by the 2016 Kumamoto Earthquake using aerial photos and 3D model.

Keywords: The 2016 Kumamoto Earthquake, Aso volcano, aerial photo, 3D model

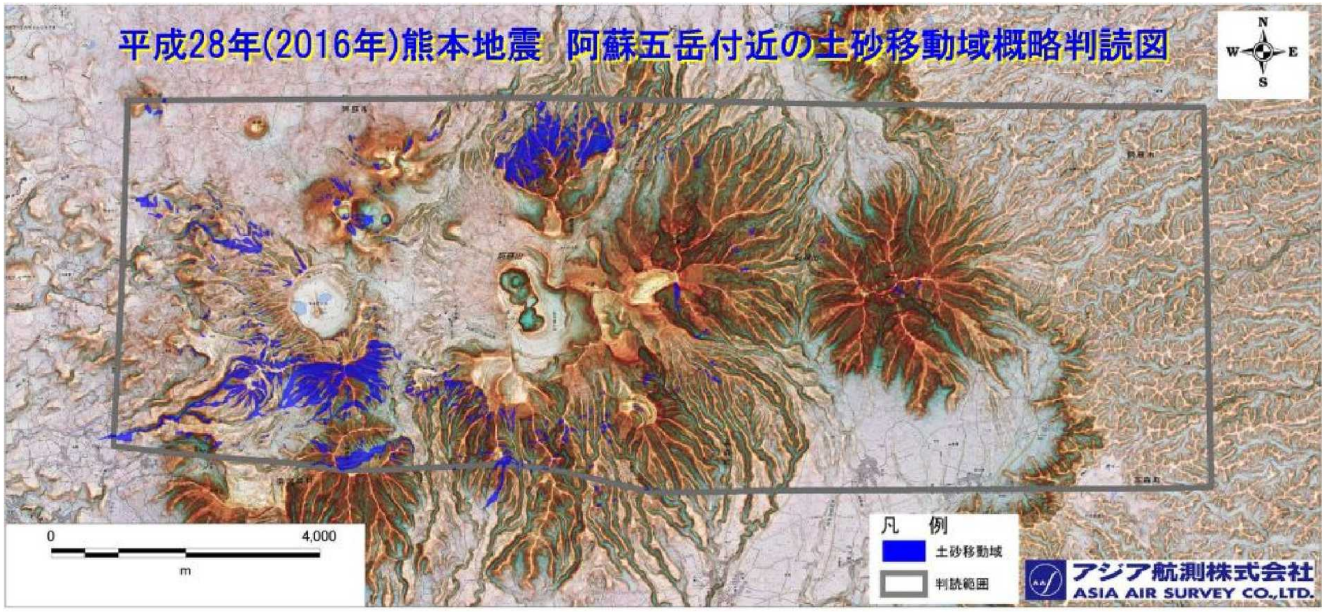

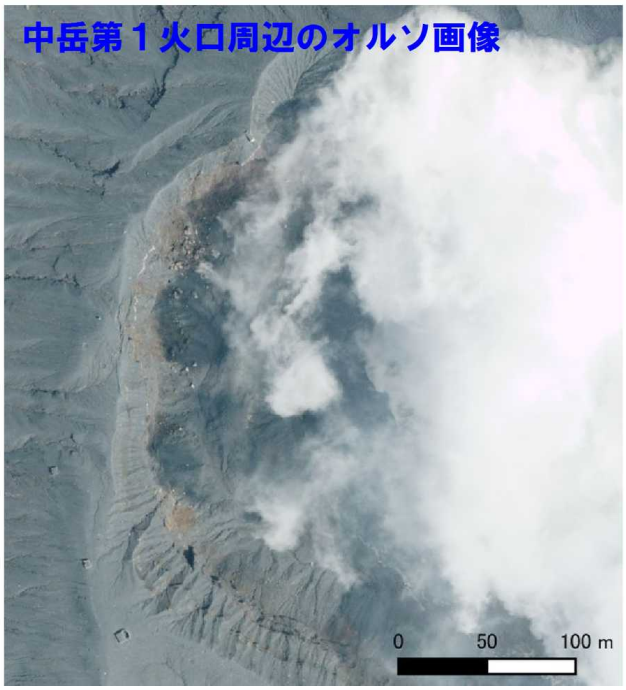

Interpretation of the Ground Disaster Occurring at Aso Area Caused by the 2016 Kumamoto Earthquake

*Tetsuro Homma[1], Hiroyuki Shimomura[1], Takeshi Honda[1], Hiroshi Yokota[1], Tooru Kobuke[1], Atsuo Noda[1], Yasuaki Honda[1]

1.PASCO CORPORATION

Introduction
The 2016 Kumamoto Earthquake triggered numerous landslides affected by the seismic ground motion. The occurrence of landslides was unclear just after the earthquake, so we needed to reveal the extent of the damage as soon as possible. After the earthquake, PASCO CORPORATION carried out aerial photographic surveys and acquired satellite images immediately, and then we interpreted landslides occurring at Aso area using acquired data. In addition, we carried out aerial laser surveying around the large-scale landslide of Tateno area, and calculated the sediment volume.

Keywords: The 2016 Kumamoto Earthquake, Landslide, Aerial photograph, Interpretation

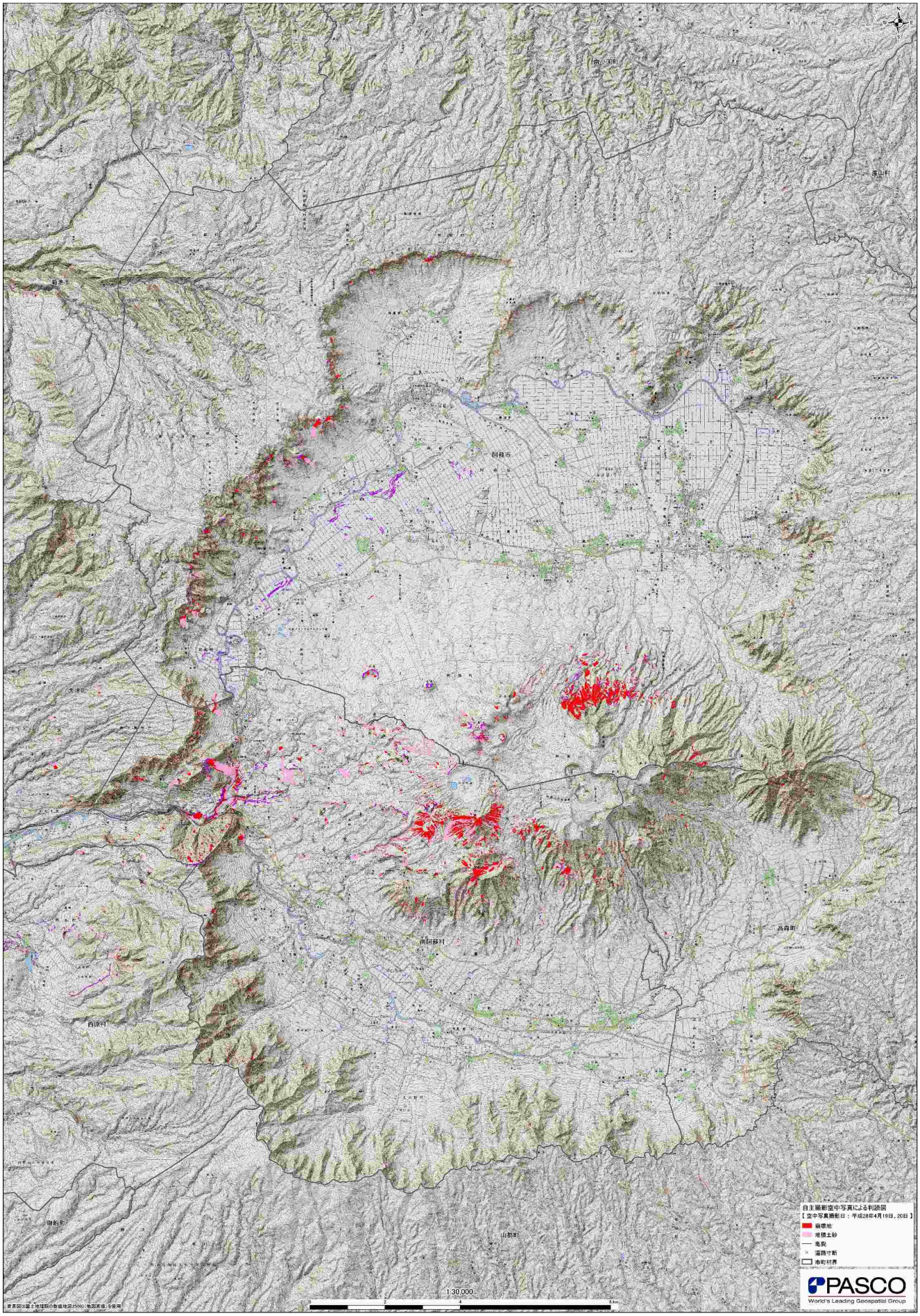

The study of coseismic dam monitoring with the Satellite data

*DAISUKE SANGO[1], YOSHIKAZU FUKUSHIMA[1], KAZUO YOSHIKAWA[1], SHO SHIMIZU[1], YASUNARI MORITA[1], HIROYUKI SATO[2]

1.PASCO, 2.Natinal Institute for Land and Infrastructure Management

Many of roads and river dike has been damaged caused by Kumamoto Earthquake (main shock) on April 16.PASCO acquired the data of stricken area from satellites and other sensing technologies as to validate and grasp the damages by the earthquake.In this series of the validation, PASCO attempted to monitor three fill dams.Some sedimentation at upper end of dam, which is located in area of 6 seismic intensity, caused by the earthquake were caught through interferometry analysis by satellite SAR.On the other hand, in dam body, which is located in area of 4 seismic intensity, any changes were not found at this moment.Pre/post earthquake optical satellite data also allows to grasp immediate change detection in dams and the surrounded area.Consequently, utilizing satellite imageries would be an effective method to monitor dams which are dotted around huge area in urgent cases.

Keywords: Satellite, Dam, Monitoring, DInSAR

Volcanic products of Aso Kusasenrigahama as revealed by surface slope collapse

*Toshiaki Hasenaka[1], Masayuki Torii[2], Yasuhisa Tajima[3]

1.Department of Earth and Environmental Science, Graduate School of Science and Technology, Kumamoto University, 2.Implementation Research and Education System Center for Reducing Disaster Risk, Kumamoto University, 3.Nippon Koei CO.,LTD.,

Kumamoto Earthquakes of April 14 and 16, 2016 caused tremendous disasters in the central part of Kumamoto prefecture, especially in Mashiki town, Minami Aso village, and Nishihara village. These areas are located close to Futagawa and Hinagu fault zones. Strong earthquake motion also caused landslides or slope collapses in the central cones and caldera walls of Aso volcano. Central cones developed after 90 ka Aso-4 caldera-forming pyroclastic eruption. Among them, 30 ka Kusasenrigahama volcano made the largest-volume eruption since Aso-4. Large-scale slope collapse made appear the interior structures of mountains around Kusasenrigahama volcano. We will discuss its products from the new geologic outcrop information.

Keywords: Aso volcano, Kumamoto earthquakes, Kusasenrigahama volcano

Preliminary report of deformation and debris flow effect at North West site Aso caldera cliff after Kumamoto earthquake.

*Shoichi Kiyokawa[1], Hiroaki Mitsuki[2]

1.Department of Earth and Planetary Sciences Faculty of sciences, Kyuushu University, 2.Fukken Co., Ltd.

At northwest area of Aso Caldera cliff area, several landslides occur along the northeast trend right-lateral faults. Our department (Kyushu university, Earth and Planetary Science) have been done of field trips every year at Novermber. Many outcrops of trip locations were damaged by the Kumamoto Earthquake at 15th and 16th April 2016. We researched 1) Kabutoiwa lookout, 2) Raputa road, 3) Muramoto rock quarry. There are several landslide along north-west site of the caldera cliff. We try to check how difference before and after earthquake topography and preserving geological evidence.
Especially the Muramoto rock quarry, which is main field trip stop in our class with big cliff and diggings hole, was highly occur land slide. Debris flow occurred during the land sliding started top of the hill (850m). Then this flow down bottom of digging hole then it clime up again opposite side of the lower cliff (30m from bottom of cliff). There are several big concrete water pipes and rock breccia within mud flow deposit. If these is not diggings holes in this quarry, debris flow went to village bellow this quarry. So it is suggest that high energy debris flow easy can pass higher mound.

Keywords: Kumamoto Earthquake, debris flow, landslide

The effects on Aso volcanic edifice by 2016 Kumamoto earthquakes

*Yasuhisa Tajima[1], Masayuki Torii[2], Toshiaki Hasenaka[3]

1.NIPPON KOEI CO.,LTD., 2.IRESC, Kumamoto University, 3.Graduate School of Science and Technology, Kumamoto University

Large earthquakes occurred in the central part of Kumamoto prefecture on 14th and 16th April, 2016. Those quakes occurred due to the north segment of the Hinagu faults and the east segment of Futagawa faults. As a result, many earthflows and landslides were triggered by those quakes.
We studied morphological analysis on Aso volcanic edifice using a space photograph published on 16th April by Google Earth (Google Earth©2016 ZENRIN). The topographical change is divided by mass movements, faults or fractures, and others.
The structure of mass movement consisted of earth flows, toes and slump blocks. We extracted the main scraps caused by mass movement. Next, we found many fresh straight fractures on the volcanic edifice. Those fractures were stretched straightly, cutting into the small hills and gullies. It is assumed those fractures were generated by faulting.
Futagawa faults is of a NE –SW direction on the west side of the Aso caldera. The straight fractures on the Aso volcanic edifice directed toward the east appeared from Kawayo to Akase, in Minamiaso village on the west side of the Aso caldera. The straight fractures spread between the edge of the south volcanic edifice and the Janoo scoria cone of North part of the edifice. Many mass movements occurred in this area. And the thick loose volcanic ash deposits are covered on the edifice in this area. These actions caused many mass movements on the volcanic edifice. It is assumed that the straight fractures on Aso volcanic edifice are correlated crater locations on the volcano. We will analyze those fractures on the volcano.

Keywords: Aso volcano, Topographical alterations, Kumamoto earthquakes

Seismic Intensity Distribution of the 1889 Meiji Kumamoto Earthquake and Its Source Location

*Masayuki Takemura[1]

1.Disaster Mitigation Research Center, Nagoya University

The earthquake (M=6.3) occurred in Kumamoto area in Meiji Period (July 28th 1889), 127 years before the Heisei events. Seismic Intensity Distribution of the 1889 Meiji event is estimated from the damage data reported by Imamura(1920). The maximum intensity is 6- in JMA scale at the area of West Ward in the present Kumamoto city, while the most severe damage region from the Heisei event is Mashiki city next to East Ward in the Kumamoto city. This difference is caused by the locations of source regions between Meiji and Heisei events. Source region of the Meiji event may be along the wast part of Futagawa Fault, while the sourece region of the foreshock (M6.5) of the Heisei event is corresponding to Hinagu Fault and that of the main shock(M=7.3) to the Eastern part of Futagawa Fault.

Keywords: Meiji Kumamoto Earthquake, Seismic Intensity Distribution, Source Region, Active Fault

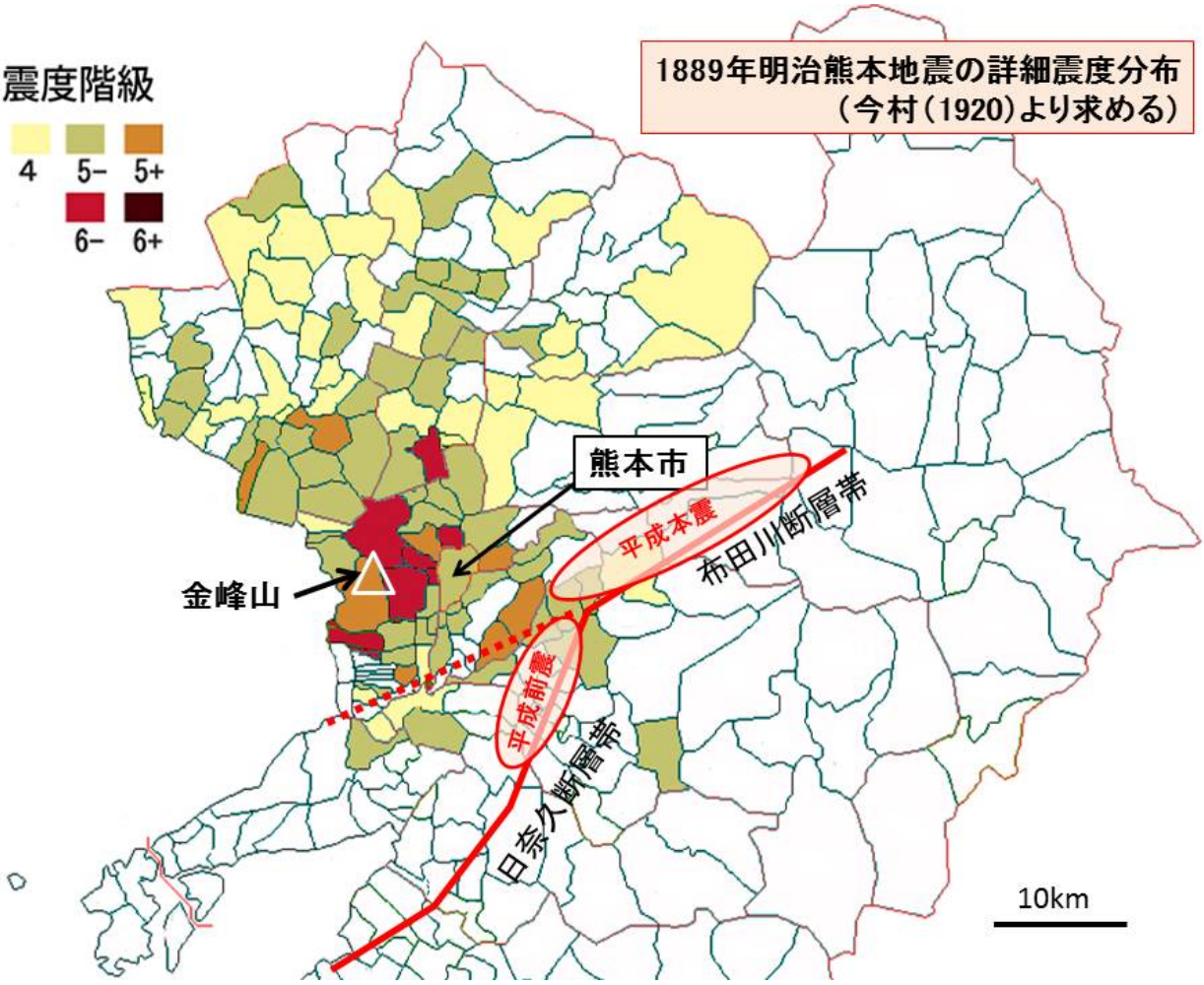

Materials related to the 1889 Meiji Kumamoto earthquake

*Satoko Murotani[1], Nobumichi Ariga[1], Fumitaka Wakabayashi[1], Masahiro Osako[1]

1.Department of Science and Engineering, National Museum of Nature and Science

The Meiji Kumamoto earthquake occurred on July 28, 1889. The ground shaking resulted in casualties of about 20, collapse of more than 230 houses, and collapse of Kumamoto Castle's stone walls. The hypocenter was estimated near Kinbo-zan, which is to the west of Kumamoto Castle, and the magnitude was estimated 6.3 (Utsu, 1982, BERI). There were 292 aftershocks within 21 days, and were 566 aftershocks within 150 days (Imamura, 1920, Reports of the Imperial Earthquake Investigation Committee). The hypocenter of this earthquake differs from that of the 2016 Kumamoto earthquake, however, many people are now interested in the Meiji Kumamoto earthquake. The National Museum of Nature and Science (NMNS) has some historical materials related to the Meiji Kumamoto earthquake. We introduce about those in this poster.
Rihei Tomishige who was a photographer in Kumamoto took some photos for the disaster of this earthquake. The 11 photos remain in NMNS today, such as the destroyed stone walls of Kumamoto Castle, the damage of military, and the scenery of temporary house. These photos are publicly available on the website of NMNS (http://www.kahaku.go.jp/research/db/science_engineering/namazu/index.html).
Prof. Bunjiro Koto, Prof. Seikei Sekiya, and Hantaro Nagaoka of Imperial University went to Kumamoto to survey this earthquake. Nagaoka examined the damage around Kinbo-zan, and noted the investigations and sketches of damage. NMNS possesses those items as a part of archival materials on scientists.
NMNS has an illustration of the Meiji Kumamoto earthquake which was published a few days after the event. It describes the situations of collapsed houses and people buried beneath them, saying "It's a rare large earthquake we've not seen in recent years."

Keywords: Meiji Kumamoto earthquake, photo collection on the damage by earthquake, archival materials on scientists

How many times do people feel strong ground motions of the JMA's seismic intensity of 5- or greater by the 2016 Kumamoto Earthquakes?

*Hiroo Nemoto[1], Masatsune Hatakeyama[2], Masashige Minamishima[3], Akihiko Ito[4]

1.Division of Natural Sciences, J.F.Oberlin University, 2.Seikou Gakuin Secondary School, 3.Tokyo Metropolitan Ryogoku Secondary School, 4.Faculty of Education, Utsunomiya University

The 2016 Kumamoto Earthquakes occurred in earthquake sequences of foreshock-mainshock-aftershock type in and around Kumamoto Prefecture, Japan on April, 2016. There were 18 earthquakes which recorded JMA Seismic Intensity (SI) of 5- or greater at one or more of SI observation stations (SIOS) during 16 days after the foreshock.
Changing over the point of view, we want to examine how many times people feel strong ground motions of the SI of 5- or greater by the 2016 Kumamoto Earthquakes at each SIOS.
In this study, we used SI data of JMA's SI information, SI database by JMA, and strong ground motion data of K-NET and KiK-net. In addition to these data, we analyzed six "Rika" (similar to Natural Science) textbooks for year six of primary school, five and five Rika textbooks for the year seven and nine of lower secondary school, respectively, and four Science and Our Daily Life textbooks and five Basic Earth Science textbooks for year 11 and/or 12 of upper secondary school.
As a result, three SIOS recorded as the most number of SI of 5- or greater during this term, and the number of occurrences was seven. These stations are Miyazono Mashiki-machi (7 : twice, 6- : once, 5+ : once, 5- : three times), Tensui-machi Tamana-shi (6- : twice, 5+ : once, 5- : four times), and Kasuga Nishi-ku Kumamoto-shi (6+ : once, 6- : once, 5+ : once, 5- : four times). On the other hand, one SIOS had recorded as the most number of SI of 5- or greater during 16 days after the mainshock in the Mid Niigata Prefecture Earthquake in 2004 (the 2004 Chuetsu Earthquake), and the number of occurrences was 16. In this station, which is located in Jyounai Ojiya-shi, SI 6+, 6-, 5+, and 5- was recorded twice, twice, seven times, and five times, respectively. At the same time, K-NET station named NIG019, is located in Ojiya-shi, recorded SI 7 equivalent (e.g. Ishii, et al., 2007). When the mainshock and the largest aftershock was attacked SIOS of Jyounai Ojiya-shi, this SIOS was recorded SI 6+ for both. These data may suggest that SI 7 had hit soft ground area in the vicinity of these stations twice.
Furthermore, we searched the SI database of JMA by referring to the reference information such as the Headquarters for Earthquake Research Promotion (HERP) (1998). According to this search, there are no aftershocks greater than mainshock's JMA Magnitude (MJ), if the mainshock's MJ is 6.4 or greater for shallow inland earthquakes. This means we will need to reconsider the characteristics of shallow inland earthquakes because foreshock (MJ6.5) - mainshock (MJ7.3) - aftershock type occurred as the 2016 Kumamoto Earthquakes.
We also analyzed school textbooks. As a result, foreshock, mainshock, and aftershock are not written in all Rika, and Science and Our Daily Life textbooks. The word, foreshock, is written only in one of five Basic Earth Science textbooks.
In conclusion, at the moment, the 2016 Kumamoto Earthquakes revealed three problems through this study as below;
(1) Is this the first time in recorded history SI 7 has hit the same place twice in close succession in Japan?
(2) Will we need to reconsider the characteristics of shallow inland earthquakes, especially for earthquake of MJ6.4 or greater?
(We may also need to think about revision of the standards for earthquake resistance through the results of (1) and (2).)

(3) What kind of knowledge should school teachers teach about seismic activity including a large scale earthquake causing strong ground motion and its related basic concept such as foreshock, mainshock, aftershock?
In this presentation, we would like to discuss how to solve these problems in the fields of seismology, earthquake engineering, and earthquake and earthquake disaster prevention education using lessons from the 2016 Kumamoto Earthquakes.

Acknowledgment
We appreciate JMA for providing data of SI information and SI database. We also would like to thank NIED for providing K-NET and KiK-net strong ground motion data.

References
HERP, Aftershock Probability Evaluation Methods, 1988.
ISHI, Y., GOTO, H., and SAWADA, S., Ground motion characteristics affected by source rupture process at Kawaguchi during Niigata Chuetsu Earthquake, JSCE Journal of Earthquake Engineering, 29(0), 153-160, 2008.
Twenty five school textbooks for primary and secondary school students.

Keywords: The 2016 Kumamoto Earthquakes, Seismic Intensity Observation Station, Seismic Intensity, Rika (Natural Sciences) and Basic Chigaku (Basic Earth Science), Foreshock-Mainshock-Aftershock Type, Standards for Earthquake Resistance

Mechanism of creation of an "unexpected" arising from 2016 Kumamoto Earthquakes

*Mamoru HAYASHI[1]

1.University of TOYAMA

The 2016 Kumamoto Earthquakes occurred in the areas with the following aspects:

(1) Experience from earthquake disasters in recent times.

(2) Finding and sharing the knowledge of local private research organizations (NPO KSNDR = Kumamoto Society for Natural Disaster Reserch, first meeting in November 27th, 1992), catalogs and research books about earthquake.

(3) Disaster prediction and warning by the central government through elaboration of hazard maps, etc.

(4) Progress of earthquake resistance measures by the local governments of Kumamoto Prefecture, Kumamoto City and Mashiki Town.

Although it happened according to the scenario based on these predictable facts, (5) it is interesting that these earthquakes are said to be "unpredictable", saying "never expected to happen in Kumamoto", "unprecedented foreshock", "aftershock experience not applicable", etc.

Moreover, the multiple earthquakes are being considered as something extraordinary. Also, the damage caused by the multiple earthquakes of intensity 7 (the highest level in the Japanese seismic intensity scale) is seen as it would have been safe in a case of a single tremor of intensity 7. Here, it is possible to see the mechanism of an " unexpected" in order not to see the real facts and avoid taking into consideration the disaster experiences.

In the case of the 2016 Kumamoto Earthquakes, in which the intensity 7 was divided into foreshock and main tremor, the collapse of houses and buildings would have been more devasting if it were just one "main tremor". The "main tremor" occurred in the middle of the night, so the worst scenario could be avoided.

Keywords: Meiji Kumamoto Earthquake Disaster in 1889, Consider Everything as “Unprecedented”, Difficulty to take into consideration the disaster experiences, Science communication for Earth and Planetary Sciences and Society, Risk Communication

1889 Meiji Kumamoto Earth Quakes (From July 28 to August 18)

震動表

月日／震力	劇震	稍強	輕震	鳴動	合計
七月廿八日 午后十一時四十九分	一				一
仝 廿九日	一	二三	一四	三三	七〇
仝 卅日	一	五	一〇	一二	二七
仝三十一日	一	一	一二	二	一五
八月一日	一	一	六	四	一一
仝 二日	一	一	一	七	八
仝 三日 午前二時十八分	一	三	一八	一三	三五
仝 四日	一	二	一一	九	二二
仝 五日	一	一	五	六	一一
仝 六日	一	一	五	五	一一
仝 七日	一	一	三	一	四
仝 八日	一	一	五	六	一一
仝 九日	一	一	一	一	二
仝 十日	一	一	四	二	六
仝 十一日	一	一	四	二	六
仝 十二日	一	一	四	一	五
仝 十三日	一	一	四	五	九
仝 十四日	一	一	一	四	五
仝 十五日	一	一	四	六	一一
仝 十六日	一	一	五	七	一二
仝 十七日	一	一	三	三	六
仝 十八日	一	一	一	四	五
計	二	三九	一二〇	一三二	二九三

小藤文次郎：熊本地震慨察報告，地学雑誌（1889）から
21日間に292回の「余震」が熊本県庁にて観測された（事務繁雑時などの記録漏れもありえる旨の注記あり）。
7月28日午後11時49分の「本震」（M6.3）から5日後の8月3日午前2時18分に，この表で同ランクの「劇震」が発生，余震が再び活発化。

